UiT Norges arktiske universitet

Department of Pharmacy

Synthesis, bioactivity testing, and structure elucidation of antimicrobial peptide analogues derived from *Synoicum Turgens*

Johannes Kristensen

Master's thesis in pharmacy FAR-3911-1 22H May 2023

1 Acknowledgment

I would like to express my gratitude to my supervisors. First, Terje Vasskog, for assisting me with interpretation of results and the use of the various instruments as well as help in the writing process. Second, Julie Strømberg, for instructing and providing advice in the use of lab equipment and the methods used in this thesis, along with help in the writing process and interpretation of results. Third, Kine Østnes Hansen for providing feedback of the parts regarding bioactivity testing. I would also like to thank Ingrid Sofie Norberg-Schulz Hagen for her help in conducting the peptide synthesis and preparative HPLC.

Further, I would like to express my gratitude to my co-student Stine Høgetveit Hansen for discussing methods and results over the course of this thesis, as well as providing assistance in the laboratory.

I would like to thank Hege Devold and Tor Haug at Norges fiskerihøgskole (NFH) for conducting the MIC measurements of the peptides synthesized in this thesis.

At last, I would like to thank my family for always supporting me in my studies.

2 Abstract

This thesis aims to develop methods for synthesis and structure elucidation of disulfide-rich peptides (DRPs). DRPs are peptides that are rich in cysteines, and form disulfide bridges between these amino acids within the peptide, contributing to their conformation and stability. Multiple isomers of the same DRP can exist. This is due to variations in which cysteines form disulfide bonds with one another within the peptide. The first objective of the study is to develop a method for synthesizing and isolating isomers of a DRP using peptide synthesis, preparative HPLC and mass spectrometry. The second objective is to develop a method for elucidation of structures of existing DRPs. This is done by selective cleaving through reduction and alkylation of the disulfide bridges and analyzing the products using Mass Spectrometry. Further, the third objective is to investigate the impact of substituting amino acids and the configuration of the disulfide bonds have for the peptides' antimicrobial activity. In this study, the MIC of each isomer of the synthesized peptides is measured and compared to the original unsubstituted peptide, as well as the amount of each peptide isomer formed. The findings are used to gain insight in development of new DRPs and the structure-activity relationship of antimicrobial peptides, which may play a role in the development of new antimicrobial peptides.

Table of contents

3 Introduction

3.1 Background

Antibiotic resistance is a problem only increasing in severity in modern medicine. Due to overuse and lack of new products entering the market, antibiotic resistant bacteria are becoming more and more prevalent, with resistances to antibiotics that were previously effective (1). As the amount of elderly and immunocompromised humans are only increasing, new classes of antibiotics are necessary to prevent untreatable infections caused by these bacteria (2). A study has estimated an amount of 1.27 million deaths in 2019 that were directly contributed to antimicrobial resistant bacteria (3). A possible new class of therapeutics are antimicrobial peptides (AMPs), which have played a part in the first line of defense against bacteria since ancient times in all forms of life (1, 4). Several of these have been found through bioprospecting of marine organisms such as mollusks, crustaceans, and ascidians, with the latter being the source of the peptides in this study (1). As of the time when this thesis was written, there were some AMPs available as therapeutics on the Norwegian market, with some examples being bacitracin (5) and vancomycin (6).

3.2 Disulfide Rich Peptides

Disulfide rich peptides, which as the name implies, contains multiple disulfide bridges between cysteines in the amino acid chain. These bridges are essential to the function of these peptides as they not only constrain the peptide in a specific three-dimensional fold, but also contribute to the stability of the peptide (7). The increased stability that the disulfide bridges offer is one possible advantage in the use of DRPs as a therapeutic, compared to conventional peptides. One of the challenges we face using peptides as a drug is the half-life in blood plasma, as they are subjected to proteolytic cleaving in both the intestines and in plasma (4). The use of DRPs may be a solution to this hinderance, and has contributed to even allowing oral administration in the peptide drug Linaclotide(8).

There are various examples of species that produce DRPs to give them an evolutionary edge. The peptides of interest in this thesis are derived from the peptide Turgencin A, which is an antimicrobial peptide (AMP) found in the ascidian *Synoicum Turgens* (9). *Synoicum Turgens*

is an ascidian, which is a class of marine organisms that feed through the filtration of swallowed seawater (10). Through this, it filters several bacteria, which is an important food source for them (11). Invertebrates like ascidians lack any form of adaptive immune system, and thus require an effective innate immune system to deal with any pathogens that may threaten it (12). Studies have determined that it produces several DRPs, including the peptides Turgencin A and B (1).

Other examples of DRPs include α-conotoxin GI in *Conus geographus* which acts as a venom and has been used by humans in structure studies of the ligand-gated ion channel superfamily of receptors (13), and kalata B1 in the plant *Oldenlandia affinis* that was used as a uterotonic by indigenous Congolese (14).

Peptides with two or more disulfide bonds can theoretically form several isomers with different disulfide connectivity. I.e., a peptide with 4 cysteines can theoretically form three different isomers where the difference lies in what cysteines form disulfide bonds between each other. In this thesis, the configurations are named after what cysteines form disulfide pairs. If the 1st and 2nd cysteine in a peptide sequence forms a disulfide bond, then the 3rd and 4th cysteines will form a bond between each other. This configuration would then be denoted as a 1-2/3-4 configuration. The three possible isomers in an example DRP with 4 cysteines is illustrated in Figure 1. Be aware that Figure 1 is a two-dimensional illustration and does not reflect on any changes made to the three-dimensional structure of the peptide. The purpose of the

figure is only to show the different disulfide bonds between the three possible isomers.

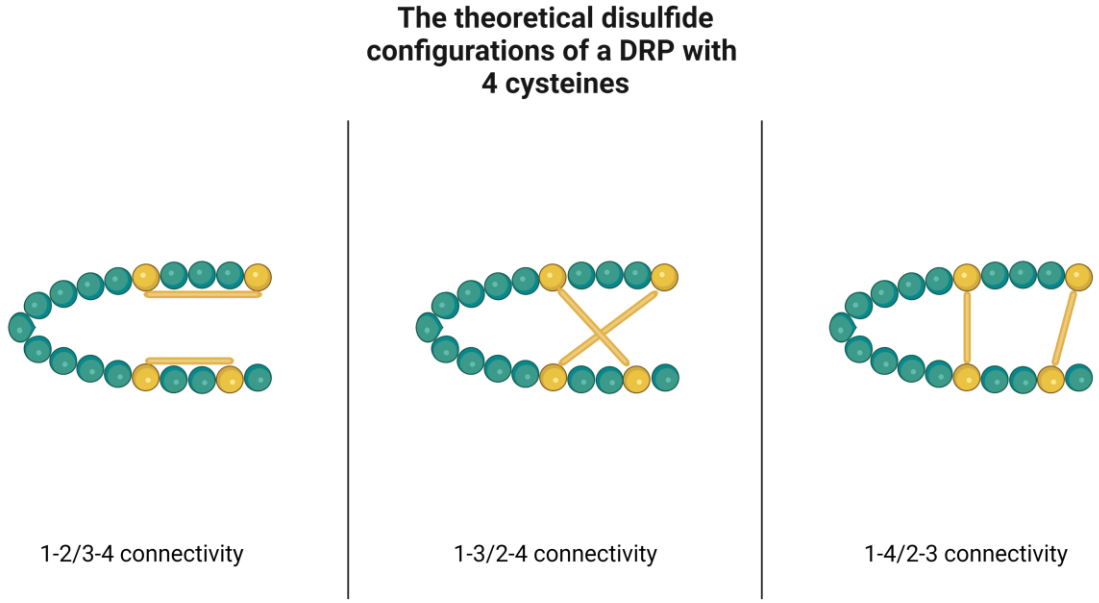

Figure 1: Illustration of an example DRP with its three possible isomers. The cysteine amino acids are highlighted in yellow, while the remaining amino acids are highlighted in teal. The disulfide bonds are illustrated as a yellow beam between the cysteine pairs. The isomers are named after what cysteines form disulfide pairs. Created with Biorender.com

The process of forming a disulfide bond between two cysteines require the oxidation of both cysteines. This results in the removal of the hydrogen bonded to the sulfur atom in the side chain of both cysteines. This results in both cysteines having an incomplete electron pair, and thus bond to each other fulfilling the octet rule. A simplified reaction showing the formation of a disulfide bond is illustrated in Figure 2.

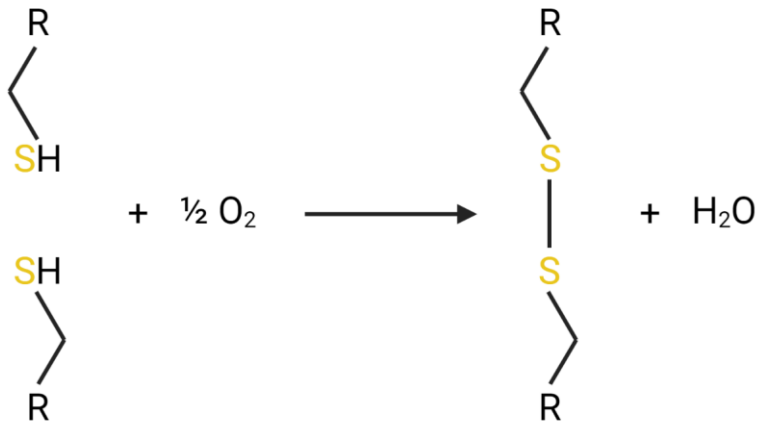

Figure 2: The formation of a disulfide bond through oxidation of a cysteine pair with oxygen. "R" is used in place of the rest of the cysteine and peptide chain. Created with Biorender.com

DRPs are able to form several isomers, but despite this in nature the peptides are usually only observed to converge into a single specific fold (13). While it is possible to control the formation of isomers during peptide synthesis, we choose to not do so in this thesis. This was done so that we could study the formation of the possible isomers, test them for their antimicrobial activity and link it to their difference in disulfide connectivity, as well as optimizing methods for determining disulfide connectivity by mass spectrometry (MS). Differing disulfide bonds will contribute to the isomers having different folds and this can contribute to drastic changes in bioactivity or a reduction of side effects (7). Therefore, the elucidation of the correct structure is of significant importance. Because the different isomers have the same amino acid sequence, they also share the same mass, which means that we cannot use mass spectrometry alone to elucidate the structure. The method used in this thesis is done by the reduction and alkylation of the disulfide bridges before analysis by MS, and is based on the method used by Albert et al. (7).

3.2.1 Peptide analogues of Turgencin A

As described earlier, Turgencin A is an AMP found in the species *Synoicum Turgens*. In this thesis, the peptides were based on a truncated version of Turgencin A named Turg_JS_001 from ongoing work. This truncated version only contains 19 of the original 36 amino acids, and 4 of the 6 cysteine amino acids from the original peptide. This means that it can only form two disulfide bridges, compared to the three that are formed in the original peptide. Therefore, the truncated peptide has 3 isomers with differing disulfide connectivity. Each of the isomers from Turg_JS_001 have shown differing levels of minimum inhibitory concentration (MIC) against different species of bacteria. MIC is the concentration of an antibiotic where the bacteria are no longer able to reproduce, and is used as a measure of how susceptible a bacteria is to an antibiotic (15). Turg_JS_001 displays relatively low antimicrobial activity, and thus a goal of this study is to improve the antimicrobial activity through minor changes to the peptide sequence.

Thus, the peptides Turg_JK_1 and Turg_JK_2 were created by modifying the sequence. The sequences of Turgencin A, Turg_JS_001, Turg_JK_1, and Turg_JK_2 can be found in Figure 3.

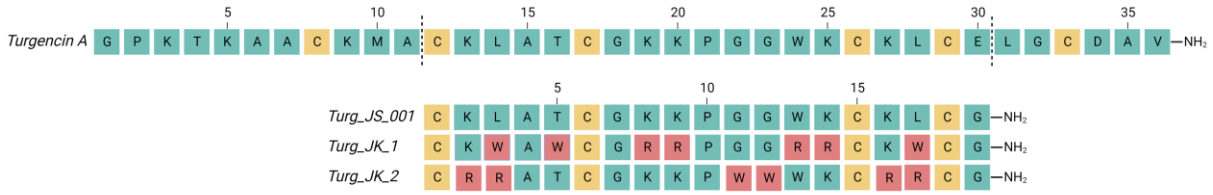

Figure 3: The amino acid sequences of the peptides in this thesis. Turg_JS_001 and its analogues are placed underneath the section of Turgencin A that they are derived from. The non-cysteine amino acids are highlighted in teal, the cysteines are highlighted in yellow and the substituted amino acids in the analogues of Turg_JS_001 are highlighted in red. Every fifth amino acid in the sequence is indicated by its respective position number. Adapted from "Multiple Sequence Alignment (Protein)", by BioRender.com (2023). Retrieved from https://app.biorender.com/biorender-templates"

The purpose of the substitution is to study the impact of this on both the bioactivity and the disulfide connectivity. In both modified peptides, several amino acids are replaced with either tryptophane or arginine, both of which are depicted in Figure 4.

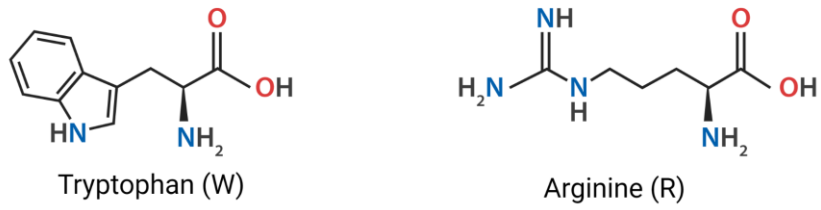

Figure 4: Structures of Tryptophan and Arginine. Created with Biorender.com.

Tryptophane is a relatively hydrophobic amino acid where the side chain contains an indole ring system, which is the main contributing factor to the hydrophobicity. Arginine contains a basic group, giving it the ability to attach a proton and obtain a positive charge. Both properties may be advantageous to the peptide's antimicrobial activity (2).

Natural AMPs are often characterized by their amount of hydrophobic amino acids and amino acids granting positive charge(s). It is thought that AMPs destabilize and disrupt the anionic outer membrane of microbes through electrostatic interactions, and then embedding into the membrane, which causes a disruption and increased permeability, leading to nutrients and electrolytes leaving the bacteria, causing bacterial death (4). Thus, substituting amino acids with either tryptophan or arginine may be a strategy in the goal of increasing the antimicrobial activity of a DRP.

Two different approaches are taken in the replacement of amino acids in Turg_JK_1 and Turg_JK_2. In Turg_JK_1 the edges of the peptide have 2 lysine amino acids and one threonine amino acid replaced with tryptophane, which leads to an increase in hydrophobicity. In the mid-part of the peptide, 3 lysine amino acids and 1 tryptophan amino acid are replaced with arginine groups. This leads to an increase in basicity. This is because while lysine has an amine in the side chain, its pKa is lower compared to the guanidino group of an arginine.

In Turg_JK_2, the other approach is taken. The edges of the peptide are made more basic by replacing two lysine and leucine amino acids there. In the mid-part of the peptide, two glycine amino acids are replaced with tryptophan, increasing the hydrophobicity there.

As mentioned earlier, we choose not to form any disulfide bonds during the peptide synthesis. The consequence of this is that we have no control over which cysteines form disulfide bonds between each other during the oxidation of the cysteine groups. Because some disulfide bonds are more easily formed than others, the probability of a peptide forming one of these isomers is higher than the other isomers. Therefore, the amount of each isomer varies between each other after the oxidation process for a given peptide.

There may occur a change in what disulfide bonds are likely to be formed during the oxidation process if the amino acids are substituted. The substituted amino acids may have differing chemical properties, such as being hydrophilic rather than hydrophobic. This can cause a change in the stability of a disulfide bond if it leads to e.g., the introduction of a hydrophilic amino acid that comes close to a hydrophobic amino acid when a disulfide bond is formed or the introduction of a larger amino acid which may sterically the formation of a specific disulfide bond. This may lead to a previously stable disulfide configuration becoming unstable or impossible, and less likely to form relative to the other disulfide configurations.

3.2.2 Elucidation of disulfide connectivity

3.2.2.1 Theory

The method used in this thesis is based on a method from Albert et al. (7). It is performed through sequential reduction of disulfide bonds and alkylation with maleimides of the cysteine pairs that formed the disulfide bridges. In this method, only a single disulfide bridge is reduced and alkylated per step, ensuring that the cysteines that form a single disulfide bridge are alkylated simultaneously with the same maleimide. The next disulfide bridge is then reduced and alkylated, but with a different maleimide. This way, the two cysteine pairs that form the two disulfide bridges are alkylated with different maleimides, making it possible to determine which cysteines form pairs. If the peptide contains more disulfide bridges, the reduction and alkylation steps can be repeated until this is performed on every disulfide bridge (7). In this thesis, the peptides that are studied contain two disulfide bridges. The sequential reduction and alkylation are illustrated in Figure 5.

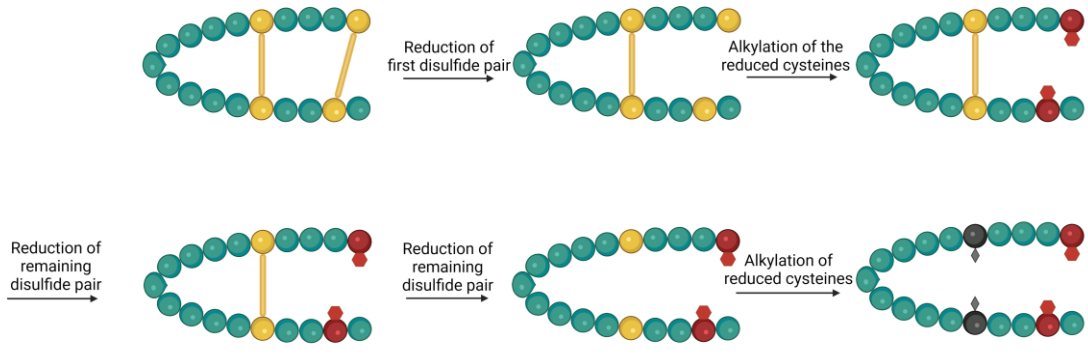

Figure 5: Reduction and alkylation of the disulfide bonds. The cysteine residues are marked with yellow. The maleimides are represented by either the red highlight and hexagon shape, or the black highlight and diamond shapeCreates with Biorender.com

The reduction and alkylation occur while the peptide is attached to a solid-phase sorbent. While attached to the sorbent, the peptides orientation is restrained, and may be attached in a way that limits the access for the reducing agent to a disulfide bridge if it is embedded into the sorbent, while the remaining cysteine pair may remain accessible for the reducing agent. This way we can limit the reduction and alkylation of both disulfide bonds in the first step, as it is necessary for the elucidation of the structure. Because the peptide is restrained by the sorbent, it also makes it more difficult for disulfide scrambling to occur (7).

The two cysteine pairs are alkylated with different maleimides as seen in Figure 5, and as such they will also differ in mass. Because of this, we can determine the alkylation pattern that is formed through peptide sequencing, and thus also determine the disulfide configuration. This is performed by fragmenting the peptide through UPLC-MS-analysis (7) and will be explained later in this thesis. When performed on isomers of a specific peptide with differing disulfide connectivity, the alkylation pattern will change accordingly when the reduction and alkylation process is performed. This makes it possible to distinguish the disulfide connectivity between isomers of the same peptide. In Figure 6 an example of how the fragments from two different isomers of the same peptide with a 1-4/2-3 and 1-3/2-4 connectivity form different alkylation patterns, and how they can be differentiated is shown.

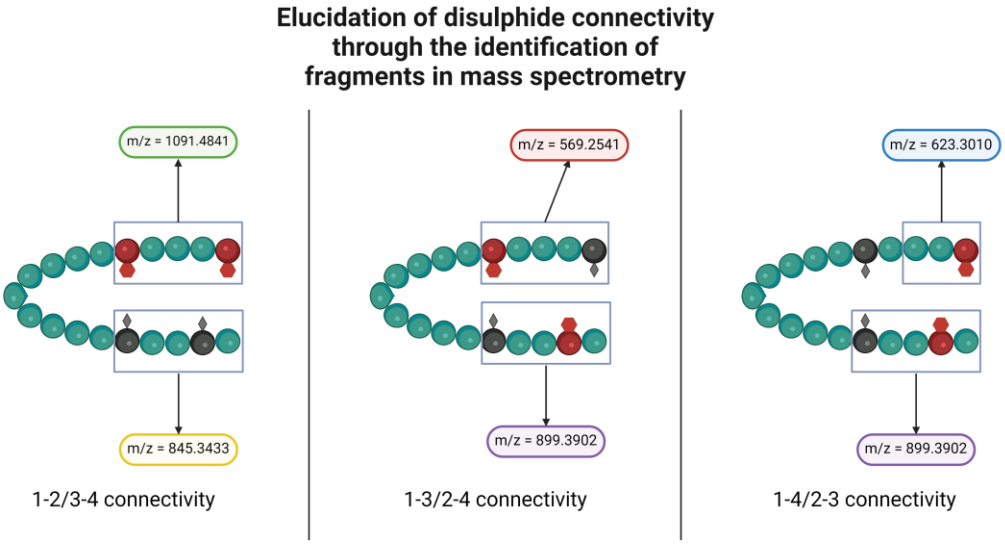

Figure 6: Figure showing the different alkylation patterns that are present for the three possible isomers of a DRP with differing disulfide connectivity. Certain fragments that can be used to determine the disulfide connectivity are highlighted, with their masses nominated. The bubbles are color coded according to their m/z value, showing what fragments are present in multiple configurations. Created with Biorender.com.

In Figure 6 the first cysteine group in the peptide sequence is alkylated with one of two different maleimides. Because of the difference in mass between the two maleimides, the highlighted fragments will differ in mass between the isomers.

Alkylation patterns that are formed will produce fragments with mass-to-charge (m/z) values that can be used to identify this pattern and thus the disulfide connectivity. First, a 1-2/3-4 connectivity will produce a fragment containing the two first or two last cysteine groups, which will both be alkylated with the same maleimide, giving it unique fragments that are not present for either of the other configurations. For both a 1-3/2-4 and 1-4/2-3 connectivity the two last cysteine groups in the sequence are alkylated with different maleimides, therefore the presence of a fragment containing two cysteine groups alkylated with the same maleimide can be used to confirm a 1-2/3-4 connectivity. The same way, the presence of a fragment with two cysteines alkylated with two different maleimides can rule out the possibility of a 1-2/3-4 connectivity. This is illustrated in Figure 6. There, the fragment containing the 5 last amino acids has an m/z value of 845.3433 and is only present for the 1-2/3-4 configuration. For the two remaining

configurations, the fragment containing the last 5 amino acids has an m/z value of 899.3902 for both configurations.

As explained, by looking at a fragment containing either the two first or last cysteines, it is possible to determine whether the peptide has a 1-2/3-4 configuration or not. If it does not, it is still necessary to distinguish between a 1-3/2-4 and 1-4/2-3 configuration. A fragment containing two cysteines cannot be used, as they will both contain one cysteine alkylated with either maleimide. Because MS can only determine the m/z of a fragment, we cannot determine the alkylation pattern this way. However, it is possible to look at fragments only containing one or three cysteines. In this explanation, fragments containing only one cysteine will be used. The isomers with 1-3/2-4 and 1-4/2-3 configurations depicted in Figure 6 have their first cysteine group alkylated with different maleimides, which is shown in the upper highlighted fragments. The consequence of this is that a fragment containing only the first cysteine will differ in mass between the two isomers. On the same note, a fragment only containing the last cysteine will produce the same fragment between both isomers as it is alkylated with the same maleimide and cannot be used to distinguish between the two.

3.2.2.2 Challenges with the approach

The example from Figure 6 assumes that the same disulfide bond is reduced and alkylated in the first step of the process for every peptide attached to the sorbent. In practice, it is possible for both disulfide bonds to be reduced and alkylated in the first step, with the remaining disulfide bond in the second step. This makes two alkylation patterns possible for a disulfide configuration of a DRP with two disulfide bonds (7). The two possible alkylation patterns for an isomer of the depicted DRP are illustrated in Figure 7.

Figure 7: Both possible alkylation patterns for this specific DRP with a 1-4/2-3 connectivity is illustrated. The hexagon shapes and red highlight represent the first maleimide used, while the diamond shapes and black highlight represent the second maleimide used. Created with Biorender.com

When analyzing the alkylated peptides by LCMS, it may be possible to separate the peptides with differing alkylation patterns, however this may vary from peptide to peptide and choice of maleimides (7). If the disulfide connectivity of the peptide is 1-3/2-4 or 1-4/2-3 it is necessary to separate the two alkylation patterns to properly elucidate the structure. This is because if there is a mix of both alkylation patterns present within the mass spectra, then it is impossible to distinguish between the two mentioned configurations. If this is the case, then there would be no unique fragments that can be used to rule out any theoretical configurations. This problem is illustrated in Figure 8.

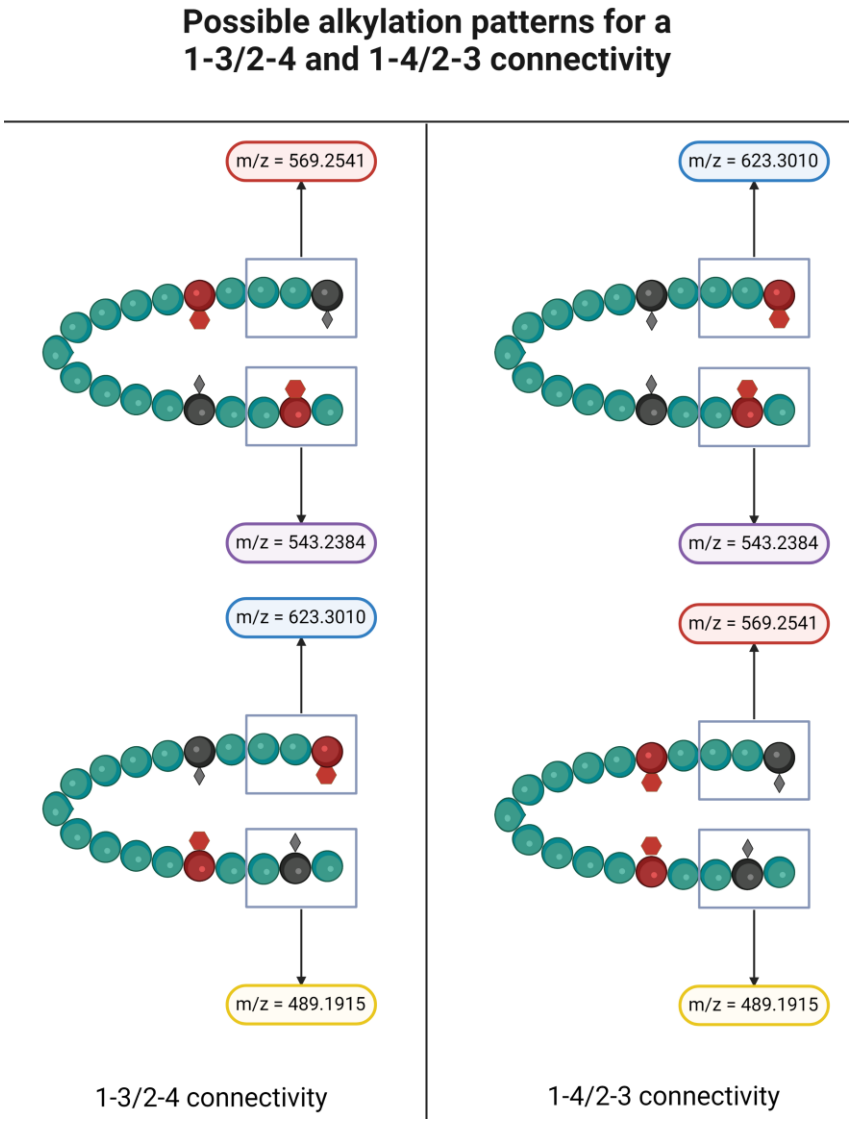

Figure 8: Both possible alkylation patterns for the depicted DRP in both 1-4/2-3 and 1-3/2-4 configurations. Certain fragments are highlighted, and the bubbles around the m/z value is color coded corresponding to the respective m/z values. Created with BioRender.com

Figure 8 illustrates that if a mix of both alkylation patterns is present within the mass spectra, it will be impossible to properly distinguish between a 1-3/2-4 and 1-4/2-3 connectivity.

As explained earlier, a fragment only containing the first or fourth cysteine in the peptide can be used to differentiate between the two isomers. A fragment containing three cysteines can also be used for this purpose, but only fragments containing one cysteine is used for this

explanation. However, this is only the case if there is only one alkylation pattern present in the chromatographic peak. If both alkylation patterns are present, then there are no fragments that can be used to determine which configuration is present. A fragment containing only a single cysteine alkylated with the first maleimide can be found in both configurations, and therefore cannot be used. This is illustrated by the fragment in the purple bubble with an m/z of 543.2384 in Figure 8.

The 1-2/3-4 configuration does, however, still possess unique fragments even when there is a mix of both alkylation patterns and is therefore unaffected by this problem.

The solution to this problem is to separate the two alkylation patterns during the liquid chromatography if they possess differing retention times. Then, a fragment containing one or three cysteines will differ in mass between the two configurations and can therefore be used to determine the disulfide configuration.

3.3 Peptide Synthesis

Peptide synthesis is a process, through a condensation reaction forming amide bonds between the amine and the carboxyl group for two amino acids, in which a peptide is formed. Because every amino acid has both a carboxyl and an amine group, they can bond to another amino acid on either end. An example of how an amide bond between two amino acids is formed is shown in Figure 9.

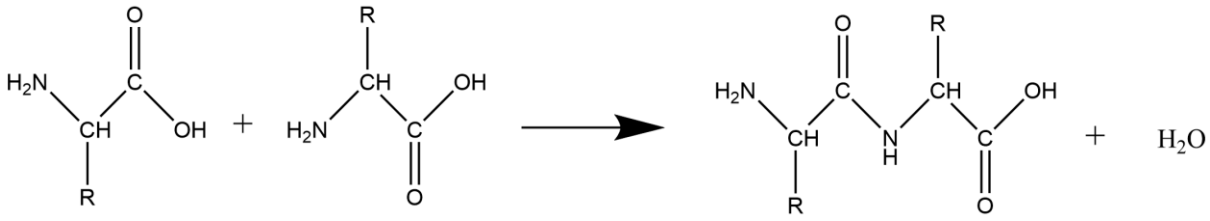

Figure 9: A condensation reaction between two amino acids, forming an amide bond between the two and creating a water molecule. "R" is used in place of the side chain.

It is also necessary to avoid any unwanted reactions, such as the formation of unwanted peptide chains. This is done by protecting the active groups in an amino acid that may cause undesirable

reactions, such as the formation of any unwanted peptide chains between the reagents. Protecting groups will be explained in more detail later in this chapter.

When synthesizing peptides in a research setting, it is necessary to be able to effectively synthesize a peptide with the desired amino acid sequence. A way of achieving this is through solid-phase peptide synthesis (SPSS).

SPSS is a method often used in research settings, as it allows for a relatively simple process with high yields allowing adequate material for conducting studies (16). The principles of an SPSS method are simple. The synthesis takes place within a reactor that contains an insoluble resin, which is a polymer that is used to anchor the peptide chain throughout the synthesis. The first amino acid in the chain is chemically bonded to the resin, and from which point the remainder of the peptide chain is built from that amino acid. The amino acids must through several steps to bond to each other or the resin, which include deprotection, activation, and coupling reactions. Throughout the synthesis the peptide is anchored to the resin. This makes it possible to add a reagent to the reactor, before filtering it away. This happens without any loss of the peptide because it is anchored to the resin and thus not washed away. Measures are taken ensure the selectivity of the desired reactions, i.e., ensuring that the only reaction that can take place is between the carboxyl group of the free amino acid and the amine of the last attached amino acid in the peptide chain. This measure is that the amino acids have protection groups attached to their amines and any other groups in the side chain that may cause undesirable reactions (16, 17). These undesirable reactions include e.g., the carboxyl group of the free amino acids binding to an amine in the side group of an amino acid in the peptide chain, instead of the N-terminal amine.

There are two main approaches to perform SPSS, and this is defined by the choice of protecting group at the amine end of the amino acid. These protecting groups are tert-butoxy-carbonyl (Boc) and fluoren-9-ylmethyloxycarbonyl (Fmoc). The main difference between the two is that Boc requires the use of a strong acid such as trifluoroacetic acid (TFA) to be removed from the amino acids, while the Fmoc group requires the use of a relatively mild base such as piperidine instead (16, 17).

When performing an SPSS method, the choice of both resin and reagents can be changed depending on what is needed. The resin is what keeps the peptide chain from being washed away along with any excess reagent after every step. When the peptide synthesis is finished, the peptide is cleaved from the resin. The resin is a polymer that has the necessary functional groups to bond to the first amino acid. Some of the important characteristics of a resin are that it needs to be mechanically and chemically stable across a range of temperatures and solvents and needs to be able to swell up to 5-6 times. The swelling properties are especially important, as the resin must swell for the amino acids to be able to access its active regions, which is the group that the first amino acid is attached to (16, 17). The resin chosen for this thesis was a H-Rink amide ChemMatrix® resin. and comes with a rink amide linker. The linker is responsible for attaching the amino acid to the resin. It also determines the functional group at the C-terminus of the peptide, which can be either an acid or an amide. Most resins require the use of a strong acid such as TFA for cleavage to occur between the linker and the peptide once the process is finished (16, 17). The linker used in this thesis is rink amide, which produces an amide at the C-terminus.

When the amino acids are attached, the process must go through a deprotection, activation, and coupling reaction. The amino acids used in the synthesis are modified with protecting groups that cover some of their active groups, such as the N-terminal amine and any potential functional groups within the side chain, such as amines or carboxyl groups (16, 17).

The amine of the amino acid backbone is protected by either a Boc or Fmoc group, depending on the choice of approach. The side chains are protected by various groups, each depending on the amino acid and whether the Boc or Fmoc approach is being used. For the Fmoc method, the side groups are protected by acid labile groups, which ensures that they are not removed until the final cleavage process where an acid such as TFA is used (16, 17). Some examples used in this thesis include Boc and Triphenylmethyl (Trt) groups. Boc is used to protect the amine group in lysine, while the Trt group is used to protect the thiol group in the cysteines.

Before an amino acid is attached to either the linker or the previous amino acid, the protection group covering these are removed to expose the active group. This step is crucial, as it allows

the active groups to participate in the subsequent reaction for the next amino acid attachment. Without this deprotection step, the free amino acids cannot form new peptide bonds between them and the linker or peptide chain (16, 17).

The next step is the activation step. This is performed through the addition of a coupling reagent to the carboxyl group. The coupling reagent is used to facilitate the formation of peptide bonds between the free amino acids and linker/peptide chain. The reagent used in this thesis is O-(1H-6-Chlorobenzotriazole-1-yl)-1,1,3,3-tetramethyluronium hexafluorophosphate or as it is more commonly called, HCTU. HCTU works by having a part of the molecule replace one of the two oxygens in the carboxyl groups, which acts as an excellent leaving group. This causes the then-created carbonyl to be more susceptible for nucleophilic attacks from the amine in the linker/peptide chain, and thus form a peptide bond.

After the last amino acid has been attached, the peptide needs to be cleaved from the resin, and any protecting groups protecting the side chains needs to be removed. This is done by using trifluoroacetic acid (TFA), which cleaves not only the bond between the peptide chain and linker, but also any protecting groups such as Boc protecting the side chains of amino acids where necessary. In this process there are formed several reactive cations that form unwanted products by reacting with the peptide. Therefore it is necessary to add “scavengers” to the cleaving cocktail, that will react with any cations that are formed, protecting our peptide from any unwanted reactions (17). In this thesis, water, 1,2-ethandithiol (EDT) and triisopropyl silane (TIS) are used for this task.

3.4 HPLC – High Performance Liquid Chromatography

3.4.1 Introduction

High Performance Liquid chromatography (HPLC) is a method of analysis that is often used in pharmaceutical industry, in medical settings such as hospitals, research in analytical chemistry etc. Its ability to separate compounds within a sample based on their chemical properties makes it an invaluable tool in analytical methods.

In HPLC, compounds are solved in a liquid mobile phase, which is then pumped through a column. The instruments most important components consist of a solvent delivery pump, which provides a steady flow of the mobile phase. Further it contains an injector, which injects the sample that is to be analyzed into the mobile phase. It contains the column, which is responsible for the separation of compounds within the sample. Lastly there is the detector, which generates a response for every compound that elutes from the system. There are several types of the detectors, but some examples include UV detectors which can measure the UV-absorbance of the mobile phase exiting the column. Another example is a mass spectrometer, which is often paired with an HPLC-system (18).

3.4.2 Principles

The time it takes for a compound to travel through the column, is referred to as retention time (Rt), and is the key to separate the different compounds in the sample. The Rt is based on the interaction between the compounds and mobile phase/stationary phase within the column.

There are several types of columns, examples include reverse phase columns and normal phase columns. A reverse phase (RP) column is a column that has a hydrophobic stationary phase, and a common column within this class is a C_{18} column. The stationary phase of a C_{18} column consists of silica particles with octadecyl groups ($-C_{18}H_{37}$) attached. This forms a hydrophobic layer on the particles, and thus classifies it as a RP column. In this type of column, the hydrophobic layer is important in the separation of compounds. A lipophilic compound will have a greater degree of interaction with the stationary phase as it travels through it compared to a more polar compound and will therefore have a longer Rt (18). A normal phase (NP) column is a type of column that has favorable interactions with hydrophilic compounds. A common column in this class is a silica normal phase column. This type of column has a stationary phase that consists of silica particles, but without any groups attached to them. This leaves free -OH groups at their surface, which are responsible for interactions with compounds that enter the column. Normal phase columns give favorable interactions with hydrophilic compounds and cause these compounds to eluate later than more hydrophobic compounds (18).

The mobile phase is one of the most important parts of an HPLC-system. It is responsible for carrying the analyte through the entire system and contribute to the separation of the compounds within a sample. The mobile phases usually used in RP chromatography are water along with one or several organic solvents that are miscible with water. For RP, water is usually denoted as the "Weak mobile phase" while the organic solvents are denoted as the "Strong mobile phase". This is because a lipophilic compound will prefer the hydrophobicity of the stationary phase in an RP column, compared to the highly hydrophilic water. Organic solvents on the other hand, are able to more efficiently break the interaction between a lipophilic compound and the stationary phase as the lipophilic compounds will also interact with them. Some organic solvents are stronger than others, and thus are able to break the interactions more efficiently. Thus, adjusting the proportion and choice of organic solvents used in a mobile phase determines its "strength". A stronger mobile phase will break the interactions between compounds and the stationary phase and result in a shorter Rt (18). Figure 10 shows an example of the importance of adjusting the proportion of acetonitrile (ACN), which is an organic solvent, in the mobile phase

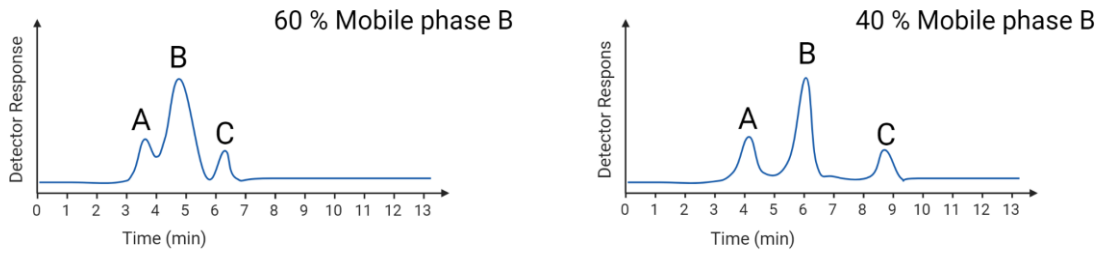

Figure 10: Illustration showing Impact of proportion of mobile phase B in the mobile phase when using isocratic elution. The left chromatogram used a mobile phase consisting of 60 % mobile phase B, while the right chromatogram has a mobile phase consisting of 40 % mobile phase B. Illustration is inspired by figure in "Introduction to pharmaceutical analytical chemistry" (18). Created with BioRender.com

In Figure 10 compounds A and B elute close to each other and are not fully separated from each other when the mobile phase consists of 60 % mobile phase B, as seen in the left chromatogram.

Decreasing the proportion of ACN in the mobile phase to 40 % provides better separation between the two, as seen in the left chromatogram. Some disadvantages of using a weaker mobile phase include an increased time of analysis, which is seen as all three peaks elute later in the left chromatogram. The chromatographic peaks tend to broaden when the time of analysis is increased as well, which is often undesirable.

As explained, choosing the proportion of the strong mobile phase is an important parameter to achieve proper separation of compounds. If the proportion of mobile phase remains the same throughout the process, it is what is known as isocratic elution. However, it is also possible to change the proportion of mobile phases throughout the chromatography. This is what is known as gradient elution. This can be useful to reduce the time of elution for analytes that elute late, while still keeping the analytes that elute early separated (18).

3.4.3 Areas of application

HPLCs have numerous areas of application. Some examples include identification of compounds and purification of compounds, which will be explained in this chapter.

HPLCs can be used to identify compounds within a sample. When running a compound through an HPLC, a lot of information can be gathered that are characteristic of that compound. The Rt should be the same between runs given the conditions of the run stay identical (composition of mobile phase, flow rate, column, temperature etc.). The output from the detector can also be used for identification. A compound may e.g., possess a distinctive UV-absorbance that can be used for identification. Another possibility is to couple it with a mass spectrometer, which will be explained in more detail later in this chapter.

The separation is also useful in processes requiring the purification of a compound from a complex matrix. One such example is using a preparative HPLC to purify an analyte from e.g., biproducts from a synthetic process. As an analyte most likely only elutes within a specific timeframe, it is possible to collect the fraction containing the compound, while discarding the rest. For this purpose, a fraction collector can be used. A fraction collector is an instrument that the mobile phase containing compounds from the HPLC column is sent to. Depending on the settings of the run, the fraction collector can either collect the fraction in a container or discard

it. There are several ways signal the fraction collector to collect the fraction. The criteria for what determines if a fraction is collector or not can be adjusted based on the properties of the peak and/or the matrix. One such method is by using the output or a chromatic peak from a UV-detector. If the signal from the detector reaches a certain threshold or a set time frame, the fraction collector can collect the "chromatographic peak" where the desired analyte elutes, that fulfills the set criteria. An illustration showing how an HPLC can be used for this purpose is shown in Figure 11.

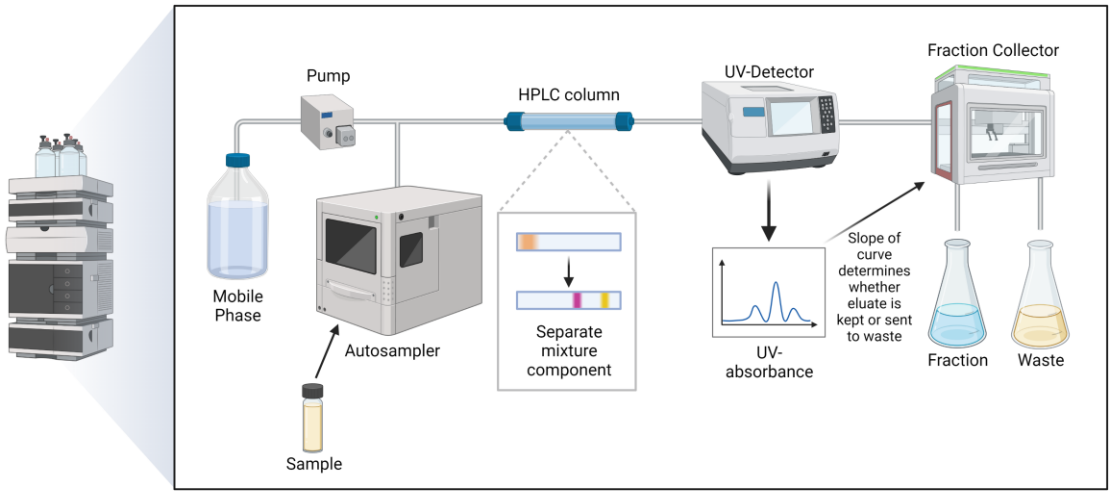

Figure 11: Diagram showing how preparative HPLC can be performed. Adapted from "High Performance Liquid Chromatography (HPLC)", by BioRender.com (2023). Retrieved from https://app.biorender.com/biorender-templates"

HPLCs are also extensively used in combination with mass spectrometers (MS). Not only can a mass spectrometer be used as a detector, but its capabilities are enhanced when used with an LC system. An LC can separate an analyte from the components of the matrix, which if not separated can cause interference such as ion suppression. In the identification of compounds, both the Rt and the m/z ratio can be used to identify a compound (18). If an analyte has/displays matching Rt and m/z for what is known for a given compound, the probability of it being that compound increases compared to if only one of these properties were compared. It is also

possible to differentiate between two analytes with similar retention times, but different mass. A mass spectrometer measures the mass-to-charge ratio, and thus will give a different signal for each compound, allowing the identification of both where it would be difficult if only LC was used (18). Mass spectrometers will be explained in more detail in chapter 3.5.

A variant of HPLC named ultra high performance liquid chromatography (UPLC) has emerged, which is capable of running HPLC at higher pressures. This type of instrument is used in this thesis, and is coupled with the mass spectrometer as well as the PDA detector used in the analysis, which will be explained in further detail in chapter 5.

3.5 Mass spectrometry

3.5.1 Introduction

Mass spectrometry (MS) is a method of analysis that is used in several areas, such as medical research and doping analysis. MS can be used both quantitively to determine the amount of a specific analyte within a sample, or qualitatively to determine the identity of an analyte(18).

In a mass spectrometer, the analytes are measured by their mass-to-charge ratio (m/z). The first step is to ionize the analyte, and the method varies depending on if the system is coupled with liquid or gas chromatography (18). In this thesis, a liquid chromatography mass spectrometry (LCMS) system is used, thus the content of this thesis will focus on LCMS.

In this type of system, a method of ionization known as electrospray ionization (ESI) is often used, as it allows for ionization of analytes within a solution (19). ESI works by spraying the mobile phase through an inlet capillary towards the MS inlet. The inlet has an electrical potential applied between it and the inlet, which leads to the mobile phase forming what is known as a “Taylor cone”. A Taylor cone will release charged droplets containing the analytes, which are headed for the MS inlet. On this path, the droplets are sprayed with a heated sheath gas, which causes the droplets to dry. As the size of the droplets decrease, the space between the charged molecules decreases before what is known as “Coloumbic explosion” occurs. In a coloumbic explosion repulsion between the charged molecules overcome the surface tension and creates several smaller droplets. This continues until all of the mobile phase has dried out,

whose absence creates what is known as “dry ions”, and is necessary for it to be possible to conduct MS (19).

ESI is what is known as a soft ionization method, which means there will not occur a high degree of fragmentation during the ionization process, compared to a hard ionization method such as electron ionization (EI) which is used in gas chromatography mass spectrometry (GCMS) (18). Furthermore, because the ionization will usually lead to either the loss or addition of a proton, the molecular ion that is analyzed will differ by the mass of one proton. If the analyte can obtain several charges, such as a peptide with several side groups that can obtain a charge, the m/z value will change drastically. This is because it is the mass-to-charge ratio that is being measured, not the actual mass of analyte. As an example, an example analyte has a mass of 1000 Da. If it is charged with a single proton, the mass will increase to approximately 1001 Da The mass-to-charge ratio would then be $\frac{m}{z} = \frac{1000\ Da + 1\ Da}{1^+} = 1001$. If the analyte were to gain two electrical charges, the calculation would look like $\frac{m}{z} = \frac{1000\ Da + 2\ Da}{2^+} = 501$, which is a little over half of the m/z ratio when the analyte only had a single charge. This also applies if an analyte loses a proton, only that the mass for the proton is subtracted. Other adducts can also be formed, such as sodium adducts, which will add a mass of 22.99 Da to the analyte(18).

There are several types of mass spectrometers, both with their strengths and weaknesses. The instrument that is used in this thesis is a Thermo IdX Tribrid Orbitrap, but other mass spectrometers such as triple quadrupole (TQ) or Time of Flight (ToF) instruments are also commonly used.

3.5.2 Triple Quadrupole (TQ) Mass Spectrometers

3.5.2.1 Introduction and areas of application

A TQ consists of three quadrupoles, as the name suggests. A quadrupole is a mass filter that consists of four rods that are placed in parallel. These rods have a constant voltage and a radio frequency oscillating voltage applied to them, with one pair having a positive- and the other a negative voltage applied (18). TQs are used extensively in the quantification of known analytes within a sample, such as the quantifying the concentration of a drug in the blood plasma of a

patient. This is because of the good sensitivity and large linear range for the signal of an analyte that a TQ can offer.

3.5.2.2 Mechanism and areas

The constant voltage and radio frequency oscillating voltage applied to the rods creates an electrical field in which ions move in complex trajectories based on their m/z ratio and the voltage of the rods. In this way it is possible to only allow ions with a certain m/z value to pass and reach either a detector or the next compartment, while the rest collide with the rods and thus are lost. By rapidly varying the voltages, it is possible to allow either a wide range or only certain m/z values to pass through the quadrupole, both which are useful depending on the purpose of the analysis (18).

The three quadrupoles that make up a TQ are often denoted as Q1, Q2 and Q3. Q1 and Q3 are quadrupoles as described in the last paragraph, while Q2 functions as a collision cell. Here the analytes that are passed through Q1 collide with an inert gas, usually N_2 or Ar. This collision can cause a fragmentation of the ions, which are then passed on through to Q3. The product ions form from a specific compound are characteristic for that compound and can thus be used in the identification of a compound. It is then possible to further filter ions and fragments with specific m/z values to pass, effectively eliminating background noise and enhance the sensitivity for the analyte (18).

3.5.2.3 Limitations

While TQs are extensively used in quantitative analysis, their use in qualitative analysis is limited due to the instrument not being able to measure m/z ratios at high resolution and mass accuracy (20). Being able to measure m/z ratios at higher resolutions means that the instrument can differentiate between ions with small differences in m/z (18). A theoretical example would be N_2 and CO, that have monoisotopic masses of 28.06147 and 27.994915 respectively. An instrument that can measure m/z ratios at higher resolutions would be able to differentiate between the two, while an instrument with a lower resolution would measure both as 28.0 (18). Sensitivity in full scan is also limited, due to scanning over a wide range of m/z values causes a significant loss of ions within the sample. Because of this, background noise can be an issue

(20). Therefore, in these types of analysis other types of mass spectrometers are more useful, such as ToFs (Time-of-flight) or Orbitraps. Their properties will be explained in their respective chapters.

3.5.3 Linear Ion Trap (LIT)

3.5.3.1 introduction and areas of application

A linear ion trap is a type of mass analyzer. They are versatile devices, in that they allow for m/z measurements, fragmentation, and storage of ions. Thus, they can be either used alone, or be coupled with other mass analyzers like an orbitrap (19).

3.5.3.2 Mechanism

A linear ion trap (LIT) is built similar to a triple quadrupole in that it consists of four rods with RF potentials applied to them. However, a linear ion trap has additional electrodes at the entrance and exit. The potential applied to the quadrupole-like rods allow them to focus the ions between them along the x- and y-axis, and the potential applied to the entrance and exit electrodes controls the movement of ions along the z-axis (19).

An ion trap can perform what is known as collision-induced dissociation (CID). This is done by changing the voltage so ions with a certain m/z value oscillate within the ion trap. This way, it is possible to cause fragmentation of only certain ions. Within the ion trap, there are gas molecules like He present, which the ions collide with during the oscillation. This collision causes energy to be transferred, which in turn can break bonds within the ion. If fragmentation occurs, then the m/z value is changed, and the ion will no longer oscillate. If needed, the fragmentation can be repeated for the generation of MS^n spectra, where the n denotes the amount of fragmentations that have been performed (19).

3.5.3.3 Limitations

The weakness of an ion trap is that it has low resolution and mass accuracy. They are not especially suited for quantifications as well, due to a larger number of ions affecting the performance (20).

3.5.4 Orbitrap

3.5.4.1 Introduction

Orbitrap instruments are of a newer technology compared to triple quadrupoles and TOFs and have certain advantages over both types of instruments. Orbitrap instruments give high mass accuracy and can give very high resolution spectra (depending on instrument version), and as such they are especially useful in the identification of compounds within a complex sample(18, 20). An example of a complex sample can be a biological sample, where there are several near isobaric compounds. A high resolution instrument like an orbitrap are also valuable tools within protein analysis (20).

3.5.4.2 Mechanism

An orbitrap consists of three electrodes. These are a central electrode and two outer electrodes. The electrodes generate an electrostatic field which causes ions to orbit around the central electrode. The ions move around the central electrode in a stable circular orbit, but in the z axis the ions move in harmonic oscillations. Because of the shape of the electrodes the movement in the z-axis is independent of movements around the central electrode and is solely dependent on the m/z of the ion. These are determined by complex equations that are outside the scope of this thesis (19, 20). A figure showing an example orbitrap is shown in Figure 12.

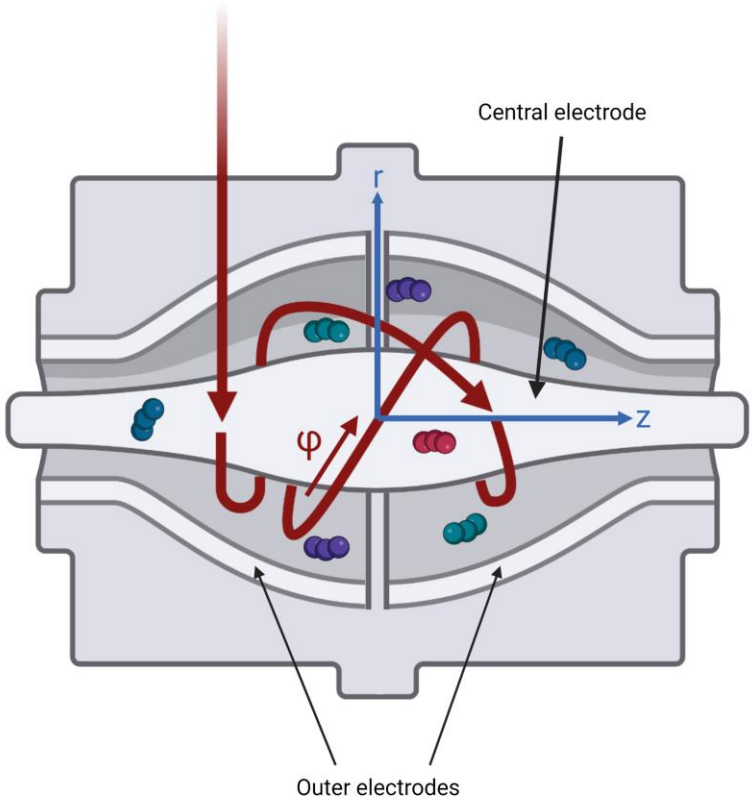

Figure 12: Illustration of an orbitrap. r and z denote the directions of the ions, while φ denotes the movement of the ions. Created with BioRender.com

3.5.4.3 Limitations

The resolution of an orbitrap can be adjusted depending on what is required by the analysis. However, an increase in resolution leads to an increase in the time of analysis as well (19). Further, while they can be used in quantitative analyses, they do not offer the same linear range and sensitivity as a triple quadrupole operating with an MRM method.

3.5.4.4 Orbitrap Id-X

Orbitraps are often used with other components such as an ion trap to further enhance its capabilities. One such example is the Orbitrap Id-X Tribrid mass spectrometer from Thermo Scientific, which is used in this thesis and is shown in Figure 13.

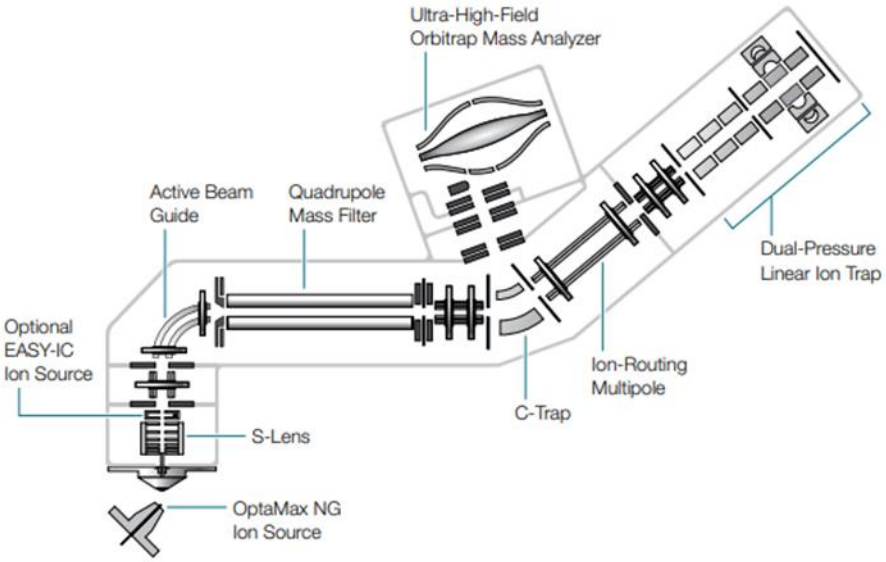

Figure 13: Diagram showing the components of an Orbitrap Id-X Tribrid Mass Spectrometer. Retrieved from Thermo Scientific (21).

The instrument contains a quadrupole mass filter, an orbitrap mass analyzer and an ion trap. The ions are sent through to the quadrupole, with the help of the S-Lens and Active beam guide. The quadrupole can be used like in a triple quadrupole to only allow ions with a certain mass to pass through, only in this case they reach the C-trap instead of another quadrupole or the detector. The C-trap collects and cools the ions sent through the quadrupole and can send it to the orbitrap at regular intervals, where their m/z value is measured (21).

The c-trap can also send selected ions through the ion-routing multipole for further analysis. The ions can be selected automatically through certain criteria, such as the ions with the highest signal in the previous mass spectrum in the orbitrap. In the ion routing multipole, higher-energy collisional dissociation (HCD) can be performed. HCD is a method of fragmentation that works by colliding gas molecules such as N_2 or He at higher kinetic energies (22). The gas molecules collide with the ions, which leads to a transfer of energy. This can cause fragmentation between the weaker bonds in an analyte. An analyte can fragment several times during HCD, as the

movement of the fragment ions is not controlled and they continue colliding with the collision gas also after the initial fragmentation (21).

As described in chapter 3.5.3, the linear ion trap can both fragment and measure the m/z of ions. This makes it possible to perform what is known as tandem mass spectrometry. Tandem mass spectrometry is performed by selective fragmentation of a single ion based on its m/z. The mass spectra that are generated contains information about the fragments that the ion forms and can be used for identification of the ion (19, 20). The ion trap can perform CID on ions with specific m/z ratios, allowing for control over the number of fragmentations that occur. This allows for the generation of MS^n spectra, where the n denotes the number of fragmentations that the ions have undergone. These ions can either be measured in the ion trap or sent back to the orbitrap (21). The measurements made in the ion trap will be made faster as they do not have to travel back to the orbitrap, but they lack the mass accuracy or resolution that the orbitrap provides.

The elucidation of disulfide bonds requires the identification of specific fragments, in which a high-resolution mass spectrometer with sufficient mass accuracy like an orbitrap is useful. Several potential fragments might have similar masses. As an example, a potential fragment from one of the peptides has an m/z value of 448,8173, whilst another has an m/z value of 448.7334. It is necessary to distinguish between these two potential fragments to avoid any uncertainty of our results.

3.5.5 Peptide fragmentation in mass spectrometry

When peptides undergo fragmentation in a e.g., collision cell or ion trap in a mass spectrometer, they typically produce specific types of fragment ions known as a-, b-, c-, x-, y-, and z-ions. These ions are product ions that form when a bond in the peptide backbone is broken, and the type of ion is determined by the position of the broken bond and which side ends up keeping the charge, if the peptide only has a single charge. Figure 14 illustrates what ions are formed

depending on the position of the broken bond when the peptide undergoes fragmentation.

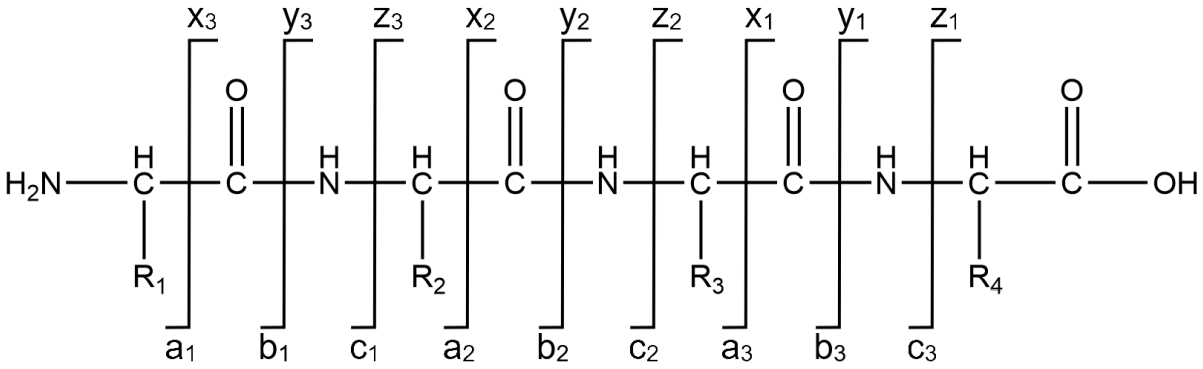

Figure 14: Example peptide with 4 amino acids. $R_{1\text{-}4}$ are used in place of the side chains. The lines indicate what types of ions are formed if the bond that it overlaps is broken during the fragmentation process, and the direction indicates what side keeps the charge when that type of ion is formed.

a-, b-, and c-ions are formed if the charge is kept at the side containing the N-terminus of the peptide after fragmentation, while x-, y-, and z-ions are formed if the side containing the C-terminus keeps the charge after fragmentation. If for example the amide bond between the first and second amino acid is broken, then either a b_1 or y_3 ion will form, depending on which side keeps the charge. The remaining side will then become a neutral loss and will not show up in the mass spectrometer as it has no charge. However, this is only the case if the peptide has a single charge. If the peptide obtains 2 charges during the ionization process, then there are two possibilities. The first is that both sides keep a charge each, and both a b_1 and y_3 ion is formed. The second is that a single side keeps both charges, creating either a b_1 or y_3 ion with two charges. What ions that form the most frequently vary, and depend on the amino acid sequence and method of fragmentation (23).

The information gained from mainly b- and y-ions can be used to determine the sequence of a peptide through tandem mass spectrometry. Tandem mass spectrometry is performed by selectively fragmenting ions with a certain m/z (peptide ions in this case) and measuring what fragment ions are formed. A way to sequence the peptide is by examining the b-ions. The first amino acid's identity can be determined by examining the m/z value of a b_1 ion, if present. Then, if the b_2 ion is present, it is possible to examine the difference between the m/z values for the b_1 and b_2 ions, and thus determine the mass and therefore identity of the second amino acid (23). A theoretical example is shown in Figure 15.

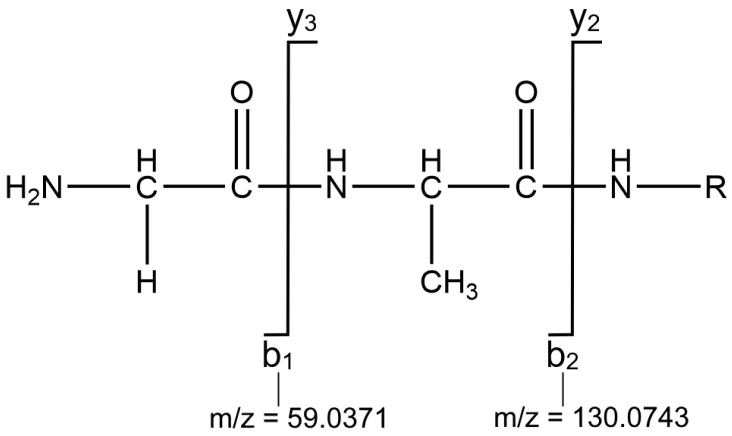

Figure 15: Theoretical example that uses a peptide with glycine (G) and alanine (A) as the two first amino acids. The R in the figure is used as a stand in for the rest of the sequence.

In Figure 15, it is possible to determine the identity of the first amino acid, by examining the m/z value of 59.0371, which is the expected m/z of a glycine when the mass of an oxygen is subtracted. Then, to identify the next amino acid the difference in m/z between b_1 and b_2 is calculated. . The difference matches up to the expected m/z of an alanine, minus an oxygen and a hydrogen atom that was lost during the formation of a peptide bond.

3.6 Bioactivity testing

One of the goals of this thesis is to study the impact that substituting the amino acids have on the antimicrobial activity of the peptide. This can be done by measuring the minimum inhibitory concentration (MIC) of a compound, which is the lowest concentration at which the compound inhibits bacterial growth. MIC is used as a measure for how susceptible a microbe is to an antibiotic, and a lower concentration suggests that the bacteria are more susceptible to the antibiotic (15). In this thesis, the peptides and their respective isomers are tested against 5 different bacterial strains, which are summarized in Table 1.

Table 1: The bacterial strains that the peptides were tested against.

Species	**Short name**	**Strain**
Gram-negative		
Escherichia coli	E.C.	ATCC 25922
Pseudomonas aeruginosa	P.A.	ATCC 27853
Gram-positive		
Corynebacterium glutamicum	C.G.	ATCC 13032
Staphylococcus aureus	S.A.	ATCC 9144
Staphylococcus epidermis	S.E.	RP62A
Bacillus subtilis	B.S.	ATCC 23857

E.C. is a species of gram-negative bacteria within the *Enterobacteriaceae* family and is an important part of the gut flora in humans. Despite this, it can cause infections such as urinary tract infections and are a growing threat as antibiotic resistant E.C. strains are becoming more prevalent (24). S.A. is a gram-positive bacteria that can be found in the normal flora in humans, and can cause infections such as local skin infections and pneumonia (25). An especially problematic type of S.A. known a methicillin-resistant *S. aureus* (MRSA) has risen in prevalence in later years, with some strains displaying resistance to several type of beta-lactams and other common antibiotics such as trimethoprim (26). C.G. is a species of gram-positive bacteria that is utilized in the production of L-amino acids such as L-Lysine (27). P.A. is a gram positive bacteria and is a common cause of infections in human such as UTIs or skin infections (28). It is well equipped to adapt to a variety of environments which causes it to cause opportunistic infections and allows for the emergence of antibiotic resistant strains (29). *Bacillus subtilis* is a gram-positive bacterium which is commonly found in sewage treatment reactors. It is thought to be one of the most important carriers of genes containing antibiotic resistance mechanisms, and often show resistance against various types of antibiotics (30). At last, S.E. is a species of gram-positive bacterium like S.A., but is an important part in the normal flora in humans. *Staphylococci* is commonly found in the skin and in mucous membranes in humans, with S.E. being the most frequently isolated species. While it is usually harmless to humans, it may cause opportunistic infections such as nosocomial infections through indwelling medical devices (31).

From a study in 2022, E.C., S.A., and P.A. were among the 6 leading pathogens that were associated with deaths attributable to AMR (3). They are therefore especially of interest when developing new antibiotics.

4 Aims of the thesis

The aim of the thesis was to develop a method for synthesis and structure elucidation of disulfide rich peptides, as well as improving antimicrobial activity by peptide modifications. To accomplish the main aim of the thesis several sub-goals were set:

- Synthesis of new peptide analogues with different disulfide connectivity patterns
- Developing a method for sequential reduction and alkylation for structure elucidation
- Developing analytical methods and interpret mass spectrometric results for identifying disulfide connectivity
- Evaluate the impact of both substitution of amino acids and disulfide connectivity patterns on antimicrobial activity for the peptides in this study

5 Materials and methods

5.1 Peptide synthesis

5.1.1 Chemicals

Table 2 provides a summary of the chemicals used in the peptide synthesis.

Table 2: List of chemicals used during the peptide synthesis.

Chemicals	Purity (%)	CAS-number	Supplier
Fmoc-Lys(Boc)-OH	≥ 97.0 % (HPLC), ≥ 98 % (TLC)	71989-26-9	Novabiochem®, Darmstad, Germany
Fmoc-Leu-OH	≥ 97.0 %	35661-60-0	Sigma-Aldrich®, Burlington, Massachusetts
Fmoc-Cys(Trt)-OH	≥ 95.0 % (sum of enantiomers, HPLC)	103213-32-7	Sigma-Aldrich®
Fmoc-Pro-OH	≥ 99.0 % (HPLC)	71989-31-6	Sigma-Aldrich®
Fmoc-Ala-OH	95 %	35661-39-3	Sigma-Aldrich®
Fmoc-Gly-OH	≥ 98.0 % (T)	29022-11-5	Sigma-Aldrich®
Fmoc-Arg(Pbf)-OH	≥ 98.0 % (HPLC)	154445-77-9	Sigma-Aldrich®
HCTU	≥ 98 % (HPLC)	330645-87-9	Novabiochem®
H-Rink amide ChemMatrix® resin			Sigma-Aldrich®
N,N-Dimethylformamide	≥ 99.8 %	68-12-2	Sigma-Aldrich®
N-Methyl-2-pyrrolidinone	≥ 99.0 %	872-50-4	Sigma-Aldrich®
Trifluoroacetic Acid	≥ 99 %	76-05-1	Sigma-Aldrich®
1,2-ethandithiol	≥ 98.0 %	540-63-6	Sigma-Aldrich®
Triisopropyl silane	99 %	6485-79-6	Sigma-Aldrich®
N,N-Diisopropylethylamine	≥ 99%	7087-68-5	Sigma-Aldrich®
Dichloromethane	≥ 99.8 %	75-09-2	Sigma-Aldrich®
Trifluoroacetic Acid	≥ 99 %	76-05-1	Sigma-Aldrich®
Acetonitrile	99.95 %	75-05-8	VWR, Radnor, Pennsylvania
Ultrapure water from a Puranity UV 15+			VWR
Diethyl ether	100 %	60-29-7	VWR
Piperidine	99 %	110-89-4	Sigma-Aldrich®

5.1.2 Weighing and dissolution of the necessary chemicals

The peptide synthesis was performed using a Biotage® Initiator+ Alstra™ with an Fmoc-protocol. The sequence as well as the conditions of the synthesis were programmed to the instrument. From this information, a calculation table that listed the necessary amounts of amino acids and other chemicals to synthesize 330 mg of peptide was generated. These amounts were 4 mole equivalents of most chemicals, and 8 mole equivalents of DIEA of what was needed synthesize 330 mg of the peptides. This information was then exported to a sequence summary file for both peptides, as well as a report once the synthesis had finished. Both can be found for Turg_JK_1 in the appendix 10.1.1. Unfortunately, as the power went out during the synthesis of Turg_JK_2, no report was generated, so only the calculation table is in the appendix in chapter 10.1.2.

The amino acids, HCTU and Resin were kept at room temperature for at least 30 minutes before weighing. The plastic vials and spatula used in the weighing process were placed on the scale before taring, except for the resin. The resin was weighed in the cartridge that was to be inserted into the peptide synthesis reactor. The amino acids and HCTU were then dissolved in N,N-Dimethylformamide (DMF) using the spatula used during the weighing process. N,N-Diisopropylethylamine (DIEA) was also measured by volume and dissolved in NMP (N-Methyl-2-pyrrolidinone). The vials were then placed according to the diagram generated in the calculation table.

The resin was set to pre-swelling before the peptide synthesis. This is done to ensure sufficient swelling of the resin before the synthesis, so the reagents and peptide have ample access to the active part of the resin and are not sterically hindered (17). The cartridge containing the resin was set on top of a vacuum manifold with the valve closed before DCM is added until it covered the whole resin and was left for 20 minutes. After this the DCM was removed by creating a vacuum inside the manifold and opening the valve.

5.1.3 Instrumentation

The loop systems containing DMF (S1) and N-Methyl-2-pyrrolidone (NMP) S2 were primed three times each to remove any air in the tubing. The synthesis was then initiated and lasted about 24 hours for both peptides.

5.1.4 Cleavage and extraction from resin

When the peptide synthesis is complete, the cartridge containing the resin and crude peptide was removed from the reactor. It is necessary to cleave the peptide crude from the resin and separate it to another container, which is the purpose of this process. The cleavage and extraction of the peptide crude from the resin is illustrated in Figure 16, and is used in the explanation.

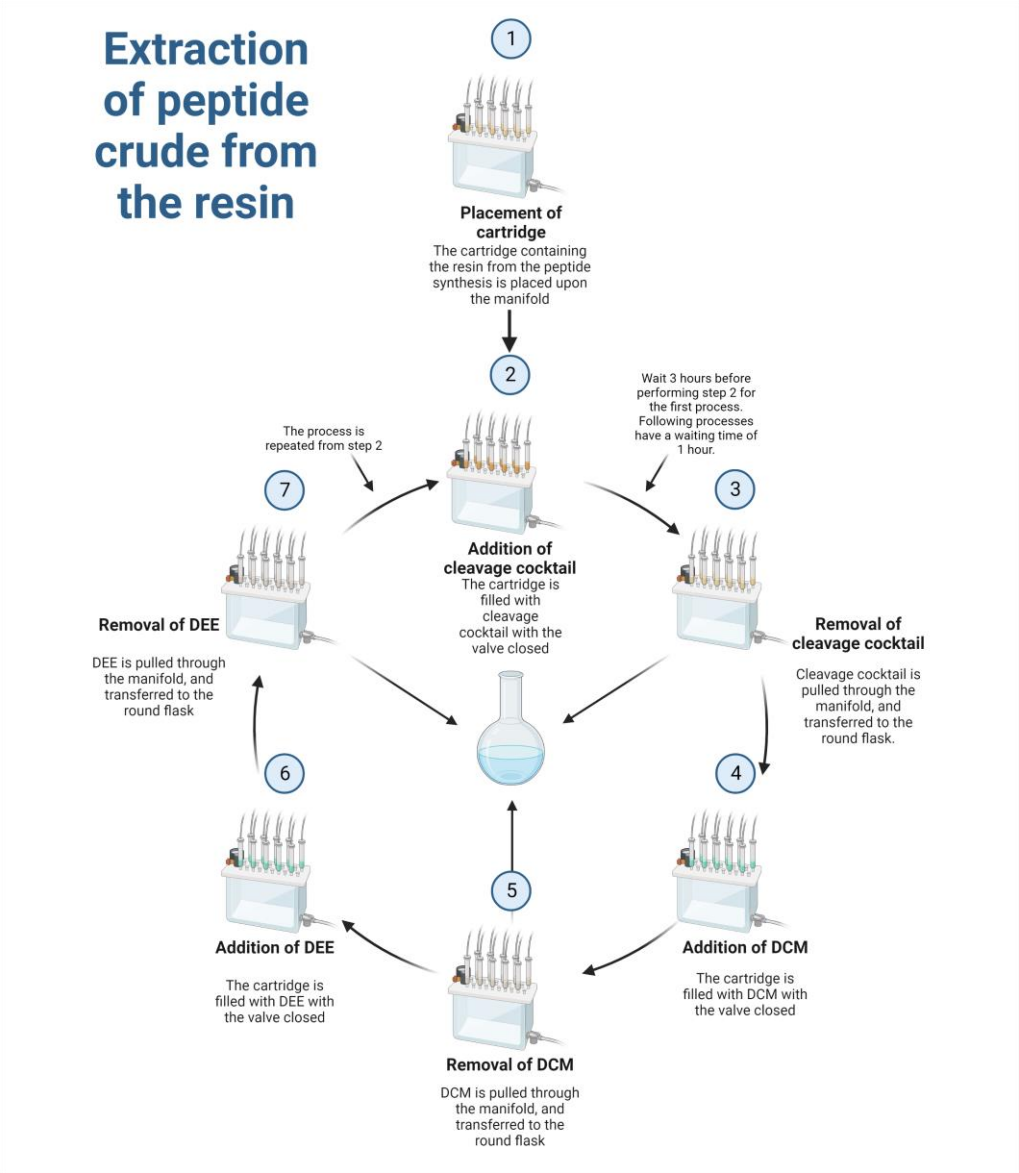

Figure 16: Figure describing the cleavage process of peptide crude from the resin after the peptide synthesis. Created with BioRender.com

In step 1, the cartridge was placed on top of a Supelco. Visiprep™ SPE Vacuum Manifold vacuum manifold with the valve closed. The cleavage cocktail was then made in a 10 mL measuring cylinder, before being transferred to the cartridge by using a glass pipette in step 2. The cleavage cocktail consisted of 9.4 mL TFA, 0.25 mL ultrapure water, 0.25 mL EDT and

0.1 mL TIS. All of the water used in this thesis is ultrapure water, unless otherwise specified. The cartridge was then left for an hour before step 3 was performed, to ensure that ample time was given to cleave the bond between the peptide and the resin. In step 3 vacuum was turned on inside the manifold, and the valve was opened, resulting in the cocktail being pulled through the manifold. This liquid was pulled through and into a glass tube inside the manifold. The vacuum was then turned off, and the eluate was transferred to a 250 mL round flask. Next in step 4 the valve was closed again, and the cartridge was filled with DCM, which caused the resin to collapse and drastically decrease in volume. The DCM was then pulled through the manifold in step 5, and the eluate was transferred to the same round flask as earlier. For step 6 the valve was closed again, and the cartridge was filled with DEE which was then in step 7 pulled through the manifold and transferred to the round flask in the same way. During these processes, parts of the peptide crude end up dissolving in the cleavage cocktail, DCM, and DEE, and it is therefore necessary to transfer these over to the round flask after extraction.

After step 7, the process was repeated from step 2. Another 10 mL of cleaving cocktail was made and transferred over to the cartridge after closing the valve on the manifold. It was then left for 3 hours this time, with stirring taking place every hour using the same glass pipette used in the transfer of the cleaving cocktail. After three hours step 3 was performed as earlier. Steps 4-7 were then repeated as earlier.

5.1.5 Further preparation of the crude peptide

The extract in the round flask from the previous process was then evaporated using a Büchi Rotavapor R-124, while the flask was partly submerged in tap water with a temperature of about 38-40 °C until all the liquid had evaporated. The round flask was removed from the rotavapor, and ice-cold DEE was added to the round flask until it was about half-full. The flask was stirred by moving the flask in a circular motion, and the stopper was placed on top and the flask is left overnight. The crude for both peptides formed a precipitation at the bottom of the flask.

The next day as much DEE as possible was removed by using a glass pipette with a volume of about 40 mL. The crude at the bottom of the flask should not be removed during this process. After this, ice-cold DEE was added until the flask is about half-full and was left for 2 hours.

The process was repeated, removing as much DEE as possible and adding new ice-cold DEE. As much DEE as possible was removed when 2 hours had passed once more. The remaining DEE was then evaporated using a rotavapor. During this the flask was not submerged in water. The rotavapor was left on until the peptide crude was dry and grainy. When the evaporation process was finished, the flask was removed and left without the stopper on to dry overnight in a fume hood.

5.1.6 Purity Analysis

The purity analysis used a Waters Acquity UPLC Sample Manager – FTN coupled with a Waters Acquity Quaternary Solvent Manager, with Acquity BEH C18 1.7µm 2.1x50 mm Column and a Waters Acquity PDA Detector.

After the evaporation, 1 mg of peptide crude was weighed and dissolved in 1 mL of water with 0.1 % TFA. This was then vortexed and centrifuged, before 25 µL was pipetted and diluted to 100 µL water with 5 % acetonitrile (ACN) and 0.1 % TFA. This was further injected into a Waters Quaternary Solvent manager that used the two mobile phases A (Water with 0.1 % TFA) and -B (ACN with 0.1 % TFA). The flow rate was set to 0.5 mL/min with a gradient of 0.5 % to 99.5 % mobile phase B over 10 minutes. The PDA detector was set to measure at x nm.

5.2 Sample preparation of the crude

5.2.1 Instrumentation, chemicals, and methodology

Table 3 provides a summary of the chemicals used in the peptide synthesis.

Table 3: List of chemicals used in the sample preparation of the crude.

Chemicals	Purity (%)	CAS-number	Supplier
Trifluoroacetic Acid	≥ 99 %	76-05-1	Sigma-Aldrich®
Ultrapure water			VWR
Acetonitrile	99.95 %	75-05-8	VWR
Methanol	≥ 99.9 %	67-56-1	VWR
Formic Acid	> 99 %	64-18-6	Thermo Fisher Scientific™

The peptide crude had to be purified to remove any biproducts or other contaminants before further preparation of the peptide could take place. The preparative HPLC was fitted with a pump Waters 1525 Binary HPLC Pump, a Waters 2998 Photodiode Array Detector (PDA), a Waters Fraction Collector III and a Waters 2707 Autosampler. The PDA detector was set to measure at 214 and 254 nm. Mobile phase A consisted of 0.1 % TFA in H_2O and mobile phase B of 950 mL ACN, 50 mL H_2O and 1 mL TFA. The needle wash consisted of 80% methanol and 20% water. The HPLC used a SunFire® Prep C18™ 5µm 19x250 mm column.

The gradients of mobile phase used during the purification process for both peptide crudes were determined experimentally. This was done by testing several gradients while injecting some of the dissolved peptide crude into the HPLC. The methods used were the ones that were found to best separate the chromatographic peak determined to contain the peptide from other contaminants. The peak containing the peptide was determined by analyzing each fraction that was collected by mass spectrometry.

Mass spectrometry was performed using a Thermo Scientific Id-X Tribrid Orbitrap, coupled with a Thermo Scientific Vanquish Autosampler and UPLC Pump., with an Acquity Premier BEH C_{18}, 1.7 µm, 2.1 x 100 mm column. The mobile phases used by the UPLC mobile phase A which consisted of water with 0.1 % formic acid (FA) and mobile phase B consisted of 95 % ACN, 5 % water and 0.1 % FA. The gradient was set from 0.5 % to 95 % Mobile phase B over 10 minutes. The column temperature was set to 60 °C, and the left preheater was set to 50 °C. The MS method was a data-dependent acquisition in which a full scan was performed, and the ions with the highest signals were then selected for fragmentation and were scanned in the orbitrap to generate MS^2 spectra. The resolution for each full scan was 120 000 and for the ms^2 scans it was 30 000. The full list of parameters can be found in Table 12 in chapter 10.2 in the appendix.

5.2.2 Turg_JK_1

In the final method for Turg_JK_1 about 10 mg of peptide crude was dissolved in 200 µL ACN and 800 mL H_2O in an Eppendorf-tube, which were pipetted using an Eppendorf Research plus pipette. Each sample was vortexed with a VELP SCIENTIFICA WIZARD IR Infrared Vortex Mixer for about 4 minutes, and then centrifuged with a VWR® MiniStar silverline microcentrifuge for about 15 minutes. The equipment listed in this paragraph was used for the rest of this thesis, unless otherwise specified. Even after using the vortexer for several minutes, there was a precipitate at the bottom of the tube. However, there was observed a greater output from the UV-detector for the peak containing the peptide when weighing in increased amounts of the crude, suggesting an increased concentration of the peptide despite the formation of the precipitate. This may suggest that the precipitate consists of a biproduct from the peptide synthesis. The precipitate did not dissolve in 100 % DMF either. The total flow of mobile phase was set to 10 mL/minute. The gradient for mobile phase B used during the chromatography was a starting concentration of 20 % which was linearly increased to 30 % over a timeframe of 25 minutes. Then, the system was set to equilibrate the column by changing the concentration of mobile phase B for 10 minutes to prepare it for further injections. The collector was set to measure the slope of the PDA-detector, which was measuring wavelengths at 214 and 254 nm. This was found to make the fraction collector collect 3-4 fractions. From analysis through mass spectrometry, the 1st and 2nd fractions contained unknown contaminants. The 3rd fraction contained a peptide that was missing the first cysteine group, suggesting difficulty attaching this cysteine group during the peptide synthesis as it is attached last. The 4th fraction contained the linear peptide, which was then isolated and later oxidized.

5.2.3 Turg_JK_2

For Turg_JK_2 the same method was used as for Turg_JK_1, with some differences. The first being that the mobile phase used a linear gradient of 20-25 % mobile phase B in a time frame of 25 minutes. Like for Turg_JK_1 the column was then equilibrated for 10 minutes by changing the gradient to 20 % mobile phase B to prepare it for further injections. The total flow of mobile phase was set to 10 mL/minute. Unlike Turg_JK_1, the crude dissolved almost completely. Unfortunately, the chromatographic peak containing the peptide co-eluted with a

contaminant in the solution. We were not able to completely solve this issue, but the degree of co-elution was decreased as much as possible.

5.2.4 Freeze-drying of the fractions

Both peptides went through the sample preparation until there was about 50 mg of the crude left in each round flask. This was stored for later studies. The fractions that contained the peptide were placed in plastic tubes with filter paper beneath a lid with holes in it. The plastic tubes were placed in the freezer at -82 °C for at least three hours. The plastic tubes were then placed in the freeze dryer for about 3 days, ensuring the removal of all water.

5.3 Oxidation process

5.3.1 Instrumentation, chemicals, and methodology

Table 4: Table listing the chemicals used in the oxidation process.

Chemicals	Purity (%)	CAS-number	Supplier
Ultrapure Water from a Puranity PU 15 UV+			VWR
Acetonitrile	0.9995	75-05-8	VWR Chemicals
Methanol	≥ 99.9 %	67-56-1	VWR Chemicals
Formic Acid	> 99 %	64-18-6	Thermo Scientific™

Each peptide was oxidized in parallels of 5 mg each. This amount was chosen due to previous work finding it to be a suitable amount where polymerization is unlikely to occur, but large enough so that the process is efficient. Polymerization would make it impossible for further studies of the peptides. Therefore, should this occur in a parallel, only that parallel would be affected. The linear peptide was weighed in plastic tubes. The peptides were dissolved in 20 mL of H_2O in glass tubes while being subjected to stirring by magnet. The transfer of the peptide was done as slowly as possible, to avoid polymerization of the peptide. The plastic tube containing the linear peptide was washed with water to ensure that the linear peptide was completely transferred to the water in the glass tube. The upper edges of the glass tube were also rinsed with water ensuring that nothing was left above the water surface.

Each of the glass tubes were placed on a rack. In order to supply each parallel with oxygen, aplastic tubing was attached to an oxygen tank. The tubing was then split using y-splitters to make sure that every parallel is supplied with oxygen. At the end of each plastic tube a glass Pasteur pipette was attached and submerged into the glass tubes containing the peptide. To monitor the oxidation process, samples were taken out of each parallel during the process and analyzed using MS with the same instrument and method used in chapter 5.2.1, except that an Acquity Premier HSS T3 1.8µm 2.1x100 mm column was used in the UPLC for some of the samples. The oxidation continued until the signal for the mass of the linear peptide and any intermediate products had disappeared. The oxidized peptides are expected to create three chromatographic peaks, each corresponding to an isomer of the oxidized peptide with differing disulfide connectivity. As discussed in chapter 3.2.1, this is because of both peptides containing 4 cysteine amino acids. This gives us 3 possible configurations of disulfide connectivity.

5.3.2 Freeze-drying of the oxidized peptides

When the oxidation process was deemed complete, the water containing the oxidized peptide isomers in each parallel was transferred to a plastic tube with filter paper beneath a lid with holes in it. These were placed in the freezer at -82 °C for at least three hours, before they were placed in the freeze-dryer for about three days.

5.4 Separation of the isomers of the oxidized peptide

5.4.1 Instrumentation, chemicals, and methodology

The instrumentation, chemicals and methodology were the same as used in chapter 2.3.1.

5.4.2 Turg_JK_1

The peptide was purified in batches of 1 mg per injection, due to difficulties separating the suspected isomers at larger amounts. Like for the linear version of the peptide, each batch was dissolved in 200 µL ACN and 800 µL water. The initial gradient of mobile phase B used during the chromatography started at 20 % and was increased to 25 % over 25 minutes. The fraction collector was set to collect each fraction at set time intervals. This was due to the fact that there was not sufficient signal at every chromatographic peak to collect using the “slope” setting.

After performing liquid chromatography, the oxidized peptide displayed 5 chromatographic peaks. Peaks 2 and 3 eluted very close to each other, with the same applying to peaks 4 and 5 as well. At first this was suspected to be due to each isomer creating two conformers, by having the same disulfide connectivity, but with the spatial orientation of each amino acid being slightly different. This was however proven to be unlikely and may rather have been caused by the peptide forming an adduct with the TFA in the mobile phase. This splitting was not present during the MS analysis, in which a mobile phase with formic acid was used rather than TFA.

During the preparation of the last oxidized parallel the conditions of the runs were changed. This was done to solve the problem of the splitting peaks. During the dissolution of the oxidized peptide, 10 µL of a 10 % TFA solution was added to the sample and was left for 10 minutes before injection through the autosampler. Further, a gradient of mobile phase B starting at 20 % and ending at 40 % over 25 minutes was used, rather than 20 % to 25 % like earlier parallels. Likely because of the added TFA before the run, there was no longer any splitting observed in any of the chromatographic peaks. Instead, three chromatographic peaks were observed. We theorize that this may be because of the TFA forming the adduct with the peptide before the chromatography, causing only one peak to form. However, the first peak containing the first isomer flattened dramatically compared to earlier. MS analysis of the fraction collected at the expected timeframe from earlier runs proved the isomer to be present in the fraction, but the peak was widened over a timespan over several minutes, for unknown reasons.

5.4.3 Turg_JK_2

For the oxidized isomers of Turg_JK_2 unfortunately, no method was found that would provide sufficient separation of isomers 2 and 3. 1-5 mg of oxidized peptide was dissolved in 200 µL ACN and 800 µL water, and 10 µL 10 % TFA. Like for Turg_JK_1, the solution was left for 10 minutes before injection through the autosampler. The final method ended up using a gradient starting at 20 % mobile phase B increasing to 25 % mobile phase B over 40 minutes. However, this was not adequate to separate the chromatographic peaks. Further, such a mild slope caused a widening of the peaks which is not ideal. Further studies may be required for

proper separation between isomers 2 and 3. A possibility could be to use another column that provides better separation between isomers 2 and 3.

5.4.4 Freeze-drying of the fractions

The fractions containing the same isomers were pooled together in plastic tubes with filter paper beneath a lid with holes in it. The plastic tubes were placed in the freezer at -82 °C for at least three hours. The plastic tubes were then placed in the freeze dryer for about 3 days.

5.4.5 Purity analysis

1 mg of a peptide isomer was weighed out and dissolved in 1 mL of ammonium formate buffer 50 mM. 25 µL was then pipetted and diluted to 100 µL water with 5 % acetonitrile (ACN) and 0.1 % TFA. The rest of the process was identical to the one described in chapter 5.1.6.

5.5 Elucidation of disulfide bond configuration

5.5.1 Chemicals

Table 5 provides a summary of the chemicals used in the elucidation of the disulfide bond configurations.

Table 5: List of chemicals used in the elucidation of disulfide bond configurations.

Chemicals	Purity (%)	CAS-number	Supplier
Tris(2-carboxyethyl)phosphine hydrochloride		51805-45-9	Sigma-Aldrich®
N-Cyclohexylmaleimide	97 %	1631-25-0	Sigma-Aldrich®
N-Methylmaleimide	97 %	930-88-1	Sigma-Aldrich®
N-Ethylmaleimide	≥ 98.0 %	128-53-0	Sigma-Aldrich®
Ammonium Formate	≥ 99.0 %	540-69-2	Sigma-Aldrich®
Ultrapure Water from a Puranity PU 15 UV+			VWR
Methanol	≥ 99.9 %	67-56-1	VWR
Formic Acid	> 99 %	64-18-6	Thermo Fisher Scientific™

5.5.2 Optimization of the method

It was necessary for the method to be optimized to ensure that sufficient amounts of the peptide isomers are alkylated with two NMM/NEM groups and two NCM groups. This was done experimentally by adjusting the TCEP concentration and time of reaction in the cleavage of the first disulfide bond to ensure that most of the peptide had undergone a single reduction and alkylation. As the different isomers have differing conformations, the way they bind to the sorbent are likely different. Therefore, it may be either easier or more difficult for the reducing agent to cleave a disulfide bond between each isomer. While it is impossible to avoid some of the peptide having none or both of the disulfide bridges cleaved, the amount should be kept to a minimum, but at the very least be lower than the amount of peptide with a single cleaved disulfide bond. A concentration used for isomer I may then be excessive for isomer II, which would result in most of the peptide having both disulfide bridges alkylated with the same maleimide.

During the optimization of the first reduction and alkylation step the peptide was directly eluted to an HPLC-vial after the first reduction and alkylation, foregoing the remaining cleavage and reduction of the disulfide bonds. The eluate in the HPLC-vial was using the same mass spectrometer and method as in chapter 5.2.1. In the chromatograms certain m/z values are extracted from the total ion chromatogram (TIC) and studied. These values were the m/z values for the oxidized peptide with no cleaved disulfide bonds, the peptide with a single disulfide bond reduced and alkylated and the peptide with both disulfide bonds reduced and alkylated with the same alkylating agents. The alkylating agents used in the first step was either NEM or NMM. Table 6 provides a summary of these m/z values.

Table 6: Summary of m/z values for Turg_JK_1 alkylated with different combinations of maleimides at a range of charges. The non-alkylated cysteines were oxidized during the calculation of the mass.

		Charge						
First alkylating agent	Attached groups	+1	+2	+3	+4	+5	+6	+7
NMM	2 NMM + 2 NCM	2845.3319	1423.1696	949.1155	712.0884	569.8722	475.0614	407.3394
	2 NMM	2485.127	1243.0671	829.0472	622.0372	497.8312	415.0272	355.8815
	4 NMM	2709.2067	1355.1070	903.7404	678.0571	542.6472	452.3739	387.8929
NEM	2 NEM + 2 NCM	2873.3632	1437.1852	958.4593	719.0963	575.4785	479.7333	411.6441
	2 NEM	2515.174	1258.0906	839.0628	629.5489	503.8406	420.0351	360.1739
	4 NEM	2765.2693	1383.1383	922.428	692.0728	553.8597	461.7176	395.9019

By examining the TIC and the extracted m/z values, we were able to determine the approximate relative amount of peptide that had no reduced disulfide bonds, peptide with a single reduced and alkylated disulfide bond and peptide with both disulfide bonds reduced and alkylated in the first step. If there was an abundance of peptide with no reduced disulfide bonds, the TCEP concentration or time of reaction were increased, and then studied using MS the same way. These parameters were adjusted until the amount of peptide with only a single reduced and alkylated disulfide bond was satisfactory, while the amounts of peptide with none or both reduced and alkylated disulfide bonds were reduced to a minimum.

5.5.3 Method

The method is based on the method suggested by Albert et al. (7). A figure illustrating the workflow can be found in Figure 17.

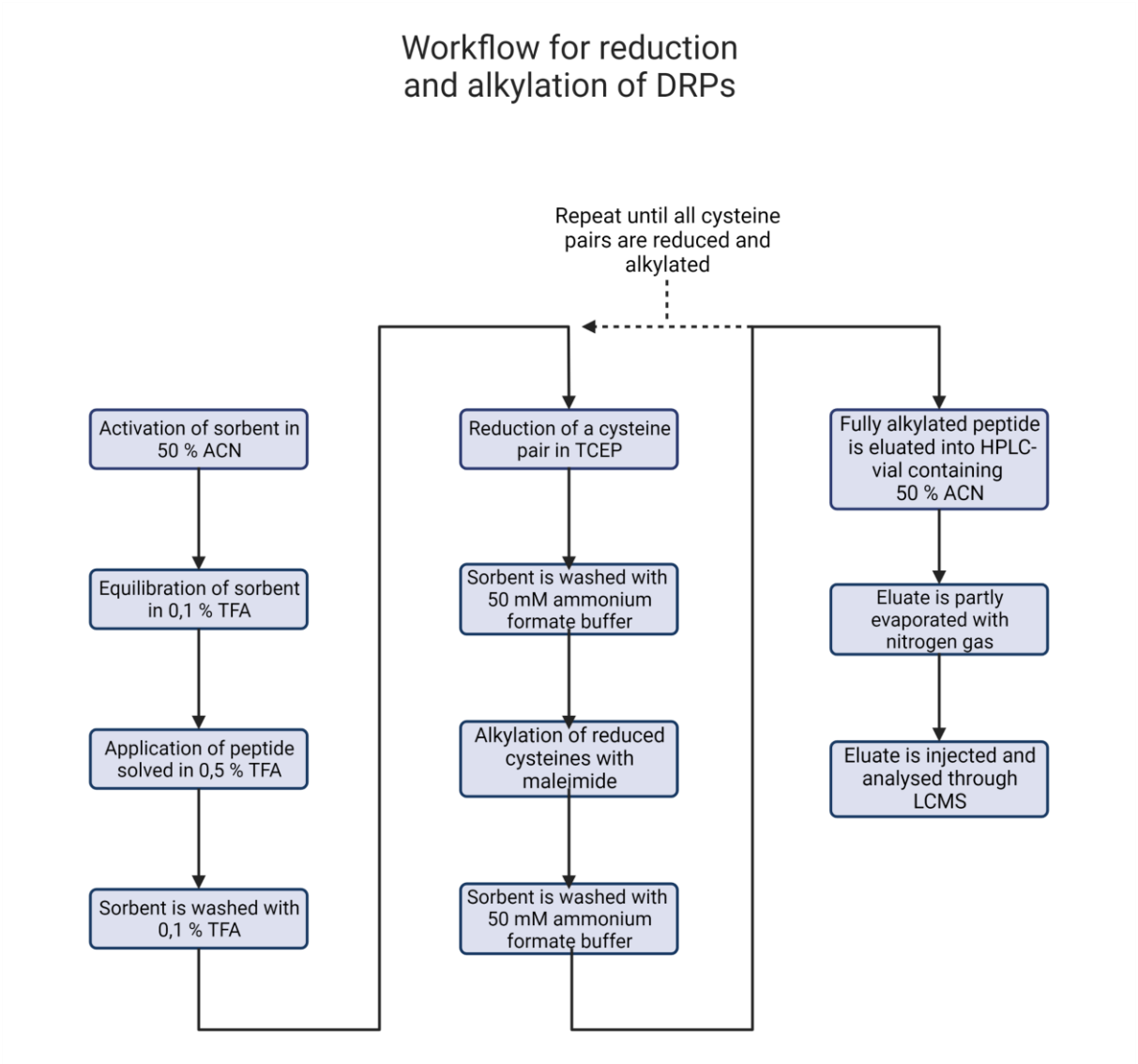

Figure 17: The workflow for the reduction and alkylation is illustrated. The dotted arrow shows that the reduction and alkylation must be repeated depending on the amount of disulfide bridges present in the peptide. Created with Biorender.com.

A list of solutions made for the method are listed in Table 7.

Table 7: List over solutions used in the sequential reduction and alkylation with their concentrations.

Solution	Concentration
Ammonium Formate Buffer	50 mM
Peptide Isomer Stock in ammonium formate buffer 50 mM	1 mg/mL
TFA in water	0.5 %
TFA in water	0.1 %
TCEP in ammonium formate buffer	(Varies)
NEM/NMM in ammonium formate buffer	20 mM
NCM in ACN	100 mM
ACN in water	50 %
Methanol	100 %

5.5.3.1 Activation and equilibration of the sorbent

The Omix C_{18} pipette tip containing the sorbent was fastened to a micropipette, and then activated by submerging it in an Eppendorf tube containing ACN. Then, the ACN was drawn in and out of the peptide 10 times, by pushing the plunger of the micropipette down, before retracting it. This was done to ensure that the whole sorbent comes into contact with the liquid. While the liquid was drawn in and out of the pipette, the surface of the liquid did not go below the sorbent surface. This was done by avoiding pushing the plunger all the way down. This process illustrated in Figure 18.

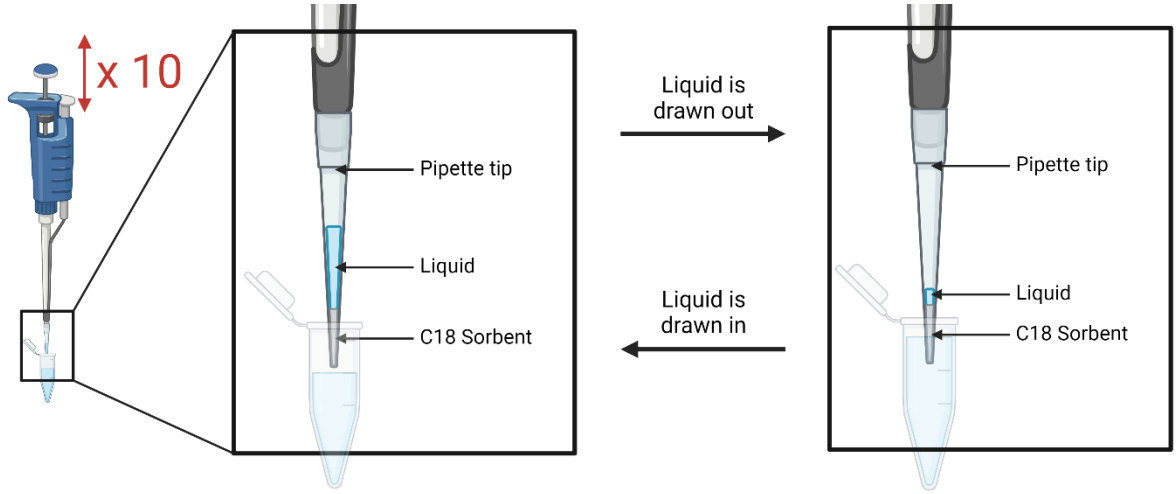

Figure 18: Illustration showing the process of drawing the liquid in and out of the pipette tip from an Eppendorf tube, while keeping the surface of the liquid above the sorbent. The box on the left shows the pipette tip with the liquid drawn in. The box on the right shows the pipette tip with the liquid pushed out until the surface is just above the sorbent. Created with BioRender.com

After the plunger was pushed down and retracted 10 times, the ACN was ejected while keeping the liquid above the sorbent as illustrated in the second box of Figure 18. Then the pipette tip was submerged in another Eppendorf tube of ACN, and the liquid was drawn in and ejected out like in the previous step. Then, the process was repeated in two Eppendorf tubes containing 0.1 % TFA to equilibrate the sorbent.

5.5.3.2 Application of the peptide to the sorbent and wash

10 µL of the peptide isomer stock and 90 µL of 0.5 % TFA was added to an Eppendorf tube, and vortexed. Then, the pipette tip was submerged in the peptide solution, and was drawn in and out of the pipette tip without the surface of the liquid going below the sorbent. While the liquid was drawn into the pipette tip, it was left for a minute to allow for the peptide isomer to bind to the sorbent. After a minute had passed, the peptide solution was pushed out of the pipette tip until the surface of the liquid was just above the sorbent and was inserted into an Eppendorf tube containing 200 µL of 0.1 % TFA. The TFA solution was then drawn into the pipette tip, which was then completely ejected of its content as waste. This was repeated until there was no TFA solution left.

5.5.3.3 Cleavage and reduction of the first disulfide bond and wash

The sorbent was submerged in 200 µL of TCEP solution, and the solution was drawn in and out of the pipette tip 10 times while the surface of the solution was kept above the sorbent. Then, the solution was drawn into the pipette tip, and was left for a certain amount of time depending on the peptide isomer. This is so the TCEP can reduce the disulfide pairs, resulting in cleavage of the disulfide bond. The concentration and duration of reaction is listed in Table 8.

Table 8: Summary of TCEP concentration and reaction times used for the cleavage of the first disulfide bond for each tested isomer.

		First Reduction		Second Reduction	
Peptide	Isomer	TCEP concentration	Duration of reaction	TCEP concentration	Duration of reaction
Turg_JK_1	I	0.5 mM	5 minutes	5 mM	10 minutes
Turg_JK_1	III	1 mM	1 minute	1 mM	10 minutes
Turg_JK_1	III	0.25 mM	7 minutes	10 mM	10 minutes

The TCEP concentrations and durations of reaction were determined experimentally, as explained in chapter 50.

After the duration of the reaction had passed according to Table 8, the TCEP solution was pushed out of the pipette tip until the surface of the liquid was just above the sorbent. The pipette tip was then submerged in an Eppendorf tube containing 200 µL of 0.1 % TFA, which was drawn in and then completely ejected until the Eppendorf tube was empty.

5.5.3.4 Alkylating the first disulfide pair and wash

The pipette tip was submerged in 200 µL of either the NMM or NEM solution. The maleimide solution was drawn in and pushed out of the pipette tip 10 times while the surface of the solution was kept above the sorbent. Then, the solution was drawn into the pipette tip, and was left for about 15 minutes. This is so the maleimides completely alkylate the reduced cysteines. After these 15 minutes, the maleimide solution was pushed out of the pipette tip until the surface of the liquid was just above the sorbent. The pipette tip was then submerged in an Eppendorf tube

containing 200 µL of 0.1 % TFA, which was drawn in and then completely ejected until the Eppendorf tube was empty.

5.5.3.5 Cleavage and reduction of the second disulfide bond and wash

The steps from chapter 5.5.3.3 were repeated, but with differing concentrations and times of reaction which are listed in Table 8.

5.5.3.6 Alkylation of the second disulfide pair

The pipette tip was submerged in an Eppendorf tube containing 100 µL of 100 mM NCM in ACN. The maleimide solution was drawn in and pushed out of the pipette tip 10 times while the surface of the solution was kept above the sorbent. Then, the maleimide solution was drawn into the pipette tip, and was left for about 1 minute. Then, the maleimide solution was pushed out of the pipette tip until the surface of the liquid was just above the sorbent. The pipette tip was then submerged in an Eppendorf tube containing 200 µL of 0.1 % TFA, which was drawn in and then completely ejected. This was repeated until the Eppendorf tube was empty.

5.5.3.7 Elution of alkylated peptide into an HPLC-vial

The sorbent was then inserted into an HPLC-vial containing 50 µL of ACN and 50 µL of water. This solution was drawn in and out of the pipette tip 10 times while the surface of the solution was kept above the sorbent. Then, the solution was drawn into the pipette tip, and was left for about 1 minute. This is so the peptide's interactions with the sorbent were broken, and thus eluted into the HPLC-vial. The pipette tip then completely ejected its contents into the HPLC vial. Thereafter the pipette tip was inserted into an Eppendorf tube containing 500 µL of methanol, which was washed through the pipette tip. The pipette tip was then left in the Eppendorf tube for at least a few minutes. After a few minutes, the pipette tip was emptied and put away for later reductions and alkylations of the same peptide isomer.

After this the solution in the HPLC-vial containing the alkylated peptide isomer was evaporated under a stream of nitrogen gas for about 8 minutes. This is to remove the acetonitrile from the HPLC-vial, which could harm the chromatography during UPLC-MS, and to boost the signal by increasing the concentration of the alkylated peptide isomer.

5.5.4 Elucidation of structure through mass spectrometry

The HPLC-vials containing the alkylated peptides from chapter 5.5.3.7 are then analyzed using mass spectrometry. The instrument and methods were the same as the ones used in chapter 5.1.3.

The mass spectra were analyzed using the software Freestyle. The chromatographic peaks for the peptides with 2 groups alkylated with NMM/NEM and 2 groups with NCM were found by extracting the m/z values for these respective peptides. The respective m/z values can be found in Table 6. The Orbitrap Tribrid Id-X can as described in chapter 3.5.4 generate MS^2 spectra from the ions with the highest intensities in the full scan spectra generated by the orbitrap. The MS^2 spectra used were gathered from the full scan spectra that was closest to the middle of the chromatographic peak, and from the next full scan spectra that were not present in the former. If two chromatographic peaks are present for the peptide alkylated with two NMM/NEM- and 2 NCM groups, then this process was performed for both peaks.

The fragments present in the MS^2 spectra were then extracted from the freestyle software to Microsoft Excel. The ions with an intensity under 1.0e5 were filtered out. The m/z values that were measured were then compared to a list of theoretical fragments for every possible alkylation pattern of the corresponding peptide. This list of theoretical fragments was obtained through the MS-Product generator in the ProteinProspector tools from The Regents of the University of California (32). Through this website, a sheet was generated showing possible fragments from a given peptide sequence. A sheet was generated for every possible alkylation pattern for a given peptide. These sheets are exported into excel. The theoretical values are then transformed and put in a single column in a separate excel sheet, and the original sheet was saved for later use. By using an R script, the list of measured m/z values was compared to the list of theoretical fragments generated through MS-product. Every measured m/z value that was within 5 ppm of a generated theoretical value was output in a list with the corresponding theoretical value. The R script can be found in the appendix in chapter 10.3. The list of matches between measured and theoretical m/z values was then used to format the previously generated MS-product sheets. The theoretical values that have a match are colored to give a visualization

of what fragments are present in the sample. Then, fragments that are characteristic of a certain disulfide connectivity are identified and are then used to determine the disulfide connectivity. The characteristic fragments also undergo manual inspection to confirm their identity. The MS^2 spectrum undergoes inspection to determine if the ion had the same charge as the theoretical fragments, displayed an isomer pattern, and was the C^{12} peak of said pattern.

5.6 Bioactivity testing

Bioactivity testing was performed at NFH according to the protocol "Screening av antibakteriell aktivitet hos peptider – Minimal inhiberende konsentrasjon (MIC)" which can be found in the appendix in chapter 10.4. Do note that the document is written in Norwegian. The peptide isomers of both Turg_JK_1 and Turg_JK_2 were weighed and dissolved in water to a concentration of 1 mg/mL. Some isomers had less than 1 mg isolated after the oxidation process, and they were dissolved in lesser amounts of water than the others, which would give a concentration of 1 mg/mL. Isomers II and III of Turg_JK_2 could not be isolated from each other and were thus dissolved together in the same sample.

The peptides were tested for antimicrobial activity against several bacterial strains, including *Escherichia coli* (E.C.), *Staphylococcus aureus* (S.A.), *Corynebacterium glutamicum* (C.G.), *Pseudomonas aeruginosa* (P.A.), *Bacillus subtilis* (B.S), and *Staphylococcus epidermidis* (S.E.).

6 Results

6.1 Peptide synthesis

6.1.1 Turg_JK_1

0.3213 grams of crude was extracted after the peptide synthesis. The purity analysis of the crude is shown in Figure 19.

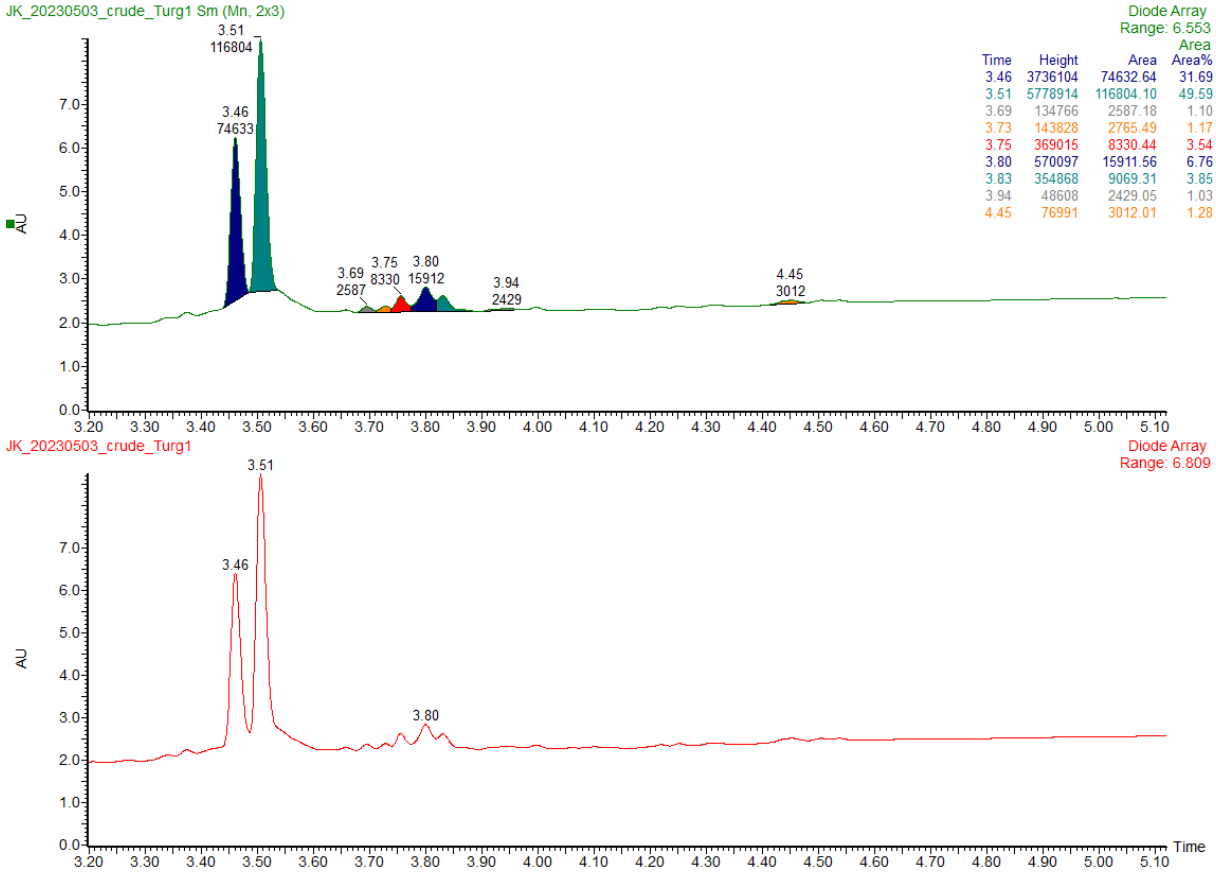

Figure 19: Chromatogram showing purity analysis of peptide crude from the synthesis of Turg_JK_1.The upper chromatogram have the peaks integrated, while the lower chromatogram is unedited.

The integrated peaks in Figure 19 does not have clear starting and ending points and both software determination and manual determination of peak areas turned out to be difficult, hence it is also difficult to be certain of the purity of the peptide eluting at 3.51 minutes.

6.1.2 Turg_JK_2

The total peptide crude from the synthesis of Turg_JK_2 was not weighed. The chromatogram from the purity analysis is shown in Figure 20.

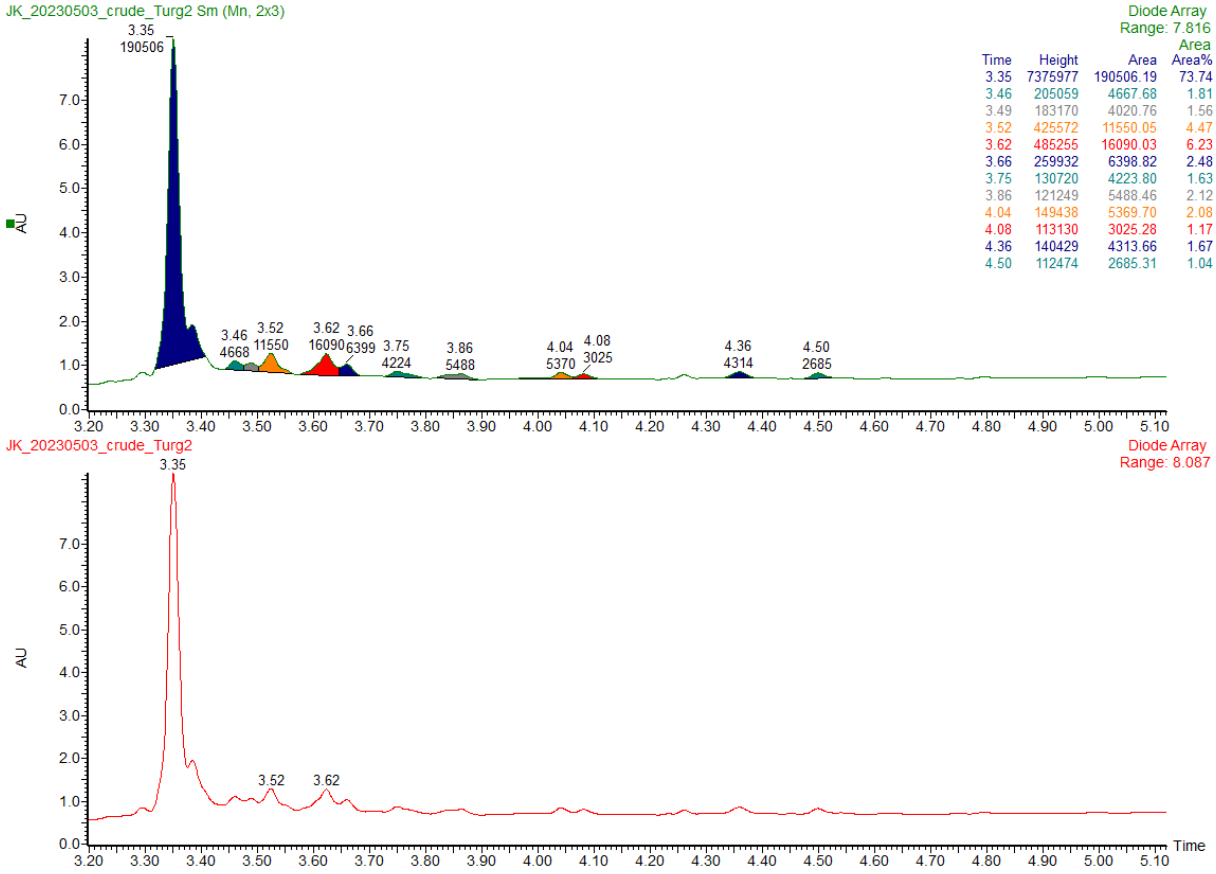

Figure 20: Purity analysis of peptide crude from the synthesis of Turg_JK_2. The upper chromatogram have the peaks integrated, while the lower chromatogram is unedited.

As for Turg_JK_1, manual editing of the integrated peaks was not performed, and it is obvious that the automatic integration has included a shoulder peak in the area, and the purity is probably lower than indicated.

6.2 Sample preparation of the crude peptides to linear peptides.

6.2.1 Turg_JK_1

During the sample preparations, the 4 peaks marked by the colored boxes in Figure 21 were collected by the fraction collector. The peaks in the red boxes contain contaminants of unknown origin. The peak in the yellow box contains the incomplete Turg_JK_1, that has a missing cysteine group. This was determined through mass spectrometry.

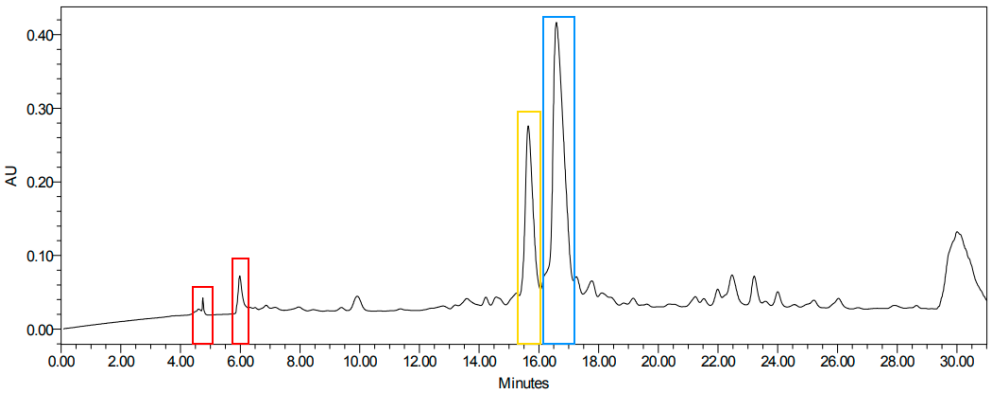

Figure 21: Chromatogram from preparative HPLC during the sample preparation of the crude peptide of Turg_JK_1. Peaks are marked in colored boxes corresponding to their identities.

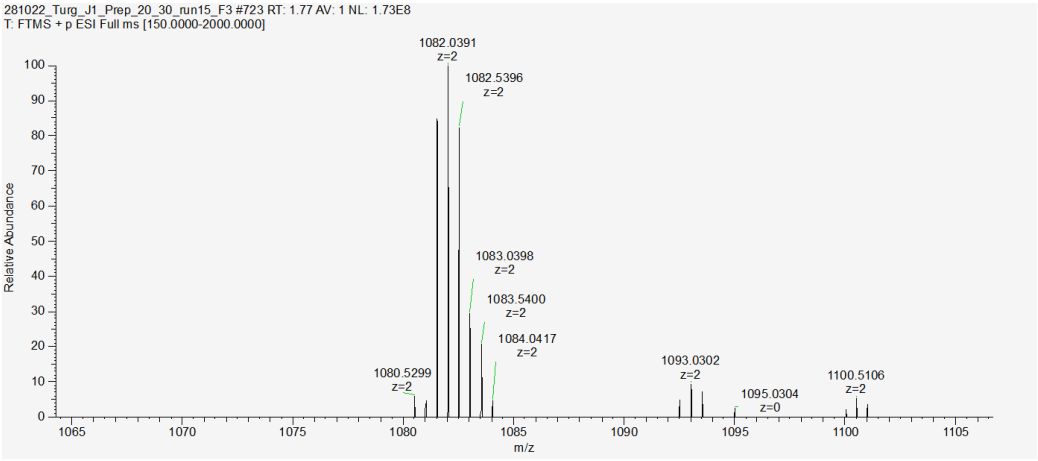

Figure 22: Mass spectrometer of the peak in the yellow box containing the incomplete peptide. Because the peptide has several groups that can obtain a charge, there are several peaks that correlate to the expected m/z values of the peptide.

In the mass spectrum of the fraction containing the peak in the yellow box in Figure 22, there is observed an ion which with 2 charges had a measured m/z value of 1081.5378. This lines up at the expected mass of the peptide chain that is a cysteine short.

The peak in the blue colored box contains Turg_JK_1, which was determined through mass spectrometry as well. The mass spectrum is seen in Figure 23

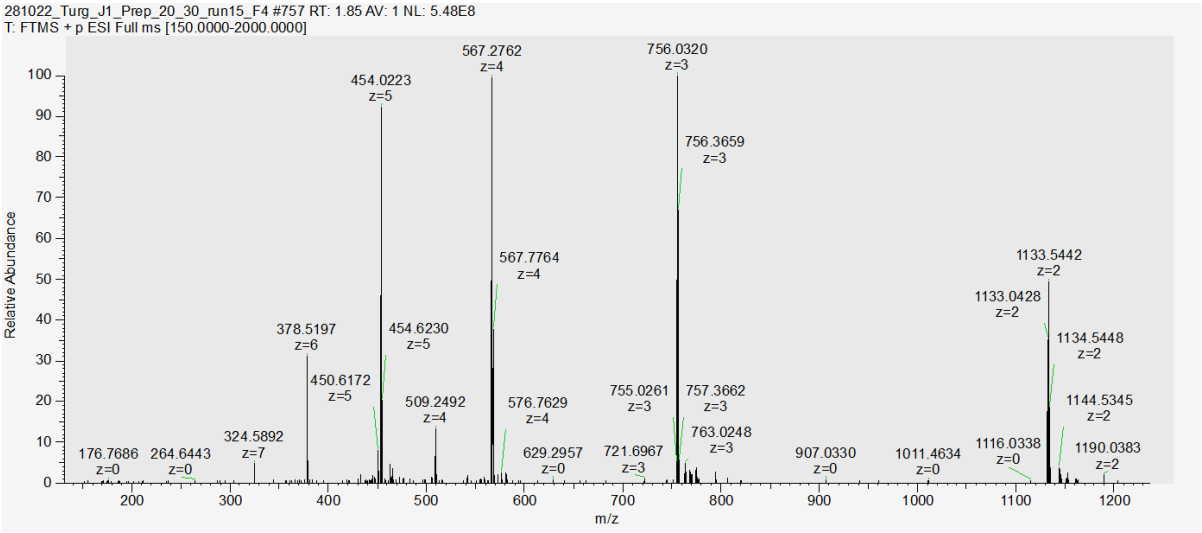

Figure 23: Mass spectrometer of the peak in the blue box containing the linear peptide. Because the peptide has several groups that can obtain a charge, there are several measured m/z values that correlate to the expected m/z values of the peptide.

Several ions were observed in the mass specter with m/z values of 1133.0428, 755.6980, 567.0251, and 453.821. These are the expected m/z values for Turg_JK_1 at 2, 3, 4, and 5 charges.

6.2.2 Turg_JK_2

Figure 24 is a chromatogram from the preparative HPLC. The red boxes contained contaminants of unknown origin like for Turg_JK_1. The blue box was determined to contain Turg_JK_2 through mass spectrometry and was collected by the fraction collector. This mass spectrum is shown in Figure 25.

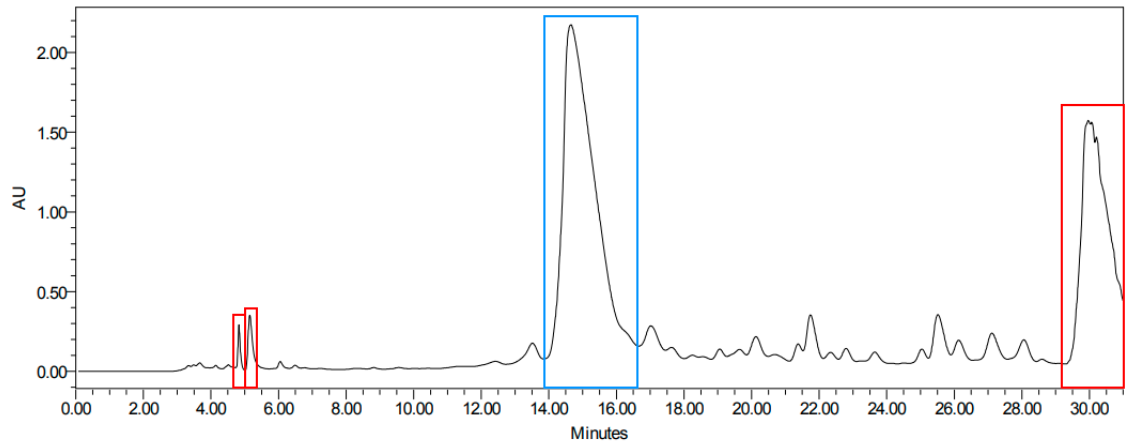

Figure 24: Chromatogram from preparative HPLC during the sample preparation of the crude peptide of Turg_JK_2. Peaks are marked in colored boxes corresponding to their identities.

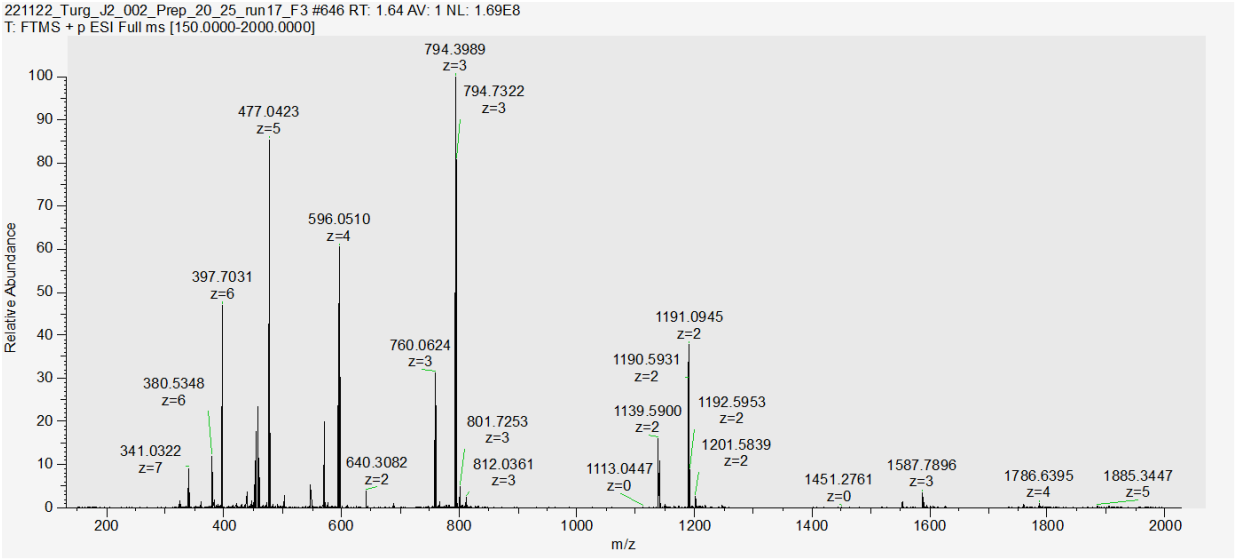

Figure 25: Mass spectrometer of the peak in the blue box containing the linear peptide. Because the peptide has several groups that can obtain a charge, there are several measured m/z values that correlate to the expected m/z values of the peptide.

In Figure 25 an ion was observed with an m/z value of 1190.5931, which correlates to the expected theoretical m/z value for Turg_JK_2 at 2 charges. Thus, the peak in the blue box in Figure 24 was determined to contain the linear peptide. In Figure 25 an ion with an m/z of 1139.0886 was measured as well. This is the expected m/z value of the incomplete peptide

chain that is missing the last cysteine, like for Turg_JK_1. The figure also shows a similar ionization pattern as for Turg_JK_1 with 2, 3, 4 and 5 charges on the peptide.

6.3 Oxidation of the linear peptides.

6.3.1 Turg_JK_1

Figures 26-28 show chromatograms from UPLC-MS analysis monitoring the oxidation process.

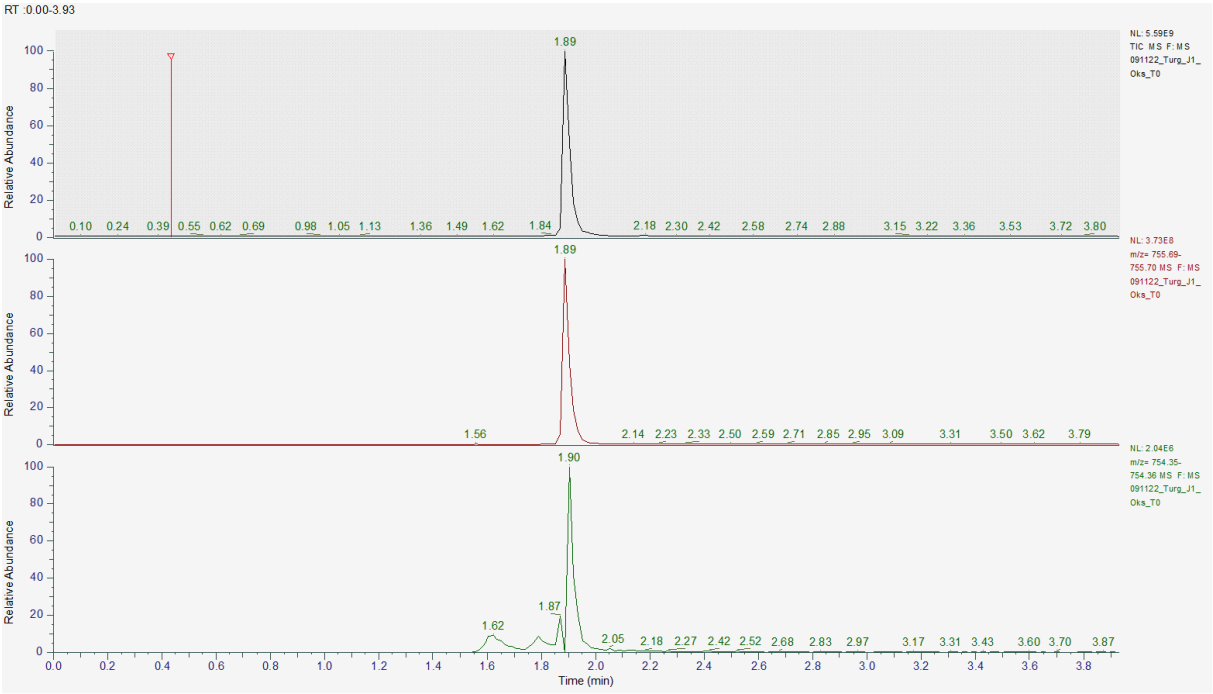

Figure 26: Chromatograms from UPLC-MS analysis of a sample taken from the glass tubes where the oxidation process is taking place at moments after start. The upper chromatogram is the total ion chromatogram. The middle is a chromatogram showing when the m/z value for the unoxidized peptide at 3 charges (755.69-755.70) was detected in the MS. The lower chromatogram is showing when the m/z value for the oxidized peptide (754.36) is detected in the MS.

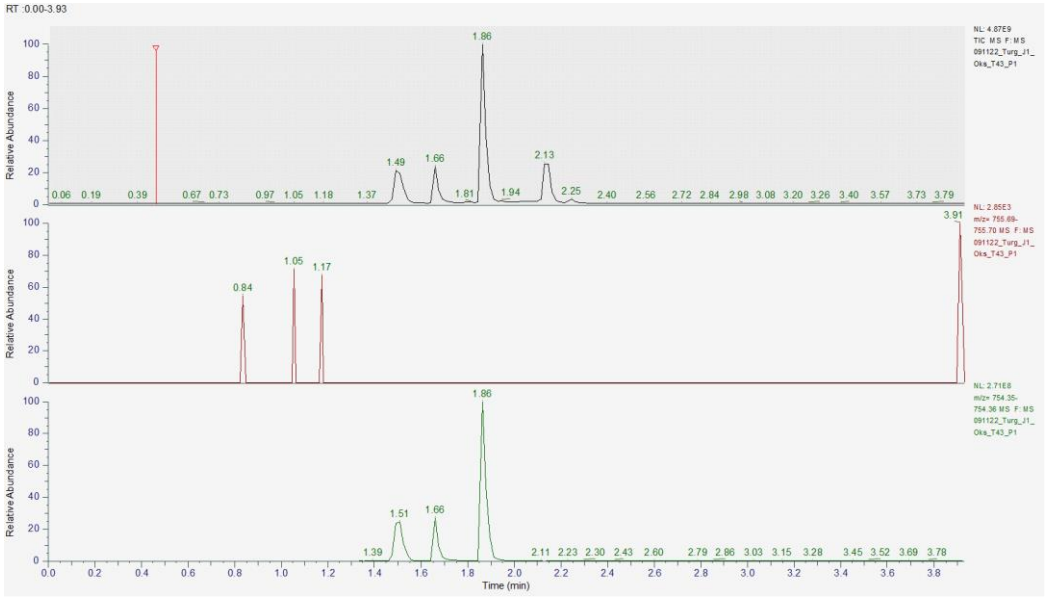

Figure 27: Chromatograms from UPLC-MS analysis of a sample taken from the glass tubes where the oxidation process is taking place at 43 hours after start. The upper chromatogram is the total ion chromatogram. The middle is a chromatogram showing when the m/z value for the unoxidized peptide at 3 charges (755.69-755.70) was detected in the MS. The lower chromatogram is showing when the m/z value for the oxidized peptide (754.36) is detected in the MS.

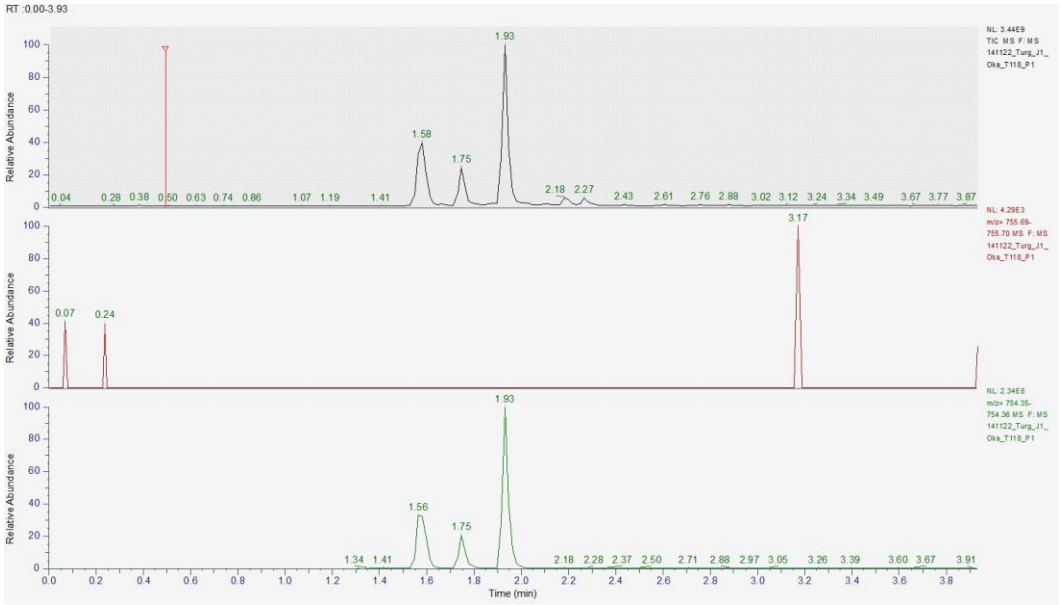

Figure 28: Chromatograms from UPLC-MS analysis of a sample taken from the glass tubes where the oxidation process is taking place at 118 hours after start. The upper chromatogram is the total ion chromatogram. The middle is a chromatogram showing when the m/z value for the unoxidized peptide at 3 charges (755.69-755.70) was detected in the MS. The lower chromatogram is showing when the m/z value for the oxidized peptide (754.36) is detected in the MS.

From Figure 26 it is shown that some oxidation has taken place right after the oxidation had started, as ions with m/z values of the oxidized peptides are detected. However, most of it remain unoxidized.

The identity of the chromatographic peak at 2.13 minutes in the TIC in Figure 27 is unknown. There, an ion with a m/z value of 792.3602 was observed, which is seen in Figure 29

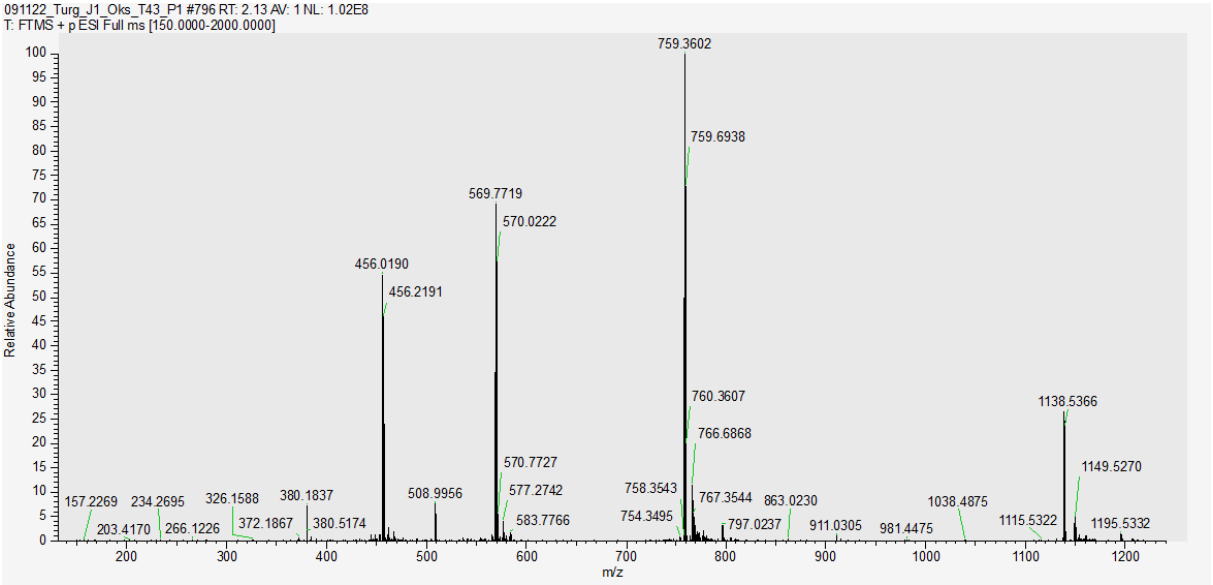

Figure 29: Mass spectrum of the peak at 2.13 from Figure 28.

The m/z values are not from any of the expected m/z values for this peptide, or Turg_JK_2. However, this peak disappeared after 118 hours in Figure 28

At 118 hours in Figure 28, the peptide is completely oxidized, as only noise is registered for m/z values for the unoxidized peptide. By visual inspection of the chromatogram for the oxidized peptides, there are 3 peaks, each corresponding to an isomer. The identification of the isomers will be described in chapter 6.5.

6.3.2 Turg_JK_2

Figures 30-31 show chromatograms from UPLC-MS analysis monitoring the oxidation process.

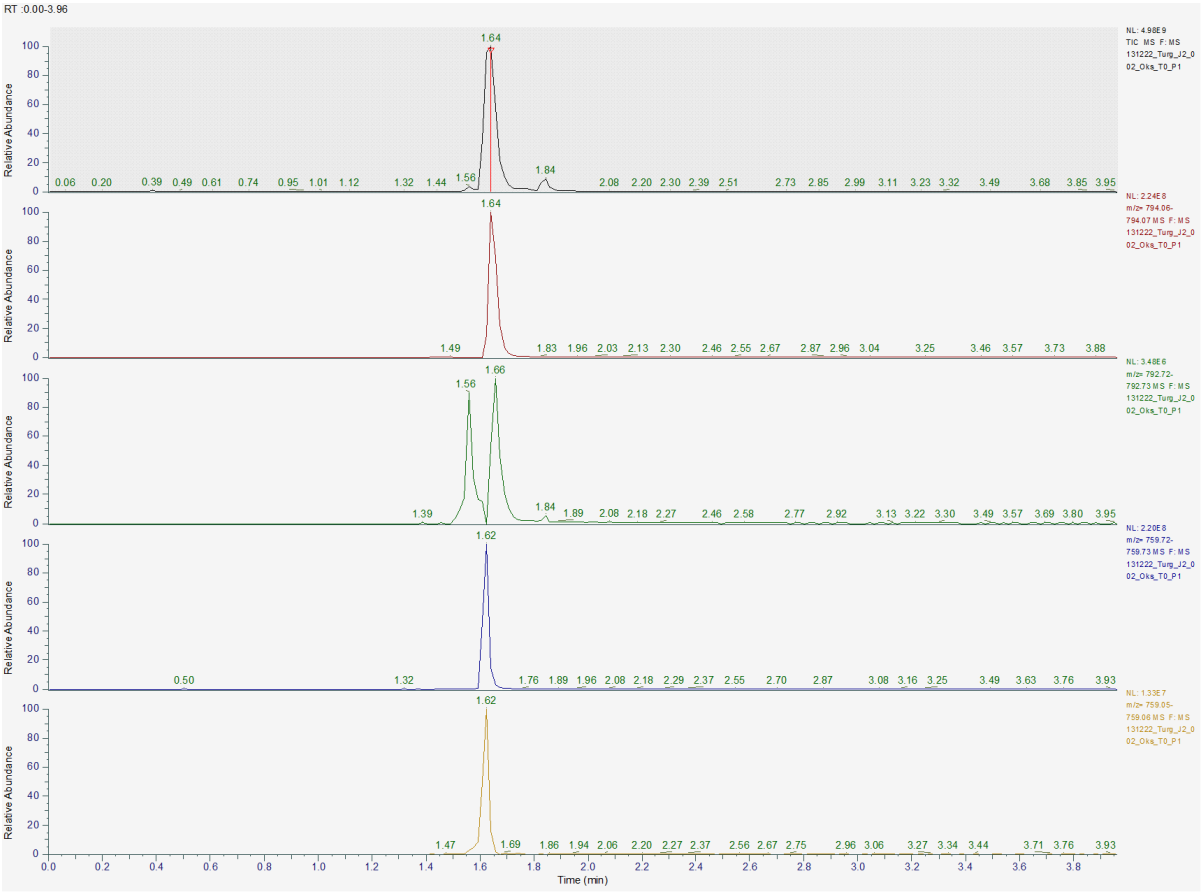

Figure 30: Chromatograms from UPLC-MS analysis of a sample taken from the glass tubes where the oxidation process is taking place at moments after start. The first chromatogram is the total ion chromatogram. The second, third, fourth, and fifth chromatograms show when the m/z values for the unoxidized peptide (794.06-794.07), oxidized peptide (792.72-792.73), unoxidized incomplete (759.72-759.73), and oxidized complete peptide (759.05-759.06) respectively are detected in the MS at 3 charges.

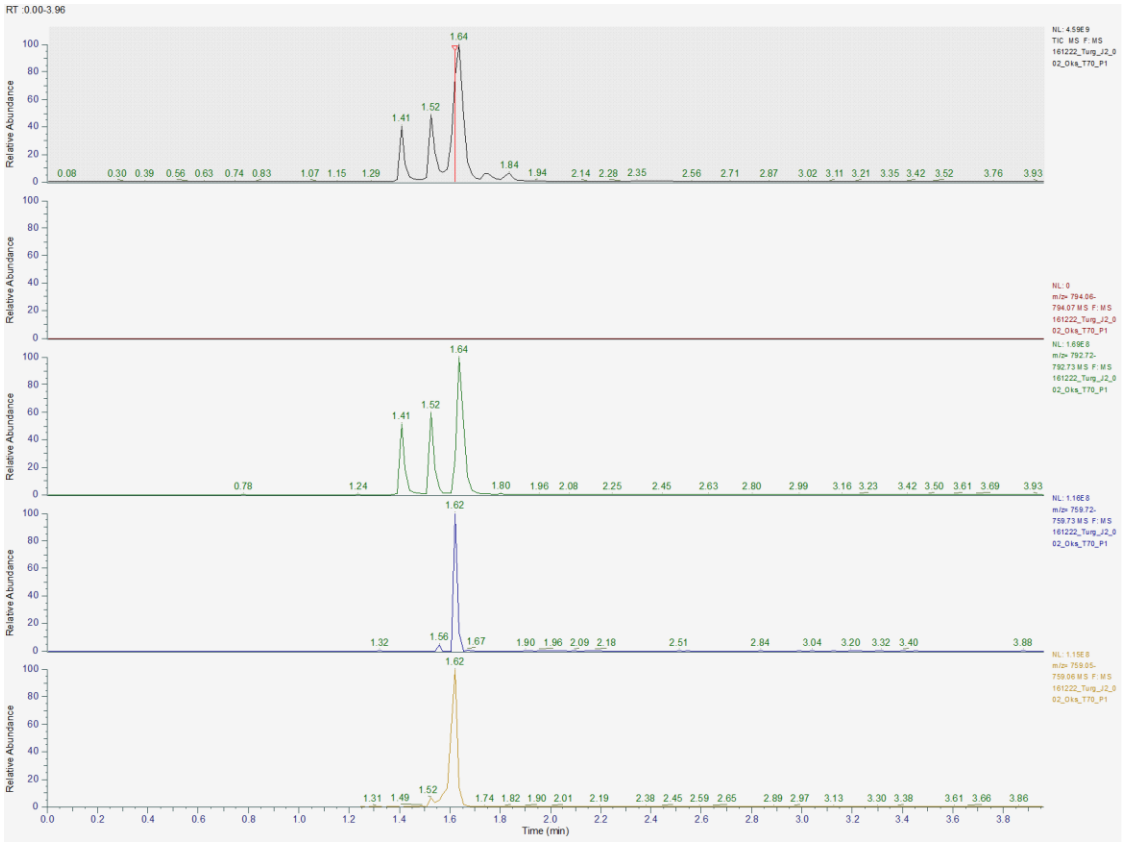

Figure 31: Chromatograms from UPLC-MS analysis of a sample taken from the glass tubes where the oxidation process is taking place at 70 hours after start. The first chromatogram is the total ion chromatogram. The second, third, fourth, and fifth chromatograms show when the m/z values for the unoxidized peptide (794.06-794.07), oxidized peptide (792.72-792.73), unoxidized incomplete (759.72-759.73), and oxidized complete peptide (759.05-759.06) respectively are detected in the MS at 3 charges.

Like for Turg_JK_1, some oxidation has already taken place at 0 hours which can be seen in the second chromatogram in Figure 30. There is also some of the incomplete peptide present, which has also been slightly oxidized, as can be seen in the third and fourth chromatograms in Figure 30. As explained in chapter 6.2.2, this is due to some of the incomplete peptide being present after the sample preparation of the crude.

After 70 hours, the peptide is completely oxidized, as seen by the lack of any signal in the second chromatogram in Figure 31. As expected, there are three peaks in the TIC and third chromatogram, all containing the expected m/z values for the oxidized peptides as can be seen in the lower chromatogram as well.

However, as seen in the fourth and fifth chromatograms of Figure 31, there is still some of the incomplete peptide which is not fully oxidized left in the sample. These form a peak approximately between the peaks in the TIC for the oxidized peptide at 1.52 and 1.64 minutes. Because of this contamination, there is a discrepancy in the form of the peaks between the TIC and the third chromatograms.

6.4 Separation of the isomers of the oxidized peptide

6.4.1 Turg_JK_1

During the sample preparations, the 4 peaks marked by the colored boxes in Figure 21 were collected by the fraction collector. The peaks in the red boxes contain contaminants of unknown origin. The peak in the yellow box contains the incomplete Turg_JK_1, that has a missing cysteine group. This was determined through mass spectrometry, as seen in Figure 32 for the peak in the blue box.

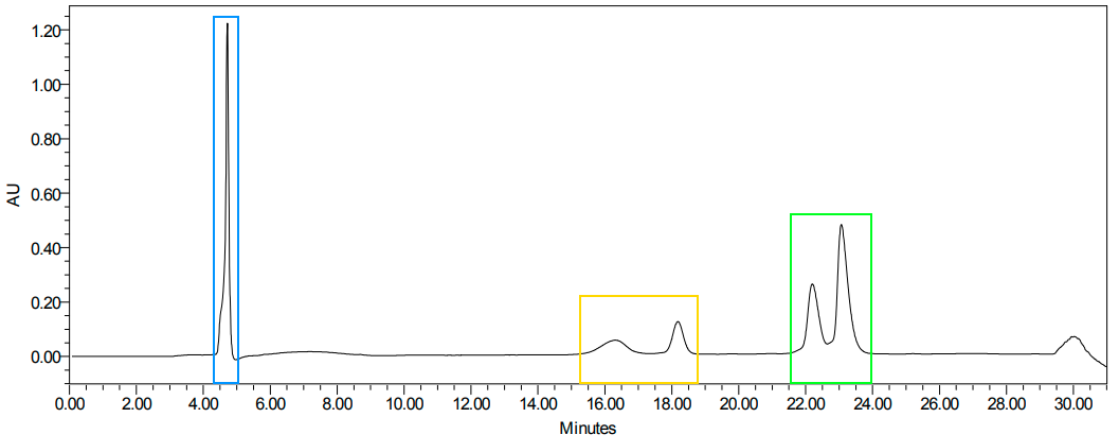

Figure 32: Chromatogram from preparative HPLC during the separation of the isomers of the oxidized Turg_JK_1. Peaks are marked in colored boxes corresponding to their identities.

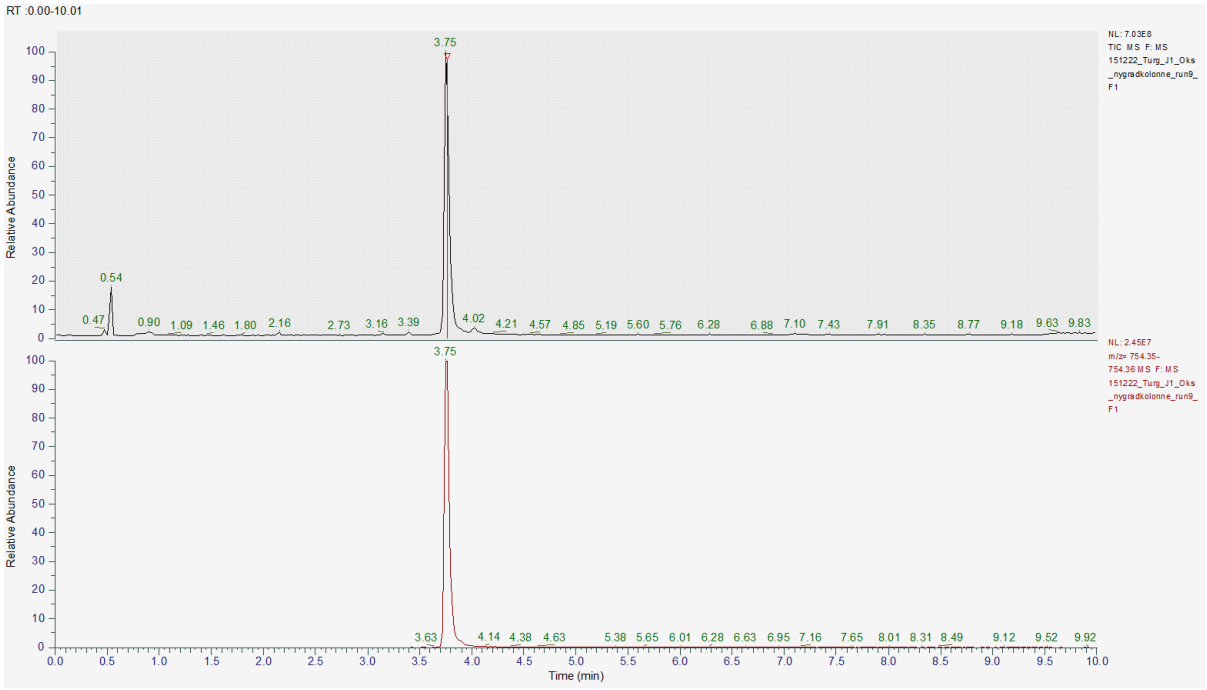

Figure 33: Chromatogram from UPLC-MS analysis of the fraction containing the peak in the blue-colored box. The upper chromatogram is the total ion chromatogram, while the lower is the chromatogram showing when ions with the mass for the oxidized peptide (754.35-754.36) at 3 charges is detected in the MS.

During the separation of the isomers of Turg_JK_1, the peaks in the colored boxes were collected. By the fraction collector. The isomer in the blue box was named “Isomer I”, the two in the yellow box were named “Isomer II” and the two in the green box were named “Isomer III”. Their identities were determined to be the oxidized peptide through mass spectrometry. The probable reason for the peak splitting of all three peaks has been explained earlier in chapter 5.4.1. There peak containing isomer I is not quite uniform, but probably did not have enough time to form two separate peaks like the other isomers because of its early elution.

MS-analysis shows that the 5 peaks that are highlighted in Figure 32 contain the isomers of the oxidized Turg_JK_1, as they all have a detector response for the m/z value of the oxidized peptide. The mass spectrum in Figure 33 shows a detector response in the second chromatogram, with the chromatograms for the rest of the peaks showing the same (Data not shown), confirming their identities. The two peaks containing isomer II did not give a clear signal at first. This was due to their fractions being diluted because their peaks were broad. Later, the fractions were pooled together, and freeze-dried, and a sample of this was analyzed

using MS (Data not shown). The result shows challenges with tailing of this compound in the chromatography, leading to a poor signal when the concentration is low.

As discussed in chapter 5.4.1, the samples were later run after adding TFA to the sample. The chromatogram from the prep-HPLC then displayed three peaks, as can be seen in Figure 34. When TFA is added to the sample, the isomers only form a single peak each as seen in Figure 34, unlike what was observed in Figure 32. The contents of the peak in the blue box was determined through MS, which is shown in Figure 35.

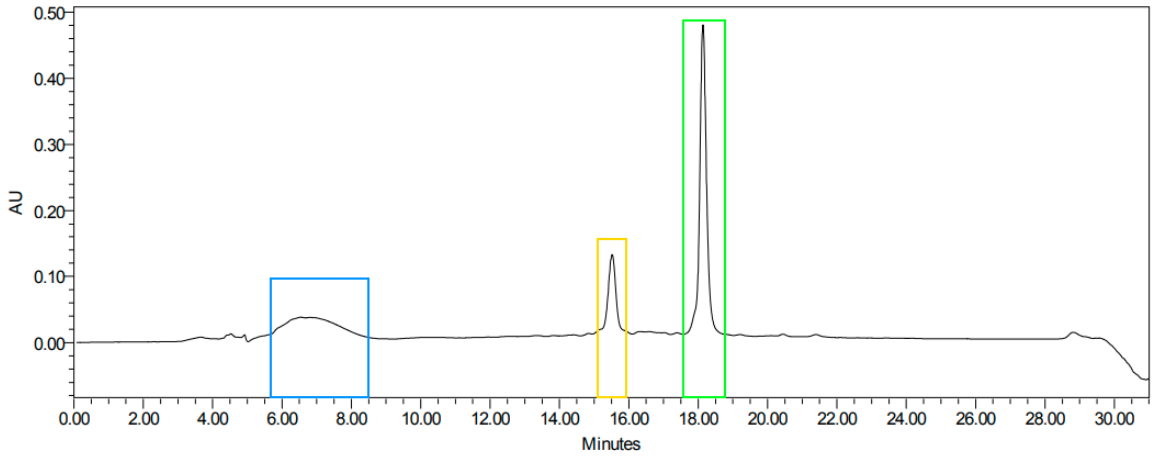

Figure 34: Chromatogram from preparative HPLC during the separation of the isomers of the oxidized Turg_JK_1 when adding TFA to the sample before injection. Peaks are marked in colored boxes corresponding to their identities.

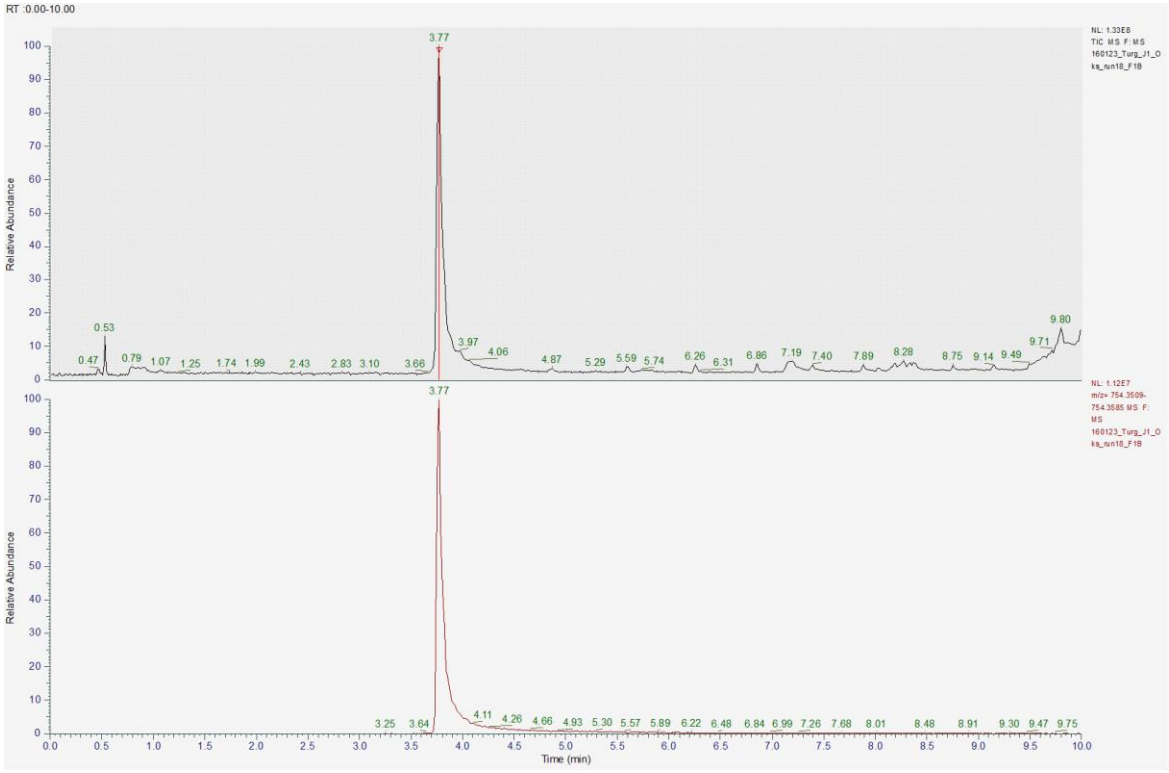

Figure 35: Chromatogram from UPLC-MS analysis of the first fraction containing the peak in the blue colored box in Figure 34. The upper chromatogram is the total ion chromatogram, while the lower is the chromatogram showing when ions with the mass for the oxidized peptide (754.35-754.36) at 3 charges is detected in the MS.

Like earlier, Figure 35 gives a detector response for the mass of the oxidized peptide, confirming its identity.

Further, the results from the purity analysis for isomer I is shown in Figure 36 and Figure 37.

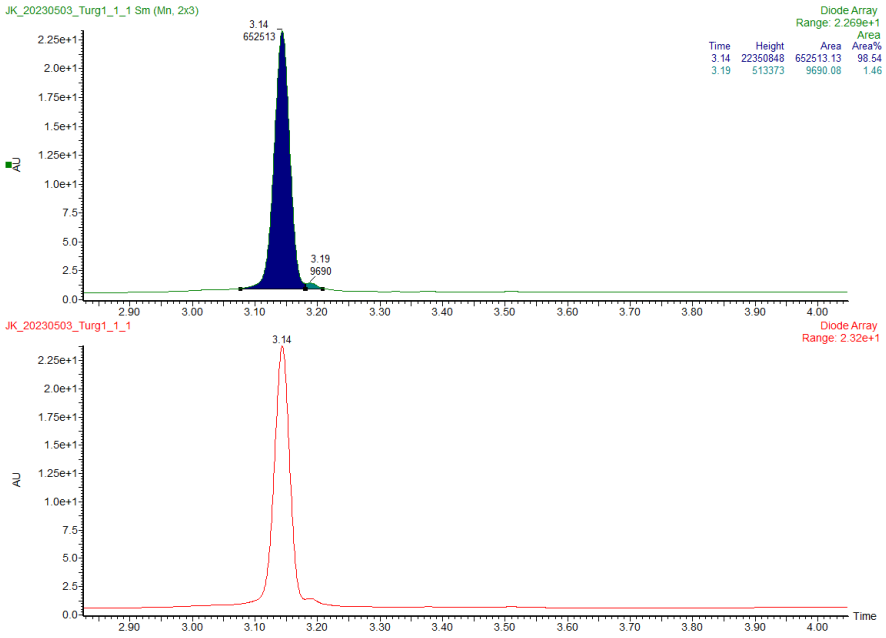

Figure 36: Chromatogram showing purity analysis of the pooled fractions containing Isomer I of Turg_JK_1. The integrated peaks have been manually edited.

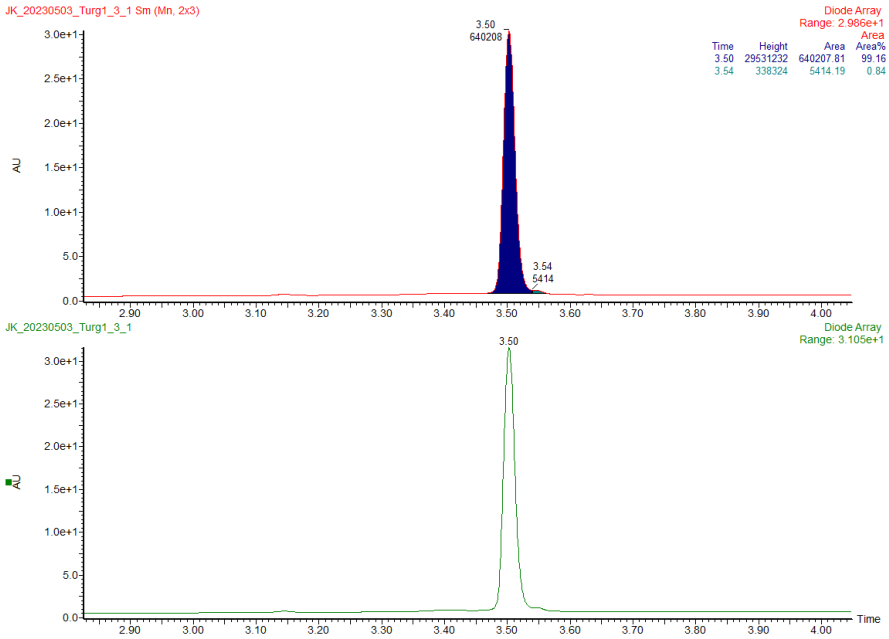

Figure 37: Chromatogram showing purity analysis of the pooled fractions containing Isomer I of Turg_JK_1. The integrated peaks have been manually edited.

Both Figure 36 and Figure 37 show a high purity for both isomers, at 98.54 and 99.16 % respectively. It should be noted that the mobile phases contained TFA, which may have caused some of the peptides to form an adduct with differing retention time as explained earlier in chapter 5.4.1. There could not be isolated enough of isomer II to conduct any purity results, as all of it was sent for bioactivity testing.

6.4.2 Turg_JK_2

The peaks highlighted in the colored boxes in Figure 38 all contain isomers of the oxidized Turg_JK_2. This was verified using mass spectrometry. The isomers were named in the same manner as for Turg_JK_1.

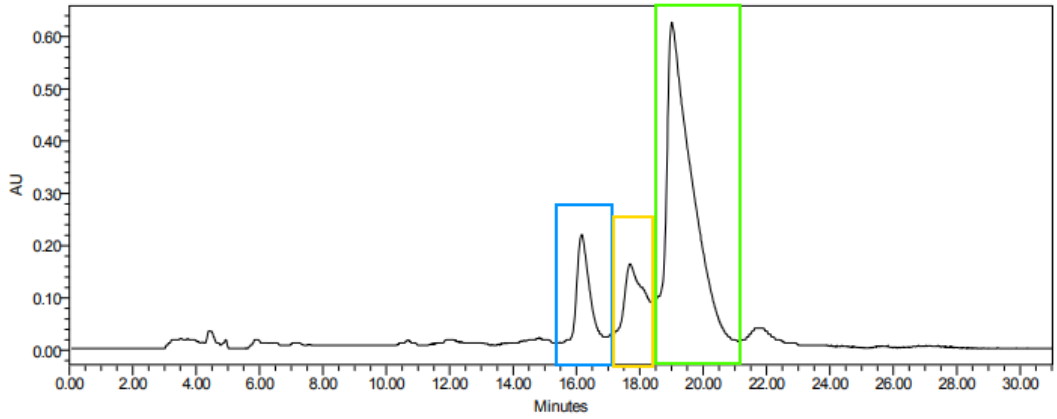

Figure 38: Chromatogram from preparative HPLC during the separation of the isomers of the oxidized Turg_JK_2. Peaks are marked in colored boxes corresponding to their identities.

From visual inspection, the fraction in the blue box containing isomer I seems to have been separated from the two other isomers. The fractions mass spectrometer is seen in Figure 39. Unfortunately, acceptable levels of separation between isomers 2 (yellow-colored box) and 3 (green-colored box) in Figure 38 was not possible. Further, the peak in the yellow box is not uniform, suggesting a contaminant. This contaminant is likely the incomplete peptide, which was present as discussed in chapter 6.4.2. Sufficient amounts of the isomers could not be

isolated for both bioactivity testing and elucidation of disulfide bonds. In Figure 40 there is a mass spectrum for the fraction containing the beginning of the green peak.

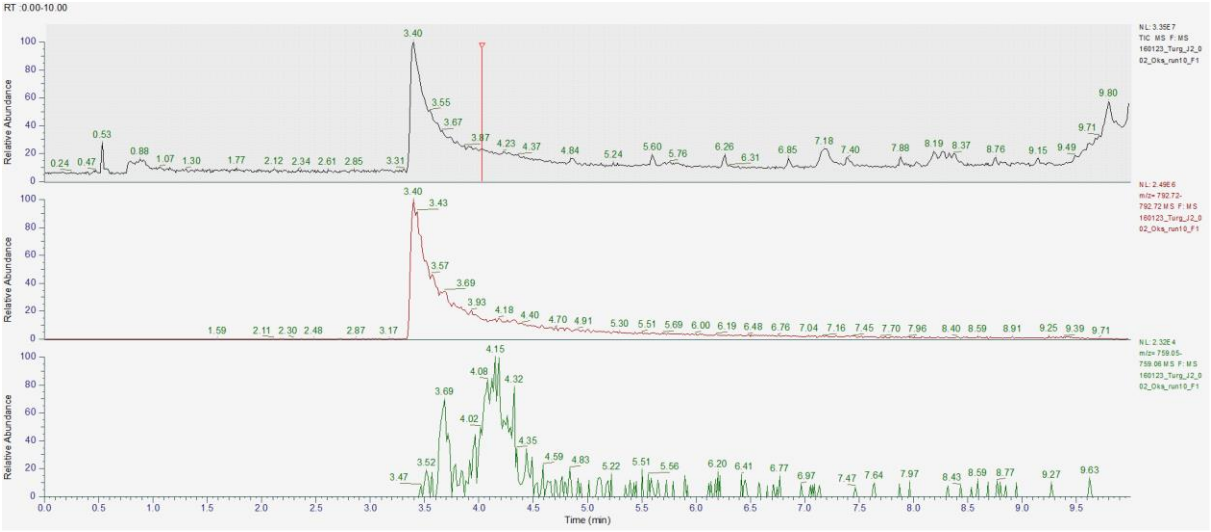

Figure 39: Chromatogram from UPLC-MS analysis of the first fraction containing the peak in the blue colored box in Figure 38. The upper chromatogram is the total ion chromatogram, the second chromatogram is showing when the m/z for the oxidized peptide at 3 charges (792.7166-792.7246) is detected. The lower chromatogram shows when an ion with the m/z for the oxidized complete peptide at 3 charges (759.0518-759-0594) is detected.

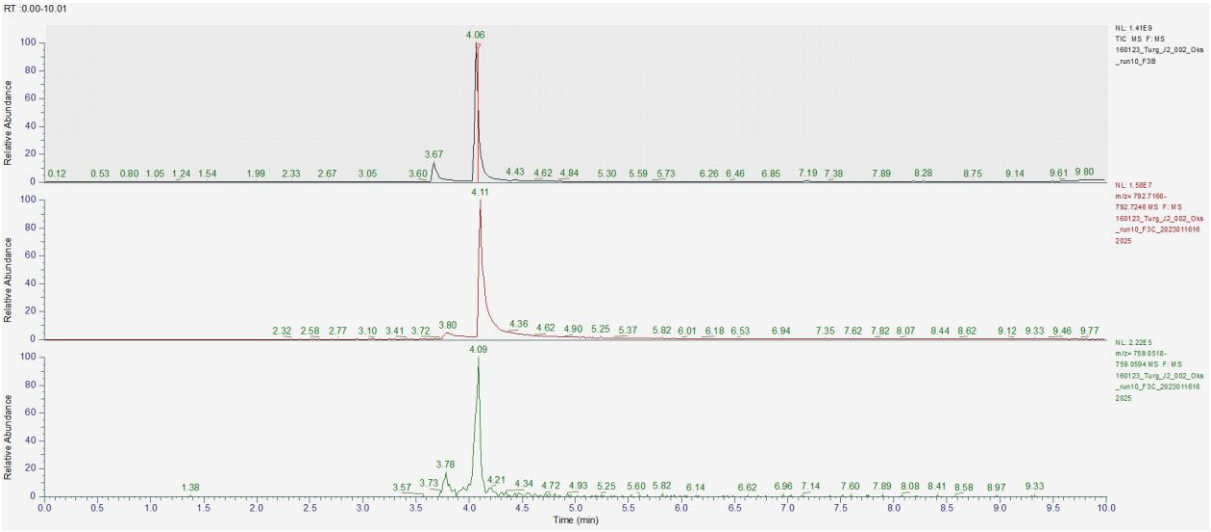

Figure 40: Chromatogram from UPLC-MS analysis of the fraction containing the beginning of the peak in the green colored box in Figure 38. The upper chromatogram is the total ion chromatogram, the second chromatogram is

showing when the m/z for the oxidized peptide at 3 charges (792.7166-792.7246) is detected. The lower chromatogram shows when an ion with the m/z for the oxidized complete peptide at 3 charges (759.0518-759-0594) is detected.

Figure 39 does show some noise that may be caused by contaminants, but there seems to only be a single isomer present. Figure 40 shows both Isomer II and III in the second chromatogram, as well as detector response for the oxidized incomplete peptide in the third chromatogram. However, in the third chromatogram some of the incomplete unoxidized peptide is detected. Isomer II was detected in the fraction containing the peak in the yellow box, with its mass spectrum showing some contaminants as well (Data not shown).

None of the isomers could be isolated in enough quantities to perform purity analysis, as the little that could be isolated was sent for bioactivity testing.

6.5 Elucidation of disulfide bond configuration

6.5.1 Turg_JK_1

6.5.1.1 Isomer I

In the mass spectrum for Isomer I of Turg_JK_1 after the sequential reduction and alkylation, the b^{+3}-ion 484.5663 and b^{+4}-ion 494.5019 were observed. These can be seen in Figure 41. The mass spectra for the remaining ions in this chapter can be found in the Appendix in chapter 10.5. These ions are formed when the bond between the 9^{th} and 10^{th} amino acid are broken, and the bond between the 14^{th} and 15^{th} amino acids respectively. These indicate that the alkylation pattern of the two first cysteines in the sequence are either 1-NEM/2-NCM or 1-NCM/2-NMM, which rules out the possibility of a 1-2/3-4 configuration. The y^{+2}-ion with an m/z of 711.8477 was also observed and supports these deductions and is caused by a fragmentation between the 9^{th} and 10^{th} amino acids. The mass spectrum for this ion is shown in Figure 43.

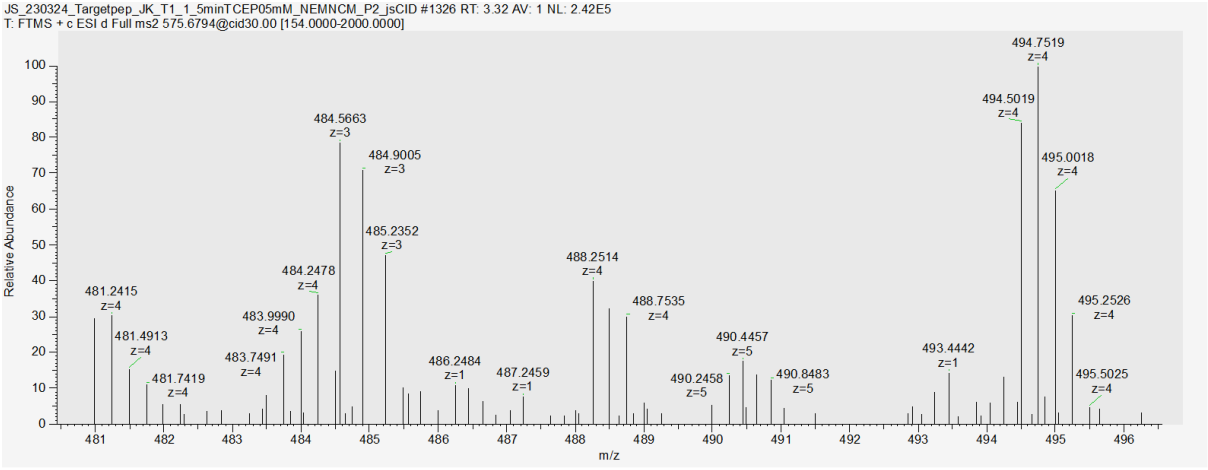

Figure 41: MS2 spectrum of ion 575.6794, which is the molecule ion for Turg_JK_1 alkylated with two NEM and NCM groups at 5 charges. The sample is of isomer I of Turg_JK_1 after sequential reduction and alkylation. b^3-ion 484.5663 and b^{+4} 494.5019 are present in the spectrum.

Further, the a-ion 312.1379 is observed as seen in, which is caused by the fragmentation of the bond between the 2nd and 3rd amino acids. The mass spectrum for this in Figure 44. This ion suggests that the first cysteine is alkylated with an NEM-group, which suggest a 1-NEM/2-NCM pattern. This is also supported by the y-ion 662.0820 which is caused by the fragmentation of the bond between the 1st and 2nd amino acid. This mass spectrum is shown in Figure 45.

Lastly, the b-ion with an m/z of 507.8502 was observed, which is caused by a fragmentation of the bond between the 17th and 18th amino acids. The mass spectrum is shown in Figure 46. The y-ion 671.3334 was also observed, which is caused by a fragmentation of the 15th and 16th amino acids. The mass spectrum is shown Both of these suggest that the last cysteine is alkylated with an NCM group. Thus, the fragmentation pattern was determined to be 1-NEM/2-NCM/3-NEM/4-NCM, which is characteristic of a 1-3/2-4 pattern.

A spreadsheet showing the two possible theoretical fragments and hits of Turg_JK_1 alkylated with two NEM and NCM groups with a 1-3/2-4 pattern is shown in Table 13 and Table 14 in chapters 10.6 in the appendix.

6.5.1.2 Isomer II

Unfortunately, we could not isolate sufficient amounts of isomer II of Turg_JK_1 for structure determination. However, this was not the case for the other peptide isomers. Then, by an elimination process, isomer II likely possesses a 1-4/2-3 configuration.

6.5.1.3 Isomer III

In the mass spectrum for Isomer III the b^{+2}-ions ion with an m/z 753.3681 and b^{+3} ion with an m/z of 502.5812 were detected. The former is shown in Figure 42, while the latter is shown in Figure 48 in the appendix. All remaining MS^2 spectra in this chapter will be found in the appendix chapter 10.7. The ions that were mentioned form when the peptide bond between the 9^{th} and 10^{th} amino acids in the sequence is broken.

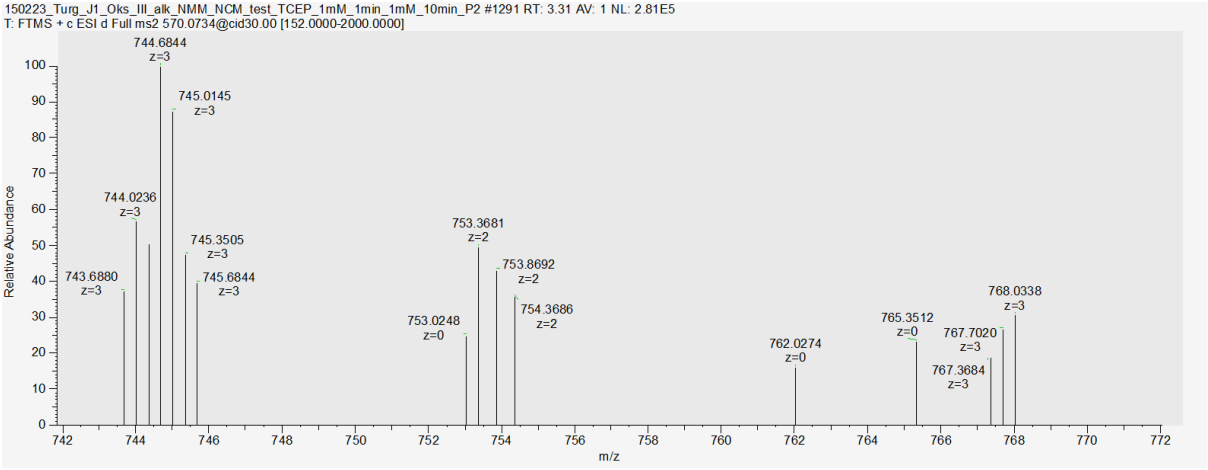

Figure 42: MS^2 spectrum of ion 570.0734, which is the molecule ion for Turg_JK_1 alkylated with two NMM and NCM groups at 5 charges. The sample is of isomer III of Turg_JK_1 after sequential reduction and alkylation. b^{+2}-ion 753.3681 is present in the spectrum.

Further, the y^{+2}-ion with an m/z of 670.8085 and y^{+3} ion with an m/z of 447.5416 were observed. The former is shown in the mass spectrum in Figure 49, and the latter in the mass spectrum in Figure 50. These y-ions form when the y-ions the bond between the 9^{th} and 10^{th} amino acid is broken. These ions suggest an alkylation pattern of 1-NMM/2-NMM/3-NCM/4-NCM, which is characteristic of a 1-2/3-4 connectivity.

A spreadsheet showing the two possible theoretical fragments and hits of Turg_JK_1 alkylated with two NMM and NCM groups with a 1-2/3-4 pattern is shown in Table 15 and Table 16 in chapter 10.8 in the appendix.

6.5.2 Turg_JK_2

Unfortunately, as sufficient amounts of the peptide isomers could not be isolated, the disulfide connectivity of any of the isomers could not be determined. Further studies are required for proper elucidation.

6.6 Bioactivity testing

Bioactivity testing was performed at NFH for all isomers of Turg_JK_1, Isomer I of Turg_JK_2, and a pooled sample containing Isomer II and III for Turg_JK_2. The results are shown in Table 9.

Table 9: MIC of Turg_JK_1 and Turg_JK_2 against several bacteria. "OXY" stands for Oxytetracycline and is used as a control.

RESULTS MIC (MICROG/ML) SAMPLE	E.C ATC 25922	C.G ATC 13032	S.A ATC 9144	P.A ATC 27853	B.S ATC 23857	S.E ATC RP62A	N=	COMMENTS
Turg_JK_1								
Isomer I	15,6	0,49	62,5	15,6	3,9	15,6	3	microgr/ml
Isomer II	31,2	0,49	31,2	31,2	3,9*)	15,6	3	microgr/ml
Isomer III	7,8	0,49	31,2	15,6	3,9	3,9	3	microgr/ml
Turg_JK_2								
Isomer I	7,8	0,49	7,8	7,8	3,9	1,9	3	microgr/ml
Isomer II and III	7,8	0,49	15,6	15,6	3,9	3,9	2	microgr/ml
OXY	0,62	0,15	0,31	10	20	0,15	2	microM
Incubation time	24h	24h	24h	24h	24h	24h		

*) n=2

7 Discussion

7.1 Peptide synthesis

7.1.1 Turg_JK_1

The peptide synthesis for Turg_JK_1 may need further optimization. As discussed in chapter 6.2.1, the peptide synthesis produced a biproduct in the form of an incomplete peptide that is missing the last cysteine group, which is shown in both the purity analysis in Figure 19 and in the chromatogram from the sample preparation of the crude in Figure 21. This may suggest difficulty attaching the last cysteine to the peptide chain during the synthesis, and therefore the conditions of the last attachment step may be a good place to start the optimization process. A possibility may be to perform the attachment step of the last amino acid twice, to ensure that it is attached to every peptide chain.

Because of the formation of the biproduct, the total amount of peptide yield was lowered for the synthesis, which likely contributed to there not being sufficient amounts of isomer II of Turg_JK_1 for disulfide bond elucidation.

7.1.2 Turg_JK_2

As for Turg_JK_1, the synthesis of Turg_JK_2 could likely be improved. The chromatogram from the purity analysis in Figure 20 shows two peaks eluting close to each other. This is further confirmed as an incomplete peptide was observed in the mass specter in Figure 25. This may have been caused by a power outage during the synthesis, which caused us to repeat the last steps of the synthesis. Another explanation may be that the synthesis is in need of optimization like for Turg_JK_1, like performing a double coupling step for the last amino acid.

7.2 Sample preparation of the crude

7.2.1 Turg_JK_1

We were able to provide acceptable separation of Turg_JK_1 from the rest of the peptide crude, including the incomplete peptide. The selectivity between Turg_JK_1 and the incomplete peptide was large enough with the given conditions, and thus the separation of the two was

solved without difficulty. If the peptide synthesis is optimized to avoid the formation of the incomplete peptide, the sample preparation would avoid the need to separate these peaks as well.

7.2.2 Turg_JK_2

For Turg_JK_2 we could not find a gradient that could provide complete separation of the peptide from the rest of the impurities/contaminants in the crude without changing the mobile phase and/or column. The final gradient used in this step was from 20 to 23 % mobile phase B over 25 minutes, which is a very gentle gradient, and is not preferred as it results in wider chromatographic peaks.

As seen in the mass spectrometer in Figure 25, this is likely caused by the incomplete peptide. However, the peptide still must go through another separation process using preparative HPLC after the oxidation process, and the level of separation in this step was therefore deemed acceptable. A solution to this problem would be the same as for Turg_JK_1, which is utilizing another column/mobile phase, or optimizing the peptide synthesis to avoid the formation of the incomplete peptide. The chromatogram from the preparative HPLC during the separation of the oxidized isomers in Figure 38 did however seem to contain more contaminants from visual inspection, compared to the same chromatogram for Turg_JK_1 in Figure 34.

A solution may be to utilize another mobile phase or use a different column that provides better separation. Another solution would be to optimize the peptide synthesis, so the peptide is completely synthesized.

Unfortunately, a substantial amount of peptide crude was lost due to human error while using the preparative HPLC. One such instance is that the pump system went dry due to running out of mobile phase, which caused the system to only pump through a single mobile phase, which in turn caused a few runs worth of peptide crude. This contributed to a lower recovery of the isomers.

7.3 Oxidation of the linear peptides.

The time needed for the oxidation process to complete seemed to vary drastically even between parallels of the same peptide. The reason for this is unknown and may depend on a variety of factors that may or may not be out of our control. A reason could be that it is impossible to control the amount of oxygen that is present within the peptide solution, which could affect the rate of oxidation.

7.3.1 Turg_JK_1

All but one parallel (parallel 7) of Turg_JK_1 were completely oxidized and yielded three isomers each. It is not known what caused parallel 7 to polymerize, but a possibility is that the peptide was transferred too rapidly to the water in the oxidation process. Whether this is the reason for the polymerization or not is difficult to confirm.

7.3.2 Turg_JK_2

Every parallel of Turg_JK_2 were completely oxidized and yielded three isomers each. As seen in the mass spectrometers, several contaminants were present. The incomplete peptide stems from there not being adequate separation in the sample preparation of the crude. Thus, the contaminants may have interfered for later studies performed on isomer II and III.

7.4 Separation of the isomers of the oxidized peptide

7.4.1 Turg_JK_1

The separation process proved at first difficult. It was thought that split peaks of isomers II and III in the chromatogram shown in Figure 32 were caused by the isomers creating two different conformers, with differing retention times. This did however prove to unlikely as adding TFA would solve this problem, as discussed in chapter 5.4.2. This made the separation easier, and a steeper gradient could also be used. It did, however, cause the broadening of the peak containing isomer I, as seen in Figure 34. The reason for this is unknown, as in Figure 32 it had formed a sharp peak at the start of the chromatogram when TFA was not added to the sample before a run.

At first it was attempted to separate between the split peaks of isomer II and III, which required a gentler gradient of mobile phase B. This in turn caused the slopes of the peaks to be too gentle to be automatically collected by the fraction collector. Thus, the collection windows had to be entered manually, which proved to be difficult as well because of variance in the retention times of the peaks. These problems combined caused unnecessary loss of peptide isomers.

We successfully isolated the peptide isomers in descending order of abundance: I, III, and II. However, during the oxidation process isomer III seems to have formed most frequently, as seen in Figure 28, assuming that the order of elution is the same between the chromatograms in Figure 28 and Figure 34. This assumption is made because a reverse-phase column is used on both systems, and the used mobile phases are the same, except that TFA is used instead of FA for pH control for the preparative HPLC.

We successfully isolated the peptide isomers in descending order of abundance: I, III, and II. However, Figure 32 and Figure 34 did not provide a clear answer as to what isomer formed the most frequently, as the peak for isomer III is split in Figure 32, and the peak for isomer I is broadened in Figure 34. The peptide that Turg_JK_1 was based on, Turg_JS_001 formed the isomer correlating to isomer III of Turg_JK_1 most frequently.

The purity analysis shows results that suggest high purity for both isomer I and III, which suggests that the separation provided excellent separation of the isomers from the rest of the matrix.

7.4.2 Turg_JK_2

Unfortunately, a gradient that provided acceptable levels of separation between isomers II and III for Turg_JK_2 could not be found. Possible solutions include using another column or mobile phase that provides better separation between the two isomers, as with the gradients used in this thesis there is a degree of co-elution. Like for Turg_JK_1, the peaks were not steep enough for the fraction collector to automatically detect the peaks, so the collection windows had to be set manually. Due to the proximity of isomers II and III along with variation in retention times per run, it was difficult to isolate isomers II and III, as seen in Figure 40. This along with limited amounts of oxidized peptide resulted poorly both in terms of amount of

peptide isolated and the separation of isomers II and III. At first, oxidized peptide used to determine a gradient was not collected and was as such unnecessarily discarded. This, along with human error during the use of the HPLC contributed to there not being enough of even a single isomer for both bioactivity testing and elucidation of the disulfide structure.

In the chromatogram from the preparative HPLC in Figure 38, the peak in the yellow box containing isomer II is not as uniform as the others. The reason for this may be that the peaks containing isomer II and III could not be separated, or the presence of contaminants. As seen in both Figure 31 and Figure 40, the oxidized peptide contained contaminants, which further complicated the chromatography.

7.5 Disulfide connectivity

7.5.1 Turg_JK_1

7.5.1.1 Isomer I

Isomer I is thought to have a 1-3/2-4 disulfide configuration from the studies conducted in this thesis. As discussed in chapter 6.5.1.1, this is because of the identification of several b-ions that are characteristic of this type of configuration.

7.5.1.2 Isomer II

Isomer II is thought to have a 1-4/2-3 disulfide configuration from a process of elimination. This is because the two other isomers possess the other possible configurations. Further studies are required to confirm this, however.

7.5.1.3 Isomer III

Isomer III is thought to possess a 1-2/3-4 disulfide configuration.

Compared to the other isomers, the disulfide bonds in this isomer make up the smallest cyclic structures in the peptide, as the disulfide pairs are closer to each other in the peptide chain. This may have played a part in its superior levels of antimicrobial activity, if the result is an orientation of the amino acids that is favorable for its antimicrobial activity. However, this is speculation, and further studies is needed to confirm this theory.

7.5.1.4 Impact of substituted amino acids

The peptide that both Turg_JK_1 and Turg_JK_2 is based on, Turg_JS_001, forms the isomer with a 1-2/3-4 configuration most frequently after the oxidation process as described in ongoing work. After the isolation of the isomers of Turg_JK_1, isomer I that possesses a 1-3/2-4 configuration was isolated in the largest amount. However, this does not necessarily mean that this formed the most frequently, as discussed in earlier chapters.

7.5.2 Turg_JK_2

Because sufficient amounts of the peptide could not be isolated, the disulfide connectivity could not be determined. Further studies are required for this, and it would be interesting to see if the ratio between the amount of each isomer formed during the oxidation process differs between the two peptides in this thesis.

7.6 Bioactivity testing

Both peptides showed an improvement in MIC compared to the peptide they were based on, Turg_JS_001, as a lower MIC was observed for all peptide isomers. Antimicrobial activity was also shown against *Staphylococcus aureus* (S.A.), where there previously was none. As theorized in chapter 3.2.1, this is likely caused by the additional tryptophane and arginine groups that substitute several amino acids within the peptide sequence.

The results suggest that replacing the amino acids seems promising, but it is still not known how this impacts the selectivity of the peptide against human cells. Previous studies with peptide analogues of Turgencin A with amino acids replaced with tryptophan and arginine were conducted. None of the changes made to the amino acid sequence resulted in significant hemolytic activity (33), suggesting that this may also apply for the peptides in this study. This, however, has to be confirmed by further studies. If the peptides are to be used as therapeutics, it is of the utmost importance that the activity against human cells is kept to acceptable levels.

7.6.1 Turg_JK_1

The decreased MIC of all isomers of Turg_JK_1 compared to Turg_JS_001 suggest increasing the hydrophobicity of the edges of the peptide and increasing the basicity of the middle of the peptide leads to a more efficient disruption of the bacterial membrane.

The three isomers of Turg_JK_1 all show antimicrobial activity, suggesting that the peptide does not need to have a specific disulfide connectivity to exert some levels of antimicrobial activity. The disulfide connectivity does make a difference, however, as isomer III is shown to be the most potent of the three. It is likely that the differing disulfide bridges cause the isomers to have different conformations, with some that can more efficiently disrupt the bacterial membranes than others. This is supported by the fact that the isomers of Turg_JK_1 had differing MICs between each other.

Isomer I seems to perform better against the gram-negative bacteria E.C. and C.G., while isomer II has better performance against S.A. when the two are compared. This suggests that the conformation of isomer I more efficiently disrupts the outer membrane of a gram-negative bacterium. Isomer II on the other hand has better activity against S.A., but the activity against the rest of the gram-positive bacteria is identical between the two.

As explained, isomer III seems to have the most activity of the three isomers. The largest reduction in MIC was about 4-fold against S.E. The activity against E.C. was also lower than the rest of the isomers by about 2-fold compared to isomer I. The MIC against the rest of the bacteria was equal to the lower MIC of the two other isomers. This does suggest that the conformation of isomer III is favored against both gram-positive and -negative bacteria. From the structure of isomer III, this suggests that the smaller cyclical regions formed by the disulfide bonds may be favorable for its activity. This may either be caused by the edges of the peptide becoming more rigid, or that the conformation of the mid-part of the peptide is relatively flexible.

7.6.2 Turg_JK_2

Turg_JK_2 has superior levels of activity compared to both Turg_JS_001 and Turg_JK_1. This suggests that increasing the basicity of the edges of the peptide and the hydrophobicity of the

middle of the peptide is a superior strategy compared to vice versa. This may be caused by either that the edges can more efficiently form electrostatic interactions with the bacterial membrane, or that the middle part of the peptide can more efficiently embed into and disrupt the membrane.

Isomer I and the mixture of isomers II and III of the peptide isomers display improved activity against the bacterial strains S.A. and P.A. compared to Turg_JK_1, while showing the same or better MIC for the rest of the bacterial strains. As for Turg_JK_1, it seems like all the isomers show antibacterial activity.

7.6.2.1 Isomer I

Out of all the peptide isomers that were isolated, isomer I displays the highest potency against the tested bacterial strains. This is especially true in activity against S.A., where the MIC is considerably lower than the activity that was shown for all isomers of Turg_JK_1. Overall, this peptide isomer seems to be the most potent antibacterial agent in this thesis.

7.6.2.2 Mixture of isomers II and III

Because the isomers were pooled together in a mixture, it is difficult to say which isomer contributed to the activity against each bacterial strain for mixture 2. As explained in chapter 7.3.2 and 7.4.2, some contaminants were present in these isomers. Thus, some of the antimicrobial activity may also have been contributed by those contaminants.

All isomer of both Turg_JS_001 and Turg_JK_1 showed antimicrobial activity, so it is likely that this is the case for Turg_JK_2 as well, but the actual antimicrobial activity per isomer is unknown.

The mixture does, however, display better antimicrobial activity than the most potent isomer of Turg_JK_1. While it does look promising, further studies are required to confirm each of the isomer's individual activity against the different strains.

It should be noted that Antimicrobial peptides in marine invertebrates are only a part of the immune response, along with both cellular responses and other humoral responses (12), and thus seldom work just on their own. This is also the case for Turgencin A, as three other

antimicrobial peptides were identified from *Synoicum Turgens* (1). It is possible that the AMPs may provide a synergistic effect with other AMPs or conventional antibiotics, by weakening the bacterial membrane. A synergistic effect similar to this is already known between aminoglycosides and cell wall-active agents such as beta-lactams (34). Thus, AMPs such as the ones in this thesis could have a place in future antimicrobial therapy by working together with conventional antibiotics and increasing their efficacy.

7.6.3 Comparison with other antimicrobial peptides and antibiotics

7.6.3.1 Other Turgencin A-based peptides

Previous work based on the same peptide by Dey et al. (33), Turgencin A, produced several antimicrobial peptides. The first peptide was based on a 10 amino acid length sequence taken from within the loop region of Turgencin A, which correlate to the amino acids between C2 and C3 in Turg_JK_1 and Turg_JK_2. This peptide was modified further, replacing the amino acids with tryptophane and arginine, creating 7 different peptides in total. These peptides were further modified to new peptides, which were cyclized by the formation of disulfide bonds and/or acylated with aliphatic fatty acids (33). The most potent isomer of this study, isomer I of Turg_JK_2 was compared to the most potent peptide in each series from the study, the MICs can be found in Table 10.

Table 10: Summary of MIC values for isomer II of Turg_JK_2 and the peptides from the study by Dey et al. (33).

RESULTS MIC (MICROG/ML)

SAMPLE	E.C ATC 25922	C.G ATC 13032	S.A ATC 9144	P.A ATC 27853	B.S ATCC 23857	S.E ATC RP62A
Turg_JK_2						
Isomer I	7,8	0,49	7,8	7,8	3,9	1,9
From Dey et al.						
cTurg-6	8	4	16	16	4	8
C12-Turg-1	8	4	8	16	4	8
c8-cTurg-2	4	2	4	8	2	4

First, when compared to the most potent peptide in the cyclized peptide series, cTurg-6, Isomer I of Turg_JK_2 displayed an equal or lower MIC against every bacteria.

When compared to the most potent peptide in the series of linear acylated peptides, C12-Turg-1, the results were the same as for the previous peptide, with the exception being C12-Turg-1 showing equal levels of activity versus S.A. compared to isomer I of Turg_JK_2 (8 µg/mL vs 7.8 µg/mL).

Lastly, isomer I of Turg_JK_2 was compared to the most potent peptide in the series of cyclized and acylated peptide, and also the most potent peptide from the study, C8-cTurg-2. When comparing the two, isomer II of Turg_JK_2 shows higher levels of activity against C.G. and S.E. Equal levels of activity against P.A. And at last, worse levels of activity against E.C, S.A., and B.S.

The comparison shows promising results, with only C8-cTurg-2 showing better results. It is worth noting that the peptides from the study by Dey at al (33) are somewhat smaller in size, compared to the peptides in this study. The peptides from the study contain 12 amino acids, versus the 19 that the peptides in this study contain. Thus, if the activity was measured in molarity instead of µg/mL, then isomer II of Turg_JK_2's results would likely be improved.

The study does however note that the latter did cause an increase in hemolytic activity, which was likely caused in part by the acyl chain elongation. The hemolytic activity isomer II of Turg_JK_2 and all of the other isomers in this study is unknown however, and thus a comparison in hemolytic activity is impossible.

7.6.3.2 Other Antimicrobial Peptides

The results for the antimicrobial activity of other AMPs and antibiotics were fetched from the study "Comparative Evaluation of the Antimicrobial Activity of Different Antimicrobial Peptides against a Range of Pathogenic Bacteria" by Ebbensgaard et al. (4). In the study, the AMPs and antibiotics were tested against 10 different strains of bacteria. Of these 10, the bacterial strains of E.C (ATCC 25922) and P.A. (ATCC 27853) were also tested in this study. While the AMPs were both tested against S.A., the bacterial strains were not the same. As such, the results are not necessarily representative of any difference in antimicrobial activity. The MIC methods used in the study was according to the methods from the Clinical and Laboratory Standard Institute (CLSI). All of the results are given in micrograms/mL, and as such take no

consideration to the molecular size of the AMP or antibiotic. As AMPs are peptides, they are larger in size than a traditional antibiotic, and as such the molar mass will be significantly larger. Further, this comparison cannot be directly used to compare efficacy *in vivo*, as the toxicity and eventual realistic plasma concentrations of the peptides in this study is unknown. The results from the study by Ebbensgaard et al. (4) can be found in Table 11.

Table 11: «Data are collected as minimal inhibitory concentrations (MICs) according to the Clinical and Laboratory Standards Institute (CLSI) and expressed in µml. All MIC determinations were carried out in duplicates for AMPs and in triplicate for antibiotics; n.d. = not determined.». Fetched from work by Ebbensgaard et al. (4). Data was transformed to remove the bacterial strains that were not tested in this study and was reformatted in the style of Table 9 for easier comparison.

RESULTS MIC (MICROG/ML)

SAMPLE	E.C. ATCC25922	S.A. ATCC29213	P.A. ATCC27853
Antimicrobial Peptides			
Cap18	4–8	≥32	4–8
Cap11	8–16	16–32	8
Cap11-1-18m 2	16–32	16	16–32
Cecropin P1	16–32	>256	>256
Cecropin B	16–32	>256	64
Bac2A-NH 2	64	128	128–256
Bac2A	256	>256	256
Sub5-NH 2	4	8	8
Myxinidin	>256	>256	>256
Melittin	16	2–4	≥64
Indolicidin	32	32	>64
Myxinidin-NH 2	>256	>256	>256
Pyrrhocoricin	>256	>256	>256
Apidaecin IA	32	>256	>256
Metalnikowin I	>256	>256	>256

The study notes that the AMP Cap18 seems to display the highest level of activity against most of the 10 bacterial strains that it was tested against. Against the bacteria that was tested in both the study and this thesis however, the AMP Sub5-NH_2 seems to be the most potent. Thus, the comparison will focus on these two peptides.

Isomer I of Turg_JK_2 has an MIC of 7.8 against all three of E.C., S.A., and P.A. Cap18 shows an activity of 4-8, ≥32, and 4-8 against E.C., S.A., and P.A. respectively. The activity against E.C. and P.A. are comparable, as they are within the same range. Isomer I of Turg_JK_2 does however show a sizable lower MIC against S.A., which is lower by about 4-fold. It is worth noting that Cap18 is a substantially larger peptide, with 38 amino acids compared to the 19 in isomer II of Turg_JK_2. Thus, results would likely improve for Cap18, if the MICs were measured in molarity instead of µg/mL

Compared to Sub5-NH_2, isomer I of Turg_JK_2 shows higher MIC values for E.C., with an MIC of 7.8 vs 4. They show similar levels of activity against both S.A. and P.A., with MICs of 7.8 for isomer I of Turg_JK_2 versus an MIC of 8 for Sub5-NH_2. Sub5-NH_2 is a somewhat smaller peptide, with 11 amino acids. Thus, the results for isomer I of Turg_JK_2 would likely improved if the MICs were measured in molarity instead of µg/mL

When comparing the MIC values to other AMPs, the results show promise for the antimicrobial activity of isomer I of Turg_JK_2, but further studies are still needed to explore its other attributes such as hemolytic activity, solubility etc.

8 Conclusion

A method was developed for synthesizing and isolating two DRPs, with varying levels of success affected by difficulties in the purification process and human error. However, it has shed light on some of the difficulties that may occur and suggestions on how they could be improved. The method developed structure elucidation through sequential reduction and alkylation of the disulfide bridges proved to be a promising method. The disulfide connectivity was elucidated for the two peptide isomers that were successfully isolated in sufficient amounts. This was done by analysis of the mass spectra that were produced from the reduced and alkylated peptide isomers.

The DRPs synthesized in this study have proven to be superior to the original peptide in terms of antimicrobial activity, suggesting that replacing amino acids with groups that are hydrophobic or can obtain positive charges is a valid strategy in improving an AMPs activity.

From the bioactivity testing, the approach taken in Turg_JK_2 proved to be superior to the one taken in Turg_JK_1. The most potent isomer in this study was isomer I of Turg_JK_2, which had an equal or lower MIC against all the bacterial strains compared to the rest of the isomers that were synthesized. The disulfide connectivity for this is unfortunately unknown.

9 References

1. Hansen IKO, Isaksson J, Poth AG, Hansen KO, Andersen AJC, Richard CSM, et al. Isolation and Characterization of Antimicrobial Peptides with Unusual Disulfide Connectivity from the Colonial Ascidian Synoicum turgens. Mar Drugs. 2020;18(1):51.
2. Hansen IKO, Lovdahl T, Simonovic D, Hansen KO, Andersen AJC, Devold H, et al. Antimicrobial Activity of Small Synthetic Peptides Based on the Marine Peptide Turgencin A: Prediction of Antimicrobial Peptide Sequences in a Natural Peptide and Strategy for Optimization of Potency. Int J Mol Sci. 2020;21(15):5460.
3. Murray CJL, Ikuta KS, Swetschinski L, Robles Aguilar G, Gray A, Han C, et al. Global burden of bacterial antimicrobial resistance in 2019: a systematic analysis. Lancet. 2022;399(10325):629-55.
4. Ebbensgaard A, Mordhorst H, Overgaard MT, Nielsen CG, Aarestrup FM, Hansen EB. Comparative Evaluation of the Antimicrobial Activity of Different Antimicrobial Peptides against a Range of Pathogenic Bacteria. PLoS One. 2015;10(12):e0144611-e.
5. Rietkötter E, Hoyer D, Mascher T. Bacitracin sensing in Bacillus subtilis. Mol Microbiol. 2008;68(3):768-85.
6. Levine DP. Vancomycin: A History. Clinical Infectious Diseases. 2006;42(Supplement-1):S5-S12.
7. Albert A, Eksteen JJ, Isaksson J, Sengee M, Hansen T, Vasskog T. General Approach To Determine Disulfide Connectivity in Cysteine-Rich Peptides by Sequential Alkylation on Solid Phase and Mass Spectrometry. Anal Chem. 2016;88(19):9539-46.
8. Diao L, Meibohm B. Pharmacokinetics and Pharmacokinetic–Pharmacodynamic Correlations of Therapeutic Peptides. Clin Pharmacokinet. 2013;52(10):855-68.
9. Hansen IKØ. Antimicrobial peptides from the Arctic ascidian Synoicum turgens: UiT The Arctic University of Norway; 2022.
10. Petersen JK. Ascidian suspension feeding. Journal of experimental marine biology and ecology. 2007;342(1):127-37.
11. TatiÁN M, Sahade R, Esnal GB. Diet components in the food of Antarctic ascidians living at low levels of primary production. Antartic science. 2004;16(2):123-8.
12. Tincu JA, Taylor SW. Antimicrobial peptides from marine invertebrates. Antimicrob Agents Chemother. 2004;48(10):3645-54.
13. Gehrmann J, Alewood PF, Craik DJ. Structure Determination of the Three Disulfide Bond Isomers of alpha-Conotoxin GI: A Model for the Role of Disulfide Bonds in Structural Stability. J Mol Biol. 1998;278(2):401-15.

14. Huang Y-H, Du Q, Craik DJ. Cyclotides: Disulfide-rich peptide toxins in plants. Toxicon. 2019;172:33-44.
15. Goering R, Dockrell H, Zuckerman M, Chiodini PL. Mims' Medical Microbiology and Immunology. 6 ed. Philadelphia: Philadelphia: Elsevier; 2018.
16. Palomo JM. Solid-phase peptide synthesis: an overview focused on the preparation of biologically relevant peptides. RSC advances. 2014;4(62):32658-72.
17. Varkey JT, Koprowski R. Peptide Synthesis. London, United Kingdom: IntechOpen; 2019.
18. Pedersen-Bjergaard S, Gammelgaard B, Halvorsen TG. Introduction to pharmaceutical analytical chemistry. Second edition. ed. Hoboken, NJ: Wiley; 2019.
19. Smoluch M, Grasso G, Suder P, Silberring J. Mass spectrometry : an applied approach. 2nd ed. Newark: Newark: John Wiley & Sons; 2019.
20. Ekman R. Mass spectrometry : instrumentation, interpretation, and applications. Hoboken, N.J.: John Wiley & Sons; 2009.
21. Scientific TF. Obitrap ID-X Tribrid Mass Spectrometer – Transforming Small Molecule Identification and Structure Elucidation 2018 [Available from: https://assets.thermofisher.com/TFS-Assets/CMD/Specification-Sheets/ps-65188-orbitrap-id-x-tribrid-ms-ps65188-en.pdf.
22. Scientific TF. Molecular Dissociation Technology Overview [Web Page]. [cited 2023 10th of may]. Available from: https://www.thermofisher.com/no/en/home/industrial/mass-spectrometry/mass-spectrometry-learning-center/mass-spectrometry-technology-overview/dissociation-technique-technology-overview.html.
23. Kinter M, Sherman NE. Protein sequencing and identification using tandem mass spectrometry. New York: Wiley-Interscience; 2000.
24. Bonten M, Johnson JR, van den Biggelaar AHJ, Georgalis L, Geurtsen J, de Palacios PI, et al. Epidemiology of Escherichia coli Bacteremia: A Systematic Literature Review. Clin Infect Dis. 2021;72(7):1211-9.
25. Tønjum T. stafylokokker [Web Page]. Oslo: Store medisinske leksikon; 2019 [updated 15th of October 2019; cited 2023 8th of May]. Available from: https://sml.snl.no/stafylokokker.
26. Turner NA, Sharma-Kuinkel BK, Maskarinec SA, Eichenberger EM, Shah PP, Carugati M, et al. Methicillin-resistant Staphylococcus aureus: an overview of basic and clinical research. Nat Rev Microbiol. 2019;17(4):203-18.
27. Kalinowski J, Bathe B, Bartels D, Bischoff N, Bott M, Burkovski A, et al. The complete Corynebacterium glutamicum ATCC 13032 genome sequence and its impact on the production of l-aspartate-derived amino acids and vitamins. J Biotechnol. 2003;104(1):5-25.
28. Sirevåg R. Pseudomonas [Web Page]. Oslo: Store medisinske leksikon; 2022 [updated 9th of October 2022; cited 2023 8th of May]. Available from: https://sml.snl.no/Pseudomonas.
29. Pelegrin AC, Palmieri M, Mirande C, Oliver A, Moons P, Goossens H, et al. Pseudomonas aeruginosa: a clinical and genomics update. FEMS Microbiol Rev. 2021;45(6):1.

30. Ul Haq H, Huang W, Li Y, Zhang T, Ma S, Zhang Y, et al. Genetic and genomic characterization of multidrug resistant Bacillus subtilis M3 isolated from an activated sludge reactor treating wastewater. Biológia. 2022;77(4):1151-60.
31. Otto M. Staphylococcus epidermidis - the 'accidental' pathogen. Nat Rev Microbiol. 2009;7(8):555-67.
32. California TRotUo. MS-Product [Web Page]. Oakland, California: The Regents of the University of California; 2023 [cited 2023 11 April]. Available from: https://prospector.ucsf.edu/prospector/cgi-bin/msform.cgi?form=msproduct.
33. Dey H, Simonovic D, Norberg-Schulz Hagen I, Vasskog T, Fredheim EGA, Blencke H-M, et al. Synthesis and Antimicrobial Activity of Short Analogues of the Marine Antimicrobial Peptide Turgencin A: Effects of SAR Optimizations, Cys-Cys Cyclization and Lipopeptide Modifications. Int J Mol Sci. 2022;23(22):13844.
34. Drew R. Aminoglycosides Waltham, MA: UpToDate; 2023 [updated 12th of December 2022; cited 2023 12th of may].
35. CLSI. Methods for Dilution Antimicrobial Susceptibility Tests for Bacteria That Grow Aerobically; Approved Standard—Ninth Edition. Wayne, PA: Clinical and Laboratory Standards Institute; 2012. Contract No.: CLSI document M07-A9.
36. Paulsen VS, Blencke HM, Benincasa M, Haug T, Eksteen JJ, Styrvold OB, et al. Structure-activity relationships of the antimicrobial peptide arasin 1 - and mode of action studies of the N-terminal, proline-rich region. PLoS One. 2013;8(1):e53326.

10 Appendix

10.1 Peptide synthesis

10.1.1 Calculation Table and report for Turg_JK_1

Biotage

Initiator+ Alstra Peptide Sequence Summary

User: Peptidgruppe
Date: 2022-09-29 10:06
Vial: 10 mL
Resin: Rink amide ChemMatrix
Resin Functionality: Amide
Loading: 0.50 mmol/g
Resin Functionality Molecular Weight: 17.0 g/mol
Molecular Weight: 2265.0 g/mol
Product Weight: 0.374 g
Quantity: 0.330 g
Scale: 0.165 mmol
UV: Off
Notes: Turg_J.1_001-20220929-JK-JS
Sequence:

C K W A W C G R R P G G R R C K W C G #1

Biotage

Table of Contents

Biotage

Calculation Table

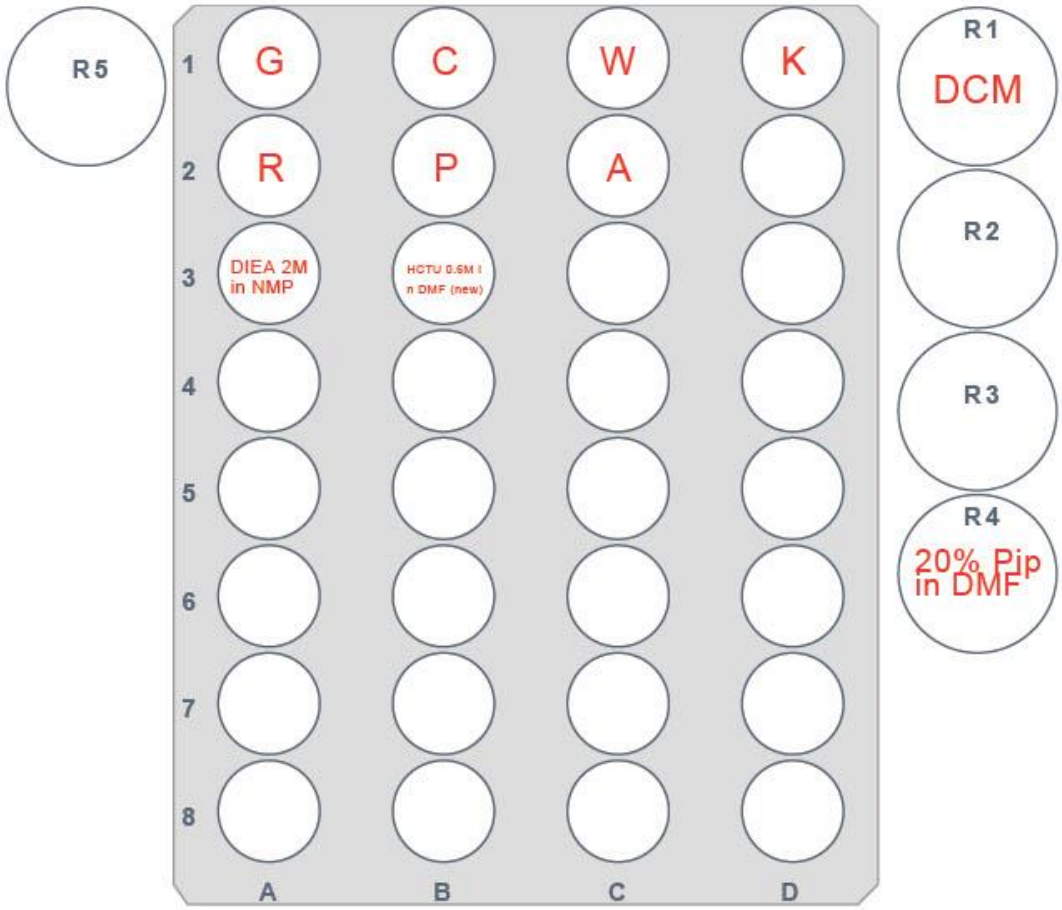

Pos	Acid	Chemical Name	Equivalents	Mol Mass [g/mol]	Mass [g]	Volume [mL]	Dissolve Volume [mL]	Concentration [mol/L]	Total Volume [mL]
A:1	G	Fmoc-Gly-OH	4.0	297.3	0.8		4.752	0.5	5.38
A:2	R	Fmoc-Arg(Pbf)-OH	4.0	648.8	1.745		3.934	0.5	5.38
A:3		DIEA 2M in NMP	8.0	129.2		4.403	8.237	2.0	12.64
B:1	C	Fmoc-Cys(Trt)-OH	4.0	585.7	1.576		4.081	0.5	5.38
B:2	P	Fmoc-Pro-OH	4.0	337.4	0.24		1.23	0.5	1.42

Pos	Acid	Chemical Name	Equivalents	Mol Mass [g/mol]	Mass [g]	Volume [mL]	Dissolve Volume [mL]	Concentration [mol/L]	Total Volume [mL]
B:3		HCTU 0.6M in DMF (new)	4.0	413.7	5.212		21.0	0.6	21.0
C:1	W	Fmoc-Trp(Boc)-OH	4.0	526.6	1.069		3.183	0.5	4.06
C:2	A	Fmoc-Ala-OH	4.0	311.3	0.221		1.246	0.5	1.42
D:1	K	Fmoc-Lys(Boc)-OH	4.0	468.5	0.642		2.217	0.5	2.74
R1		DCM				0.0			32.0
R4		20% Piperidine in DMF	54.55	85.2		34.771	141.229	2.0	176.0
S1		DMF				0.0			2218.0
S2		NMP				0.0			13.5

Cycle No: 1

G (Fmoc-Gly-OH)

Swelling DMF, 2022-09-29 10:06

Reaction: Temp: 70°C **Time (mm:ss):** 20:00 **Oscillating Mixer:** On

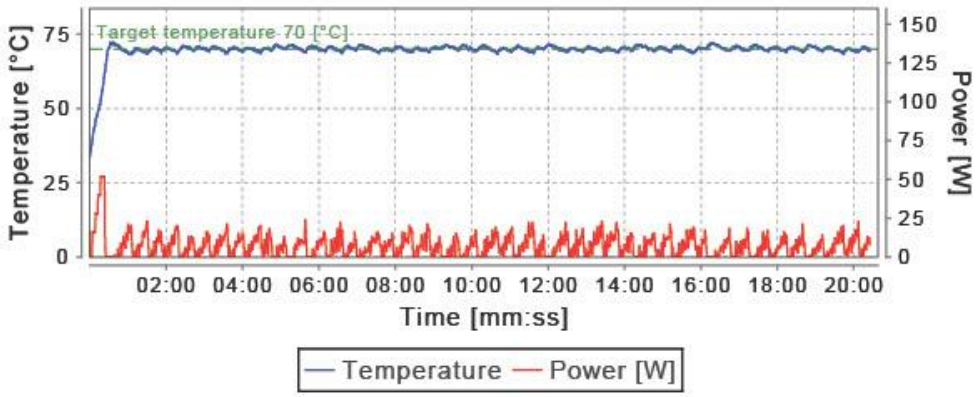

NY HCTU/DIEA mw 1=1eq, 2022-09-29 10:27

Reaction: Temp: 75°C **Time (mm:ss):** 10:00 **Oscillating Mixer:** On

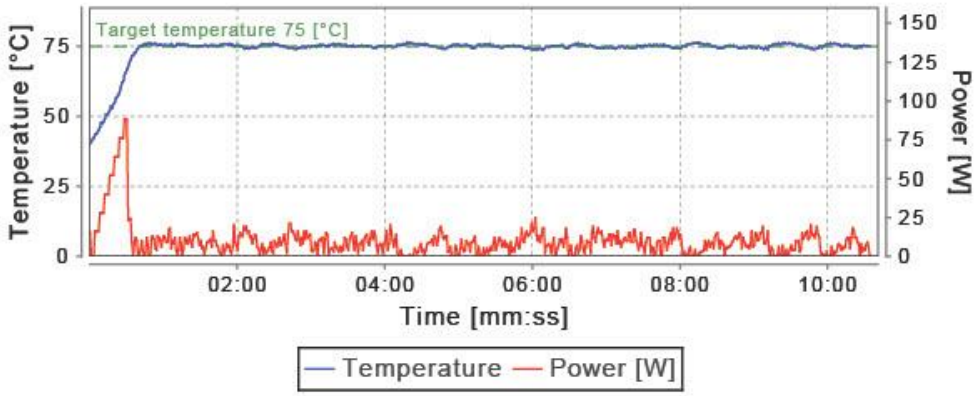

Cycle No: 2

C (Fmoc-Cys(Trt)-OH)

20% Piperidine , 2022-09-29 10:51

Reaction: Temp: Room Temperature **Time (mm:ss):** 03:00 **Oscillating Mixer:** On **Interval Mixing On/Off:** 10/15

Reaction: Temp: Room Temperature **Time (mm:ss):** 10:00 **Oscillating Mixer:** On **Interval Mixing On/Off:** 10/15

NY HCTU/DIEA r.t.1-1eq, 2022-09-29 11:17

Reaction: Temp: Room Temperature **Time (mm:ss):** 60:00 **Oscillating Mixer:** On

Cycle No: 3

W (Fmoc-Trp(Boc)-OH)

20% Piperidine , 2022-09-29 12:30

Reaction: Temp: Room Temperature **Time (mm:ss):** 03:00 **Oscillating Mixer:** On **Interval Mixing On/Off:** 10/15

Reaction: Temp: Room Temperature **Time (mm:ss):** 10:00 **Oscillating Mixer:** On **Interval Mixing On/Off:** 10/15

NY HCTU/DIEA mw 1=1eq, 2022-09-29 12:57

Reaction: Temp: 75°C **Time (mm:ss):** 10:00 **Oscillating Mixer:** On

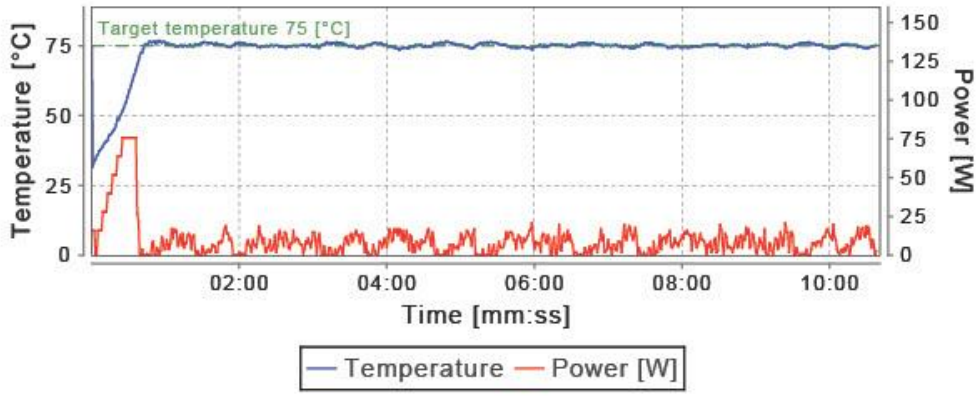

Cycle No: 4

K (Fmoc-Lys(Boc)-OH)

20% Piperidine , 2022-09-29 13:20

Reaction: Temp: Room Temperature **Time (mm:ss):** 03:00 **Oscillating Mixer:** On **Interval Mixing On/Off:** 10/15

Reaction: Temp: Room Temperature **Time (mm:ss):** 10:00 **Oscillating Mixer:** On **Interval Mixing On/Off:** 10/15

NY HCTU/DIEA mw 1=1eq, 2022-09-29 13:47

Reaction: Temp: 75°C **Time (mm:ss):** 10:00 **Oscillating Mixer:** On

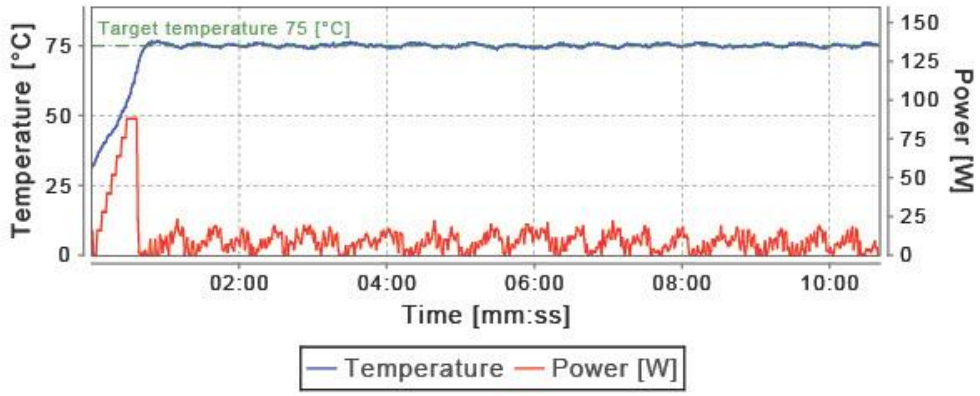

Cycle No: 5
C (Fmoc-Cys(Trt)-OH)
20% Piperidine , 2022-09-29 14:10
Reaction: Temp: Room Temperature **Time (mm:ss):** 03:00 **Oscillating Mixer:** On **Interval Mixing On/Off:** 10/15
Reaction: Temp: Room Temperature **Time (mm:ss):** 10:00 **Oscillating Mixer:** On **Interval Mixing On/Off:** 10/15
NY HCTU/DIEA r.t.1-1eq, 2022-09-29 14:36
Reaction: Temp: Room Temperature **Time (mm:ss):** 60:00 **Oscillating Mixer:** On

Cycle No: 6
R (Fmoc-Arg(Pbf)-OH)
20% Piperidine , 2022-09-29 15:49
Reaction: Temp: Room Temperature **Time (mm:ss):** 03:00 **Oscillating Mixer:** On **Interval Mixing On/Off:** 10/15
Reaction: Temp: Room Temperature **Time (mm:ss):** 10:00 **Oscillating Mixer:** On **Interval Mixing On/Off:** 10/15
NY HCTU/DIEA r.t.1-1eq, 2022-09-29 16:16
Reaction: Temp: Room Temperature **Time (mm:ss):** 60:00 **Oscillating Mixer:** On

Cycle No: 7

R (Fmoc-Arg(Pbf)-OH)

20% Piperidine , 2022-09-29 17:28

Reaction: Temp: Room Temperature **Time (mm:ss):** 03:00 **Oscillating Mixer:** On **Interval Mixing On/Off:** 10/15

Reaction: Temp: Room Temperature **Time (mm:ss):** 10:00 **Oscillating Mixer:** On **Interval Mixing On/Off:** 10/15

NY HCTU/DIEA r.t.1-1eq, 2022-09-29 17:55

Reaction: Temp: Room Temperature **Time (mm:ss):** 60:00 **Oscillating Mixer:** On

Cycle No: 8

G (Fmoc-Gly-OH)

20% Piperidine , 2022-09-29 19:07

Reaction: Temp: Room Temperature **Time (mm:ss):** 03:00 **Oscillating Mixer:** On **Interval Mixing On/Off:** 10/15

Reaction: Temp: Room Temperature **Time (mm:ss):** 10:00 **Oscillating Mixer:** On **Interval Mixing On/Off:** 10/15

NY HCTU/DIEA mw 1=1eq, 2022-09-29 19:34

Reaction: Temp: 75°C **Time (mm:ss):** 10:00 **Oscillating Mixer:** On

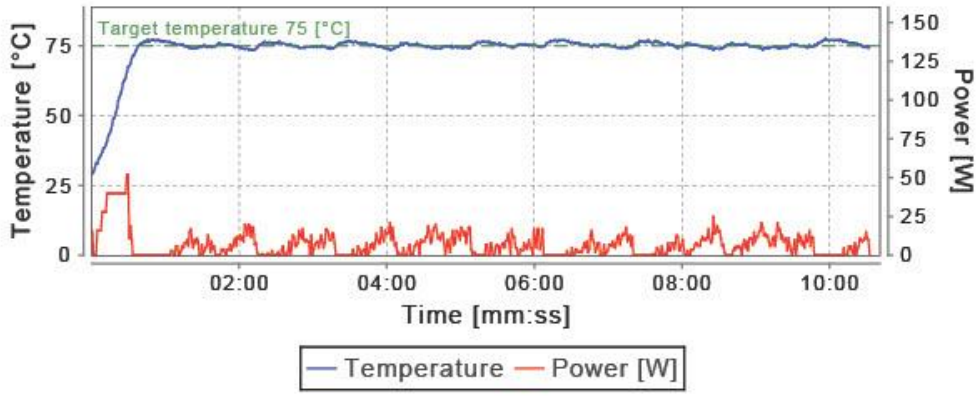

Cycle No: 9

G (Fmoc-Gly-OH)

20% Piperidine , 2022-09-29 19:57

Reaction: Temp: Room Temperature **Time (mm:ss):** 03:00 **Oscillating Mixer:** On **Interval Mixing On/Off:** 10/15

Reaction: Temp: Room Temperature **Time (mm:ss):** 10:00 **Oscillating Mixer:** On **Interval Mixing On/Off:** 10/15

NY HCTU/DIEA mw 1=1eq, 2022-09-29 20:24

Reaction: Temp: 75°C **Time (mm:ss):** 10:00 **Oscillating Mixer:** On

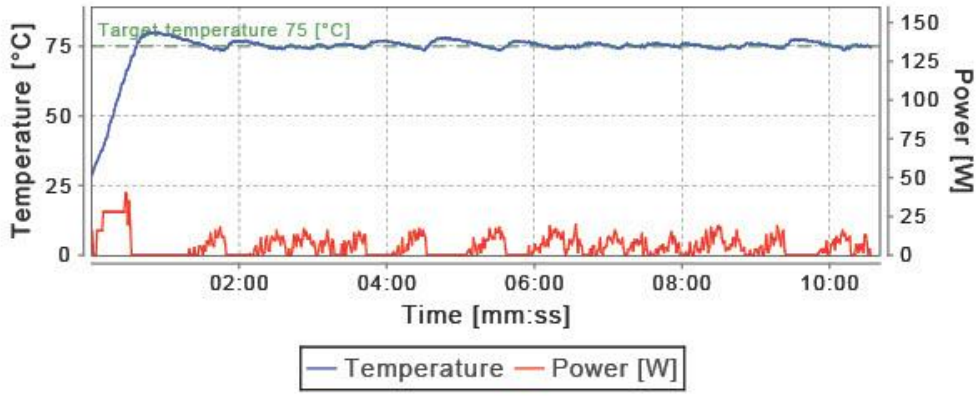

Cycle No: 10

P (Fmoc-Pro-OH)

20% Piperidine , 2022-09-29 20:47

Reaction: Temp: Room Temperature **Time (mm:ss):** 03:00 **Oscillating Mixer:** On **Interval Mixing On/Off:** 10/15

Reaction: Temp: Room Temperature **Time (mm:ss):** 10:00 **Oscillating Mixer:** On **Interval Mixing On/Off:** 10/15

NY HCTU/DIEA mw 1=1eq, 2022-09-29 21:14

Reaction: Temp: 75°C **Time (mm:ss):** 10:00 **Oscillating Mixer:** On

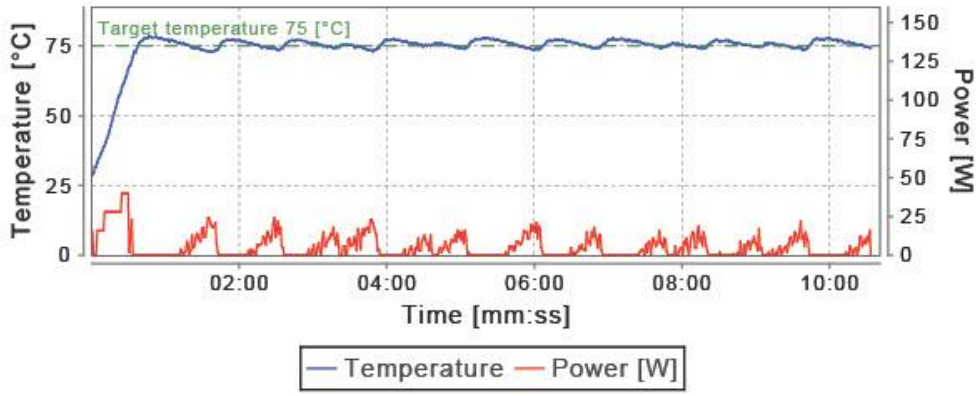

Cycle No: 11
R (Fmoc-Arg(Pbf)-OH)
20% Piperidine , 2022-09-29 21:37
Reaction: Temp: Room Temperature **Time (mm:ss):** 03:00 **Oscillating Mixer:** On **Interval Mixing On/Off:** 10/15
Reaction: Temp: Room Temperature **Time (mm:ss):** 10:00 **Oscillating Mixer:** On **Interval Mixing On/Off:** 10/15
NY HCTU/DIEA r.t.1-1eq, 2022-09-29 22:04
Reaction: Temp: Room Temperature **Time (mm:ss):** 60:00 **Oscillating Mixer:** On

Cycle No: 12
R (Fmoc-Arg(Pbf)-OH)
20% Piperidine , 2022-09-29 23:16
Reaction: Temp: Room Temperature **Time (mm:ss):** 03:00 **Oscillating Mixer:** On **Interval Mixing On/Off:** 10/15
Reaction: Temp: Room Temperature **Time (mm:ss):** 10:00 **Oscillating Mixer:** On **Interval Mixing On/Off:** 10/15
NY HCTU/DIEA r.t.1-1eq, 2022-09-29 23:43
Reaction: Temp: Room Temperature **Time (mm:ss):** 60:00 **Oscillating Mixer:** On

Cycle No: 13

G (Fmoc-Gly-OH)

20% Piperidine , 2022-09-30 00:55

Reaction: Temp: Room Temperature **Time (mm:ss):** 03:00 **Oscillating Mixer:** On **Interval Mixing On/Off:** 10/15

Reaction: Temp: Room Temperature **Time (mm:ss):** 10:00 **Oscillating Mixer:** On **Interval Mixing On/Off:** 10/15

NY HCTU/DIEA mw 1=1eq, 2022-09-30 01:22

Reaction: Temp: 75°C **Time (mm:ss):** 10:00 **Oscillating Mixer:** On

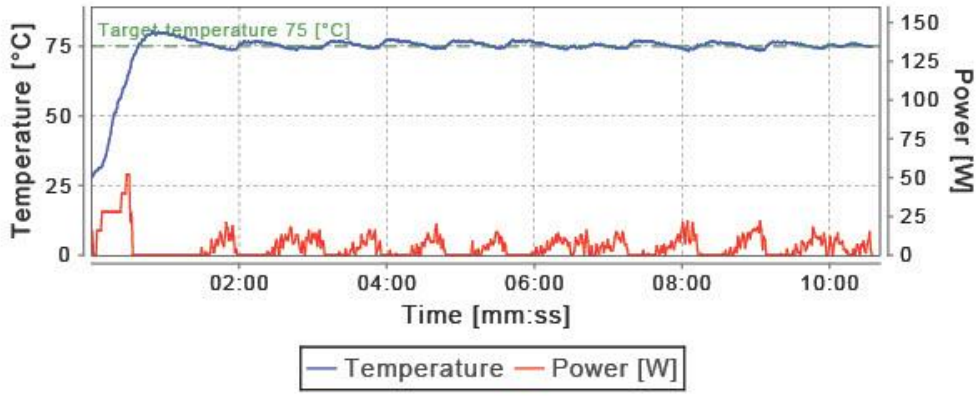

Cycle No: 14
C (Fmoc-Cys(Trt)-OH)
20% Piperidine , 2022-09-30 01:45
Reaction: Temp: Room Temperature **Time (mm:ss):** 03:00 **Oscillating Mixer:** On **Interval Mixing On/Off:** 10/15
Reaction: Temp: Room Temperature **Time (mm:ss):** 10:00 **Oscillating Mixer:** On **Interval Mixing On/Off:** 10/15
NY HCTU/DIEA r.t.1-1eq, 2022-09-30 02:12
Reaction: Temp: Room Temperature **Time (mm:ss):** 60:00 **Oscillating Mixer:** On

Cycle No: 15

W (Fmoc-Trp(Boc)-OH)

20% Piperidine , 2022-09-30 03:24

Reaction: Temp: Room Temperature **Time (mm:ss):** 03:00 **Oscillating Mixer:** On **Interval Mixing On/Off:** 10/15

Reaction: Temp: Room Temperature **Time (mm:ss):** 10:00 **Oscillating Mixer:** On **Interval Mixing On/Off:** 10/15

NY HCTU/DIEA mw 1=1eq, 2022-09-30 03:51

Reaction: Temp: 75°C **Time (mm:ss):** 10:00 **Oscillating Mixer:** On

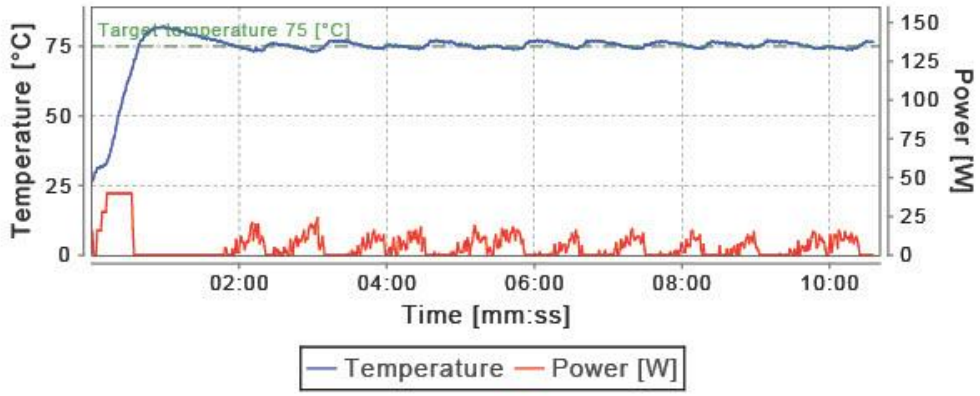

Cycle No: 16

A (Fmoc-Ala-OH)

20% Piperidine , 2022-09-30 04:14

Reaction: Temp: Room Temperature **Time (mm:ss):** 03:00 **Oscillating Mixer:** On **Interval Mixing On/Off:** 10/15

Reaction: Temp: Room Temperature **Time (mm:ss):** 10:00 **Oscillating Mixer:** On **Interval Mixing On/Off:** 10/15

NY HCTU/DIEA mw 1=1eq, 2022-09-30 04:41

Reaction: Temp: 75°C **Time (mm:ss):** 10:00 **Oscillating Mixer:** On

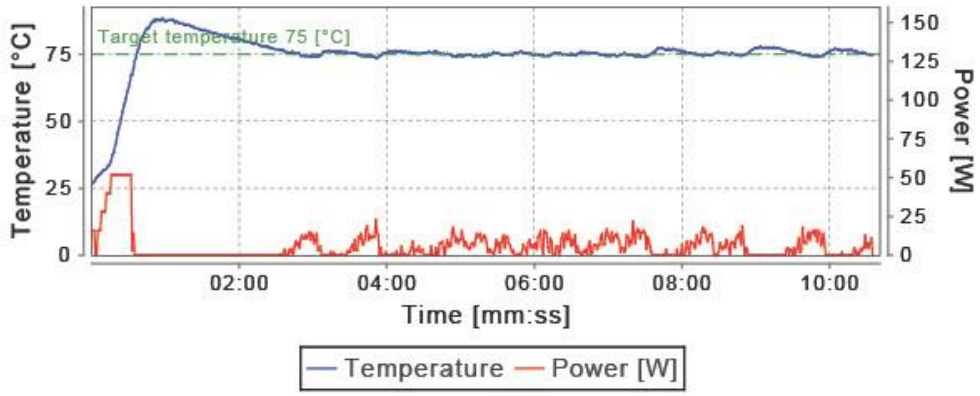

Cycle No: 17

W (Fmoc-Trp(Boc)-OH)

20% Piperidine , 2022-09-30 05:04

Reaction: Temp: Room Temperature **Time (mm:ss):** 03:00 **Oscillating Mixer:** On **Interval Mixing On/Off:** 10/15

Reaction: Temp: Room Temperature **Time (mm:ss):** 10:00 **Oscillating Mixer:** On **Interval Mixing On/Off:** 10/15

NY HCTU/DIEA mw 1=1eq, 2022-09-30 05:31

Reaction: Temp: 75°C **Time (mm:ss):** 10:00 **Oscillating Mixer:** On

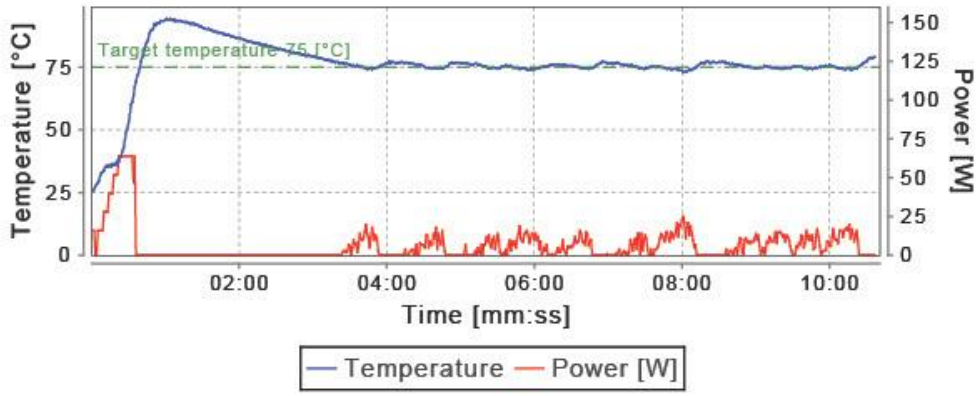

Cycle No: 18

K (Fmoc-Lys(Boc)-OH)

20% Piperidine , 2022-09-30 05:54

Reaction: Temp: Room Temperature **Time (mm:ss):** 03:00 **Oscillating Mixer:** On **Interval Mixing On/Off:** 10/15

Reaction: Temp: Room Temperature **Time (mm:ss):** 10:00 **Oscillating Mixer:** On **Interval Mixing On/Off:** 10/15

NY HCTU/DIEA mw 1=1eq, 2022-09-30 06:21

Reaction: Temp: 75°C **Time (mm:ss):** 10:00 **Oscillating Mixer:** On

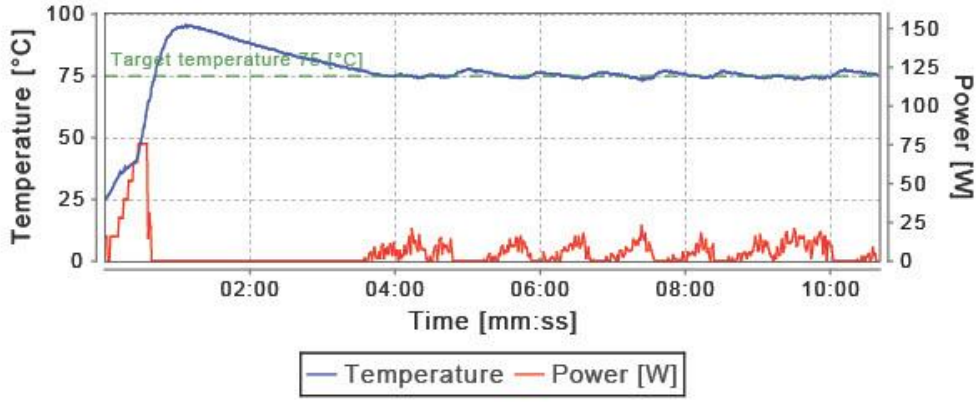

Cycle No: 19
C (Fmoc-Cys(Trt)-OH)
20% Piperidine , 2022-09-30 06:44
Reaction: Temp: Room Temperature **Time (mm:ss):** 03:00 **Oscillating Mixer:** On **Interval Mixing On/Off:** 10/15
Reaction: Temp: Room Temperature **Time (mm:ss):** 10:00 **Oscillating Mixer:** On **Interval Mixing On/Off:** 10/15
NY HCTU/DIEA r.t.1-1eq, 2022-09-30 07:11
Reaction: Temp: Room Temperature **Time (mm:ss):** 60:00 **Oscillating Mixer:** On
20% Piperidine , 2022-09-30 08:23
Reaction: Temp: Room Temperature **Time (mm:ss):** 03:00 **Oscillating Mixer:** On **Interval Mixing On/Off:** 10/15
Reaction: Temp: Room Temperature **Time (mm:ss):** 10:00 **Oscillating Mixer:** On **Interval Mixing On/Off:** 10/15
Pre-cleavage wash DCM , 2022-09-30 08:50

10.1.2 Calculation Table for Turg_JK_2

Biotage

Initiator+ Alstra Peptide Sequence Summary

Date: 2022-11-01 10:53

Calculation Table

Sequence:

C R R A T C G K K P W W W K C R R C G # 1

Resin: Rink amide ChemMatrix
Loading: 0.50 mmol/g
Mol. Weight: 2380.1 g/mol
Quantity: 0.330 g
Scale: 0.165 mmol
Vial: 10 mL

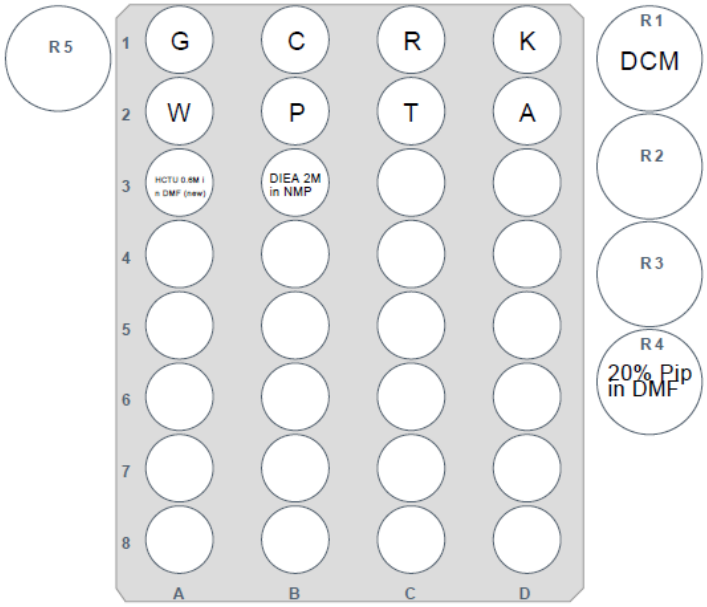

Pos	Acid	Chemical Name	Equivalents	Mol Mass [g/mol]	Mass [g]	Volume [mL]	Dissolve Volume [mL]	Concentration [mol/L]	Total Volume [mL]
A:1	G	Fmoc-Gly-OH	4.0	297.3	0.407		2.42	0.5	2.74
A:2	W	Fmoc-Trp(Boc)-OH	4.0	526.6	1.069		3.183	0.5	4.06
A:3		HCTU 0.6M in DMF (new)	4.0	413.7	5.212		21.0	0.6	21.0
B:1	C	Fmoc-Cys(Trt)-OH	4.0	585.7	1.576		4.081	0.5	5.38
B:2	P	Fmoc-Pro-OH	4.0	337.4	0.24		1.23	0.5	1.42
B:3		DIEA 2M in NMP	8.0	129.2		4.403	8.237	2.0	12.64
C:1	R	Fmoc-Arg(Pbf)-OH	4.0	648.8	1.745		3.934	0.5	5.38
C:2	T	Fmoc-Thr(tBu)-OH	4.0	397.5	0.282		1.193	0.5	1.42
D:1	K	Fmoc-Lys(Boc)-OH	4.0	468.5	0.951		3.285	0.5	4.06

Pos	Acid	Chemical Name	Equivalents	Mol Mass [g/mol]	Mass [g]	Volume [mL]	Dissolve Volume [mL]	Concentration [mol/L]	Total Volume [mL]
D:2	A	Fmoc-Ala-OH	4.0	311.3	0.221		1.246	0.5	1.42
R1		DCM				0.0			32.0
R4		20% Piperidine in DMF	54.55	85.2		34.771	141.229	2.0	176.0
S1		DMF				0.0			2218.0
S2		NMP				0.0			13.5

10.2 Full list of MS-parameters

Table 12: Full list of MS-parameters used in the MS method in this thesis.

Method Settings	
Application Mode	Small Molecule
Method Duration (min)	10
Global Parameters	
Ion Source Properties	
Parameter	Value
Ion Source Type	H-ESI
Spray Voltage	Static
Positive Ion (V)	3500
Negative Ion (V)	2500
Gas mode	Static
Aux Gas (Arb)	60
Sweep Gas (Arb)	15
Ion Transfer Tube Temp (°C)	2
Vaporize Temp (°C)	350
APPI Lamp	Not in Use
Use Ion Source Settings from Tune	False
FAIMS Mode	Not in Use
MS Global Settings	
Infusion Mode	Liquid Chromatography
Expected LC Peak Widt (s)	3
Advanced Peak Determination	True
Mild Trapping	False
Default Charge State	2
Enable Xcalibur AcquireX method modifications	False
Internal Mass Calibration	EASY-IC™
Divert Valve A	
Time (min)	0
Position	1-2
Experiment#1 [MS]	
Start Time (min)	0
End Time (min)	10
Cycle Time (sec)	1
Master Scan	
MS OT	

Detector Type	Orbitrap
Orbitrap Resolution	120000
Use Quadrupole Isolation	False
Scan Range (m/z)	150-2000
RF Lens (%)	60
AGC Target	Standard
Maximum Injection Time Mode	Auto
Microscans	1
Data Type	Profile
Polarity	Positive
Source Fragmentation	Disabled
Use EASY-IC™	True
Intensity	
Filter Type	Intensity Threshold
Intensity Threshold	1.0e5
Data Dependent	
Data Dependent Mode	Cycle Time
Time between Master Scans (sec)	1
ddMS2 OT CID	
Isolation Mode	Quadrupole
Isolation Window (m/z)	1.6
Isolation Offset	Off
Activation Type	CID
Collision Energy Mode	Fixed
CID Collision Energy (%)	30
CID Activation Time (ms)	10
Activation Type Q	0.25
Multistage Activation	False
Detector Type	Orbitrap
Orbitrap Resolution	30000
Scan Range Mode	Auto
AGC Target	Standard
Maximum Injection Time Mode	Auto
Microscans	1
Data Type	Centroid
Use EASY-IC™	True

10.3 R-script used in the finding the hits between the theoretical fragments and hits of both peptides

```
# Load the necessary libraries
library(readxl)
library(dplyr)

# Read the data from the "Theoretical Values" sheet in the "data.xlsx" file
theoretical_values <- read_excel("C:/Users/Johannes/OneDrive/Farmasi Masteroppgave/Peptidfragmenter/Turg_J1_001/Turg_J1_Oks/2_NEM_2_NCM/230220_(1-2, 3-4)_Teoretiske_Fragmenter.xlsx", sheet=1)
# Convert the data in the 'theoretical_value' column to numeric data
theoretical_values <- unlist(theoretical_values) theoretical_values <- as.numeric(theoretical_values)
# Read the data from the "575.6794" sheet in the "data.xlsx" file
measured_values_1 <- read_excel("C:/Users/Johannes/OneDrive/Farmasi Masteroppgave/Peptidfragmenter/Turg_J1_001/Turg_J1_Oks/Turg_J1_Oks_I/JS_230324_Targetprep_JK_T1_1_5minTCEP05mM_NEMNCM_P2_jsCID.xlsx", sheet = "575.6794", col_types = c("skip", "guess", "skip", "skip", "skip", "skip"))
# Convert the data in the 'measured_value' column to numeric data measured_values_1 <- unlist(measured_values_1) measured_values_1 <- as.numeric(measured_values_1)
# Use the expand.grid() function to create a data frame containing all possible combinations of 'measured_value' and 'theoretical_value' values
combinations_1 <- expand.grid(measured_values = measured_values_1, theoretical_values = theoretical_values)
# Use the abs() function to calculate the absolute difference between the measured and theoretical values
combinations_1$difference <- abs(combinations_1$measured_values - combinations_1$theoretical_values)
# Filter the data frame to only include rows where the absolute difference is between 0 and 0.005
combinations_1 <- combinations_1 %>% filter(difference >= 0 & difference <= 0.005)
# Print the resulting data frame
combinations_1

# Read the data from the "Theoretical Values" sheet in the "data.xlsx" file
theoretical_values_2 <- read_excel("C:/Users/Johannes/OneDrive/Farmasi Masteroppgave/Peptidfragmenter/Turg_J1_001/Turg_J1_Oks/2_NEM_2_NCM/230220_(1-2, 3-4)_Teoretiske_Fragmenter.xlsx", sheet=2)
# Convert the data in the 'theoretical_value' column to numeric data
theoretical_values_2 <- unlist(theoretical_values_2) theoretical_values_2 <- as.numeric(theoretical_values_2)
# Read the data from the "575.6794" sheet in the "data.xlsx" file
measured_values_2 <- read_excel("C:/Users/Johannes/OneDrive/Farmasi Masteroppgave/Peptidfragmenter/Turg_J1_001/Turg_J1_Oks/Turg_J1_Oks_I/JS_230324_Targetprep_JK_T1_1_5minTCEP05mM_NEMNCM_P2_jsCID.xlsx", sheet = "575.6794", col_types = c("skip", "guess", "skip", "skip", "skip", "skip"))
# Convert the data in the 'theoretical_value' column to numeric data
theoretical_values_2 <- unlist(theoretical_values_2) theoretical_values_2 <- as.numeric(theoretical_values_2)
# Read the data from the "575.6794" sheet in the "data.xlsx" file
measured_values_2 <- read_excel("C:/Users/Johannes/OneDrive/Farmasi Masteroppgave/Peptidfragmenter/Turg_J1_001/Turg_J1_Oks/Turg_J1_Oks_I/JS_230324_Targetprep_JK_T1_1_5minTCEP05mM_NEMNCM_P2_jsCID.xlsx", sheet = "575.6794", col_types = c("skip", "guess", "skip", "skip", "skip", "skip"))
# Convert the data in the 'measured_value' column to numeric data measured_values_2 <- unlist(measured_values_2) measured_values_2 <- as.numeric(measured_values_2)
# Use the expand.grid() function to create a data frame containing all possible combinations of 'measured_value' and 'theoretical_value' values
```

```
combinations_2 <- expand.grid(measured_values = measured_values_2, theoretical_values
= theoretical_values_2)
# Use the abs() function to calculate the absolute difference between the measured
and theoretical values
combinations_2$difference       <-       abs(combinations_2$measured_values       -
combinations_2$theoretical_values)
# Filter the data frame to only include rows where the absolute difference is between
0 and 0.005
combinations_2 <- combinations_2 %>% filter(difference >= 0 & difference <= 0.005)
# Print the resulting data frame
combinations_2

# Combine all of the data frames
combinations_1to2<-rbind(combinations_1, combinations_2)
# Combine data frames into a list
dfs_1to2 <- list(combinations_1, combinations_2)

# Create a vector of all unique values
all_values_1to2 <- unique(unlist(lapply(dfs_1to2, '[[', "theoretical_values")))
# Create a vector of values that appear in only one data frame
values_in_one_df_1to2    <-    all_values_1to2[sapply(all_values_1to2,    function(x)
sum(sapply(dfs_1to2, function(df) x %in% df$theoretical_values))) == 1]
#     Convert     vector     to     data     frame     df_values_in_one_df_1to2     <-
data.frame(values_in_one_df_1to2)

#
#
# 1-3,2-4
# Read the data from the "Theoretical Values" sheet in the "data.xlsx" file
theoretical_values_3       <-       read_excel("C:/Users/Johannes/OneDrive/Farmasi
Masteroppgave/Peptidfragmenter/Turg_J1_001/Turg_J1_Oks/2_NEM_2_NCM/230220_(1-3,   2-
4)_Teoretiske_Fragmenter.xlsx", sheet=1)
#   Convert   the   data   in   the   'theoretical_value'   column   to   numeric   data
theoretical_values_3   <-   unlist(theoretical_values_3)   theoretical_values_3   <-
as.numeric(theoretical_values_3)
# Read the data from the "575.6794" sheet in the "data.xlsx" file
measured_values_3         <-         read_excel("C:/Users/Johannes/OneDrive/Farmasi
Masteroppgave/Peptidfragmenter/Turg_J1_001/Turg_J1_Oks/Turg_J1_Oks_I/JS_230324_Targ
etprep_JK_T1_1_5minTCEP05mM_NEMNCM_P2_jsCID.xlsx", sheet = "575.6794", col_types =
c("skip", "guess", "skip", "skip", "skip", "skip"))
# Convert the data in the 'measured_value' column to numeric data measured_values_3
<- unlist(measured_values_3) measured_values_3 <- as.numeric(measured_values_3)
# Use the expand.grid() function to create a data frame containing all possible
combinations of 'measured_value' and 'theoretical_value' values
combinations_3 <- expand.grid(measured_values = measured_values_3, theoretical_values
= theoretical_values_3)
# Use the abs() function to calculate the absolute difference between the measured
and theoretical values
combinations_3$difference       <-       abs(combinations_3$measured_values       -
combinations_3$theoretical_values)
# Filter the data frame to only include rows where the absolute difference is between
0 and 0.005
combinations_3 <- combinations_3 %>% filter(difference >= 0 & difference <= 0.005)
# Print the resulting data frame
combinations_3

# Read the data from the "Theoretical Values" sheet in the "data.xlsx" file
theoretical_values_4       <-       read_excel("C:/Users/Johannes/OneDrive/Farmasi
Masteroppgave/Peptidfragmenter/Turg_J1_001/Turg_J1_Oks/2_NEM_2_NCM/230220_(1-3,   2-
4)_Teoretiske_Fragmenter.xlsx", sheet=2)
```

```
# Convert the data in the 'theoretical_value' column to numeric data
theoretical_values_4 <- unlist(theoretical_values_4) theoretical_values_4 <-
as.numeric(theoretical_values_4)
# Read the data from the "575.6794" sheet in the "data.xlsx" file
measured_values_4 <- read_excel("C:/Users/Johannes/OneDrive/Farmasi
Masteroppgave/Peptidfragmenter/Turg_J1_001/Turg_J1_Oks/Turg_J1_Oks_I/JS_230324_Targ
etprep_JK_T1_1_5minTCEP05mM_NEMNCM_P2_jsCID.xlsx", sheet = "575.6794", col_types =
c("skip", "guess", "skip", "skip", "skip", "skip"))
# Convert the data in the 'theoretical_value' column to numeric data
theoretical_values_4 <- unlist(theoretical_values_4) theoretical_values_4 <-
as.numeric(theoretical_values_4)
# Read the data from the "575.6794" sheet in the "data.xlsx" file
measured_values_4 <- read_excel("C:/Users/Johannes/OneDrive/Farmasi
Masteroppgave/Peptidfragmenter/Turg_J1_001/Turg_J1_Oks/Turg_J1_Oks_I/JS_230324_Targ
etprep_JK_T1_1_5minTCEP05mM_NEMNCM_P2_jsCID.xlsx", sheet = "575.6794", col_types =
c("skip", "guess", "skip", "skip", "skip", "skip"))
# Convert the data in the 'measured_value' column to numeric data measured_values_4
<- unlist(measured_values_4) measured_values_4 <- as.numeric(measured_values_4)
# Use the expand.grid() function to create a data frame containing all possible
combinations of 'measured_value' and 'theoretical_value' values
combinations_4 <- expand.grid(measured_values = measured_values_4, theoretical_values
= theoretical_values_4)
# Use the abs() function to calculate the absolute difference between the measured
and theoretical values
combinations_4$difference <- abs(combinations_4$measured_values -
combinations_4$theoretical_values)
# Filter the data frame to only include rows where the absolute difference is between
0 and 0.005
combinations_4 <- combinations_4 %>% filter(difference >= 0 & difference <= 0.005)
# Print the resulting data frame
combinations_4

# Combine all of the data frames
combinations_1to3<-rbind(combinations_3, combinations_4)
# Combine data frames into a list
dfs_1to3 <- list(combinations_3, combinations_4)

# Create a vector of all unique values
all_values_1to3 <- unique(unlist(lapply(dfs_1to3, '[[', "theoretical_values")))
# Create a vector of values that appear in only one data frame
values_in_one_df_1to3 <- all_values_1to3[sapply(all_values_1to3, function(x)
sum(sapply(dfs_1to3, function(df) x %in% df$theoretical_values))) == 1]
# Convert vector to data frame df_values_in_one_df_1to3 <-
data.frame(values_in_one_df_1to3)
# 1-4,2-3
#
#

# Read the data from the "Theoretical Values" sheet in the "data.xlsx" file
theoretical_values_5 <- read_excel("C:/Users/Johannes/OneDrive/Farmasi
Masteroppgave/Peptidfragmenter/Turg_J1_001/Turg_J1_Oks/2_NEM_2_NCM/230220_(1-4, 2-
3)_Teoretiske_Fragmenter.xlsx", sheet=1)
# Convert the data in the 'theoretical_value' column to numeric data
theoretical_values_5 <- unlist(theoretical_values_5) theoretical_values_5 <-
as.numeric(theoretical_values_5)
# Read the data from the "575.6794" sheet in the "data.xlsx" file
measured_values_5 <- read_excel("C:/Users/Johannes/OneDrive/Farmasi
Masteroppgave/Peptidfragmenter/Turg_J1_001/Turg_J1_Oks/Turg_J1_Oks_I/JS_230324_Targ
etprep_JK_T1_1_5minTCEP05mM_NEMNCM_P2_jsCID.xlsx", sheet = "575.6794", col_types =
c("skip", "guess", "skip", "skip", "skip", "skip"))
```

```
# Convert the data in the 'measured_value' column to numeric data measured_values_5
<- unlist(measured_values_5) measured_values_5 <- as.numeric(measured_values_5)
# Use the expand.grid() function to create a data frame containing all possible
combinations of 'measured_value' and 'theoretical_value' values
combinations_5 <- expand.grid(measured_values = measured_values_5, theoretical_values
= theoretical_values_5)
# Use the abs() function to calculate the absolute difference between the measured
and theoretical values
combinations_5$difference       <-       abs(combinations_5$measured_values       -
combinations_5$theoretical_values)
# Filter the data frame to only include rows where the absolute difference is between
0 and 0.005
combinations_5 <- combinations_5 %>% filter(difference >= 0 & difference <= 0.005)
# Print the resulting data frame
combinations_5

# Read the data from the "Theoretical Values" sheet in the "data.xlsx" file
theoretical_values_6        <-        read_excel("C:/Users/Johannes/OneDrive/Farmasi
Masteroppgave/Peptidfragmenter/Turg_J1_001/Turg_J1_Oks/2_NEM_2_NCM/230220_(1-4,   2-
3)_Teoretiske_Fragmenter.xlsx", sheet=2)
#  Convert  the  data  in  the  'theoretical_value'  column  to  numeric  data
theoretical_values_6  <-  unlist(theoretical_values_6)  theoretical_values_6  <-
as.numeric(theoretical_values_6)
# Read the data from the "575.6794" sheet in the "data.xlsx" file
measured_values_6         <-         read_excel("C:/Users/Johannes/OneDrive/Farmasi
Masteroppgave/Peptidfragmenter/Turg_J1_001/Turg_J1_Oks/Turg_J1_Oks_I/JS_230324_Targ
etprep_JK_T1_1_5minTCEP05mM_NEMNCM_P2_jsCID.xlsx", sheet = "575.6794", col_types =
c("skip", "guess", "skip", "skip", "skip", "skip"))
#  Convert  the  data  in  the  'theoretical_value'  column  to  numeric  data
theoretical_values_6  <-  unlist(theoretical_values_6)  theoretical_values_6  <-
as.numeric(theoretical_values_6)
# Read the data from the "575.6794" sheet in the "data.xlsx" file
measured_values_6         <-         read_excel("C:/Users/Johannes/OneDrive/Farmasi
Masteroppgave/Peptidfragmenter/Turg_J1_001/Turg_J1_Oks/Turg_J1_Oks_I/JS_230324_Targ
etprep_JK_T1_1_5minTCEP05mM_NEMNCM_P2_jsCID.xlsx", sheet = "575.6794", col_types =
c("skip", "guess", "skip", "skip", "skip", "skip"))
# Convert the data in the 'measured_value' column to numeric data measured_values_6
<- unlist(measured_values_6) measured_values_6 <- as.numeric(measured_values_6)
# Use the expand.grid() function to create a data frame containing all possible
combinations of 'measured_value' and 'theoretical_value' values
combinations_6 <- expand.grid(measured_values = measured_values_6, theoretical_values
= theoretical_values_6)
# Use the abs() function to calculate the absolute difference between the measured
and theoretical values
combinations_6$difference       <-       abs(combinations_6$measured_values       -
combinations_6$theoretical_values)
# Filter the data frame to only include rows where the absolute difference is between
0 and 0.005
combinations_6 <- combinations_6 %>% filter(difference >= 0 & difference <= 0.005)
# Print the resulting data frame
combinations_6

# Combine all of the data frames
combinations_1to4<-rbind(combinations_5, combinations_6)
# Combine data frames into a list
dfs_1to4 <- list(combinations_5, combinations_6)

# Create a vector of all unique values
all_values_1to4 <- unique(unlist(lapply(dfs_1to4, '[[', "theoretical_values")))
# Create a vector of values that appear in only one data frame
```

```
values_in_one_df_1to4    <-    all_values_1to4[sapply(all_values_1to4,    function(x)
sum(sapply(dfs_1to4, function(df) x %in% df$theoretical_values))) == 1]
#     Convert     vector     to     data     frame     df_values_in_one_df_1to4     <-
data.frame(values_in_one_df_1to4)
# Skriv til excel fil
# create a new workbook
library(openxlsx)
wb <- createWorkbook()

# add each data frame as a new sheet in the workbook
addWorksheet(wb, "1-2,3-4")
writeData(wb, "1-2,3-4", combinations_1to2)
addWorksheet(wb, "1-2,3-4_Felles")
writeData(wb, "1-2,3-4_Felles", df_values_in_one_df_1to2)
addWorksheet(wb, "1-3,2-4")
writeData(wb, "1-3,2-4", combinations_1to3)
addWorksheet(wb, "1-3,2-4_Felles")
writeData(wb, "1-3,2-4_Felles", df_values_in_one_df_1to3)
addWorksheet(wb, "1-4,2-3")
writeData(wb, "1-4,2-3", combinations_1to4)
addWorksheet(wb, "1-4,2-3_Felles")
writeData(wb, "1-4,2-3_Felles", df_values_in_one_df_1to4)

# save the workbook to a file
saveWorkbook(wb,   "Turg_J1_Oks_1_I_(1-2,3-4)_575.6794_matches.xlsx",   overwrite   =
TRUE)
```

10.4 Screening av antibakteriell aktivitet hos peptider - Minimal inhiberende konsentrasjon (MIC)

Mikrotiterplate test.

Denne testen baserer seg på metoder fra *Clinical and Laboratory Standards Institute* (CLSI) M07-A9 (35) med mindre tilpasninger til aktivitetstesting i våre laboratorier ved NFH og Forskningsgruppen i marin bioprospektering (36).

10.4.1 Bakterier

Valg av bakteriestammer avhenger av hvilke fraksjoner som skal testes og hvilken aktivitet som ønskes sjekket. I tabell 1 er bakterier for standard screening nevnt. Andre bakteriestammer kan benyttes til utvidet testing.

Tabell 1. Oversikt over bakterier som benyttes til primær screening for antibakteriell aktivitet. Vanligvis benyttes de fire første.

Bakterie type	*kortnavn*	Stamme
Første screening		
Gram-negativ		
Escherichia coli	*Ec*	ATCC 25922
Pseudomonas aeruginosa	*Pa*	ATCC 27853
Gram-positiv		
Corynebacterium glutamicum	*Cg*	ATCC13032
Staphylococcus aureus	*Sa*	ATCC 9144
Utvidet screening		
Vibrio anguillarum	*Va*	AL 104

10.4.2 Medium

Minimalmediet Mueller Hinton broth (MH; Difco Laboratories, USA) benyttes der det er mulig (35).

Mueller Hinton Agar plater (MHA; Difco) benyttes for dyrking av bakterier på plater. Det tillages i henhold til oppskriften fra produsenten.

Vanligvis finnes disse ferdig tillaget på kjølerommet i 3 etg.

10.4.3 Fortynning og klargjøring av prøver

Prøvene fortynnes i mQ H_2O til ønsket konsentrasjon. Dersom materialet i prøven(e) er tungt løselig (polart), kan DMSO opptil 100% brukes som løsemiddel. Ved testing derimot kan det ikke være mer enn totalt 1% DMSO til stede uten at testen påvirkes. En må derfor tenke gjennom på forhånd hvilken konsentrasjon en ønsker i stockløsningen og i arbeidsløsningen for testing. Vanligvis testes en substans i ulike konsentrasjoner, gjerne i en tofolds fortynningsrekke (appendiks 1).

Innholdet i inndampede fraksjoner fra f. eks. HPLC separert materiale, tilsettes mQ H_2O (f. eks. 500 µl, men mengde tilsatt væske avhenger av innholdet og konsentrasjonen av materialet i fraksjonene), og blandes over natt ved 4 °C om nødvendig.

Konsentrasjonen angitt i prøven kan være proteinkonsentrasjon bestemt med f. eks. BCA kit (Pierce), Nanodrop metode eller den kan være basert på utveid tørrstoff (µg tørrstoff/ml). Prøvene settes i kjøleskap eller fryses om de ikke testes samme dag.

10.4.4 Tillaging av testbakteriene (bruksløsning)

1. Bakteriene oppbevares i en -80°C frysestock. Herfra sås de ut på en MHA plate og inkuberes ved bakterienes trivselstemperatur til synlige kolonier observeres. (E. coli, C.g, S.a og P.a settes over natt (ON) i 37°C, og V. ang 1-2 dager ved RT). Deretter kan de oppbevares på agarplate i kjøleskap i inntil 14 dager før de kastes. Dersom marine bakterier benyttes, må temperaturen endres og muligens også mediet eller sammensetningen av det.
2. En koloni fra hver bakterie overføres fra agarplate til 5 ml MH i et dyrkingsrør med kork og inkuberes over natta ved risting ved samme temp som angitt overfor.

3. Neste dag overføres 20 µl av kulturene til nye 5 ml MH-medium som inkuberes ved risting i 2 timer. Kulturene er da i aktiv vekstfase (logaritmisk vekstfase).
4. 1/10 fortynning av kulturene avleses ved A_{600}.
5. Bruksløsning av bakterier lages ved å overføre 3 - 20 µl av disse 2 timers bakteriekulturene til 10 ml MHB. Tabell 2 viser forholdet mellom A_{600} og hvor mye en må benytte av en bakteriekultur for å få en gitt tetthet av bakterien[1]. Benyttes fortynning som angitt i tabell 2, blir bakterietetthet ca. 2.5-3.0 x 10^4 per ml (dvs. 1250-1500 celler i 50 µl).

Tabell 2. Forhold mellom A_{600} og tetthet av bakterier er bestemt ved utplating (coloni formende enheter; CFU), for å gi ca. 2.5-3.0 bakterier x 104 ml^{-1}.

Tetthet bakteriekultur (OD_{600})	Mengde uttak (µl) av kultur som overføres til 10 ml MH medium
0,003 - 0,010	20
0,010 - 0,030	10
0,030 - 0,075	5
0,075 - 0,100	4
0,100 - 0,150	3

[1] En kultur med OD_{600}= 0.05/0.06 tilsvarer ca. 5-6 x 10^7 bakterier ml^{-1}. Dette volumet er basert på tidligere oppdyrking av alle bakteriestammene og bestemmes av antall kim (CFU) av bakterier som detekteres i logaritmisk vekstfase. Kulturene er fortynnet og et gitt volum er fordelt på bakterieskåler, inkubert i et par dager og bakteriekolonier er telt og kim beregnet.

10.4.5 Prøveoppsett - Test av antibakteriell aktivitet.

10.4.6 Minimal inhiberende konsentrasjon

Benytt polystyrene mikrotiterplater (NUNC, Roskilde, Danmark).

1. Til hver brønn tilsettes:

- 50 µl av fraksjonene (sterilt mQ H_2O, MH-medium eller andre kontroller) eller prøver fortynnet i tofoldsfortynningsrekker (appendiks 1)
- 50 µl av bakterie-bruksløsning.

Eksempel på et oppsett er vist i fig 1.

2. Inkuber platene med forsegling ved 37°C (evt. ved RT) i 24-48 timer i EnVision avleser (Perkin-Elmer, Turku, Finland) i inkubator, med regelmessig rysting og avlesning av A_{600}. Avlesning innstilles automatisk på hver time. I plateleser oppnås vanligvis A_{600} verdier på 0.1 – 0.4 på 24 – 48 timer når metoden ovenfor benyttes. Alternativet er endepunktsmåling.
3. Analyse av resultatet. Resultatet av prøven sammenlignes først med vekst av bakterier alene (i mQ H_2O og 50% MH), dernest med kontroll med mQ H_2O uten bakterier, samt med eventuelle andre positive kontroller.

MIC verdien for en ren forbindelse (>95 % ren) defineres som minste konsentrasjon av testsubstansen som gir full veksthemning av bakteriene sammenlignet med kontroll.

		Ec											
		1	2	3	4	5	6	7	8	9	10	11	12
ufortynnet		Prøve	Prøve	Prøve	Prøve	Prøve	Prøve					Pos ktr	Ktr
1/2	A	P1	P1	P1	P2	P2	P2	Fr. 1				Pos ktr	mQ H2O
14	B	P1	P1	P1	P2	P2	P2	Fr. 2				Pos ktr	mQ H2O
1/8	C	P1	P1	P1	P2	P2	P2	Fr. 3				Pos ktr	mQ H2O
1/16	D	P1	P1	P1	P2	P2	P2	Fr. 4					mQ H2O
1/32	E	P1	P1	P1	P2	P2	P2	Etc.					mQ H2O
1/64	F	P1	P1	P1	P2	P2	P2						mQ H2O
1/128	G	P1	P1	P1	P2	P2	P2						mQ H2O
1/256	H	P1	P1	P1	P2	P2	P2						mQ H2O

Figur 1. Eksempel på oppsett av prøver i mikrotiterplate for å teste antibakteriell aktivitet. Vann benyttes som kontroll for å teste bakterievekst i en uhemmet vekst av bakteriene. Mediet i dette oppsettet blir 50% MH. Kun medium MH (50%) sammen med substansen benyttes for å teste evt. forurensing av bakterier i selve prøvene. Aktuell konsentrasjon i brønner av testsubstans er angitt i figuren som fortynning i forhold til utgangskonsentrasjon i prøven.

Referanser:

1. **CLSI. Methods for Dilution Antimicrobial Susceptibility Tests for Bacteria That Grow Aerobically; Approved Standard—Ninth Edition**. In., vol. 32. Wayne, PA: Clinical and Laboratory Standards Institute; 2012.

2. Paulsen VS, Blencke HM, Benincasa M, Haug T, Eksteen JJ, Styrvold OB, Scocchi M, Stensvag K: **Structure-activity relationships of the antimicrobial peptide arasin 1 - and mode of action studies of the N-terminal, proline-rich region**. *PLoS One* 2013, **8**(1):e53326.

10.4.7 Appendiks

10.4.7.1 Tofolds fortynningsrekke

Fortynn prøvene i tofold direkte i mikrotiterbrett ved at følgende utføres:

1. Tilsett 50 µl mQ H_2O i alle brønnene, bortsett fra i startrekka (rekke A, figur 2).
2. 100 µl prøve i 2x startkonsentrasjon tilsettes i rekke A.

3. Overfør 50 µl fra A-rekka til neste brønn nedover (rekke B). Bland godt ved å pipettere opp og ned noen ganger.
4. Gjenta 3 og 4.
5. Fjerne de siste 50 µl fra rekke H etter blanding.
6. Deretter tilsettes 50 µl bakterier i alle brønner som angitt i metoden.

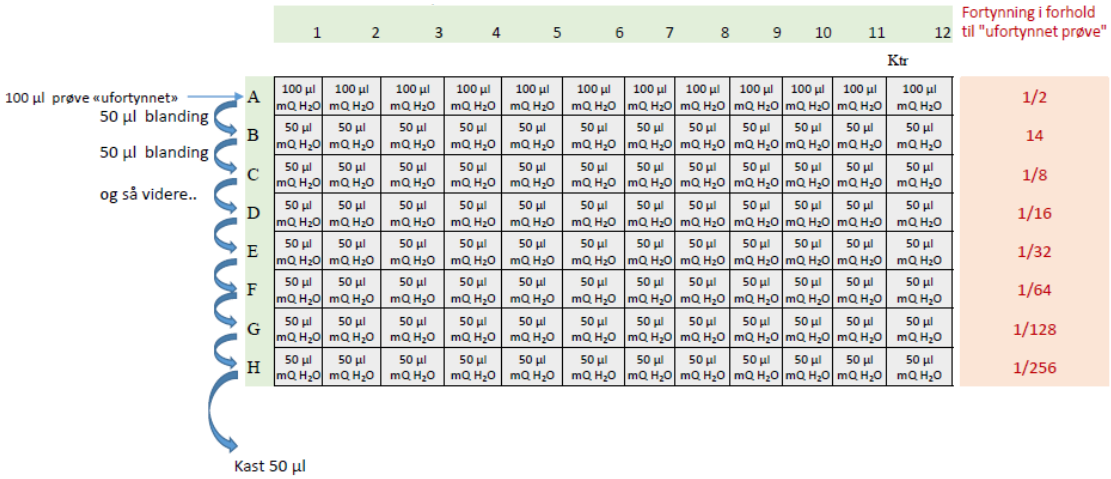

Figur 2. Eksempel på tofoldsfortynningsrekke og volum benyttet.

10.5 MS^2 spectra used in the disulfide elucidation of isomer I of Turg_JK_1

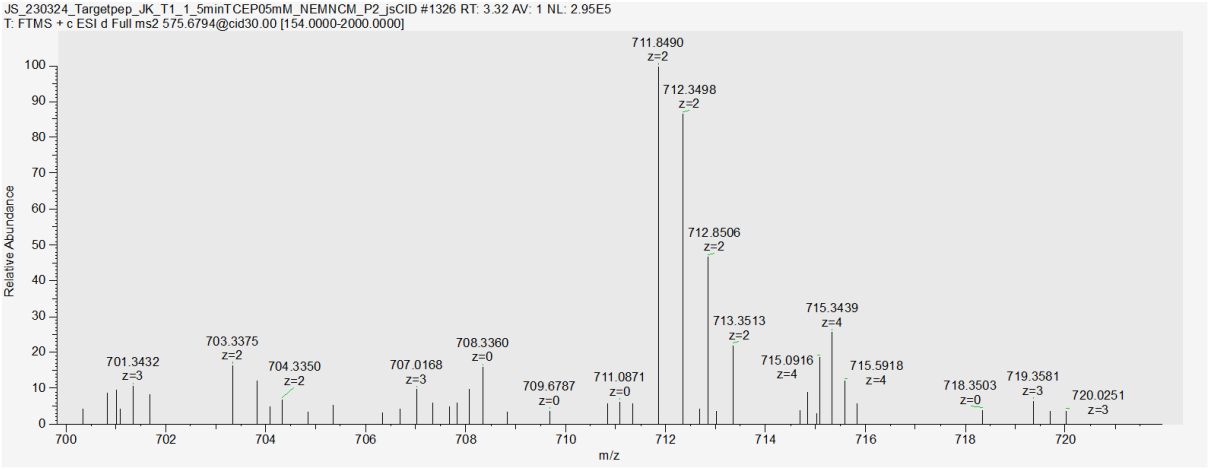

Figure 43: MS^2 spectrum of ion 575.6794, which is the molecule ion for Turg_JK_1 alkylated with two NEM and NCM groups at 5 charges. The sample is of isomer I of Turg_JK_1 after sequential reduction and alkylation. y-ion 711.8490 is present in the spectrum in the spectrum.

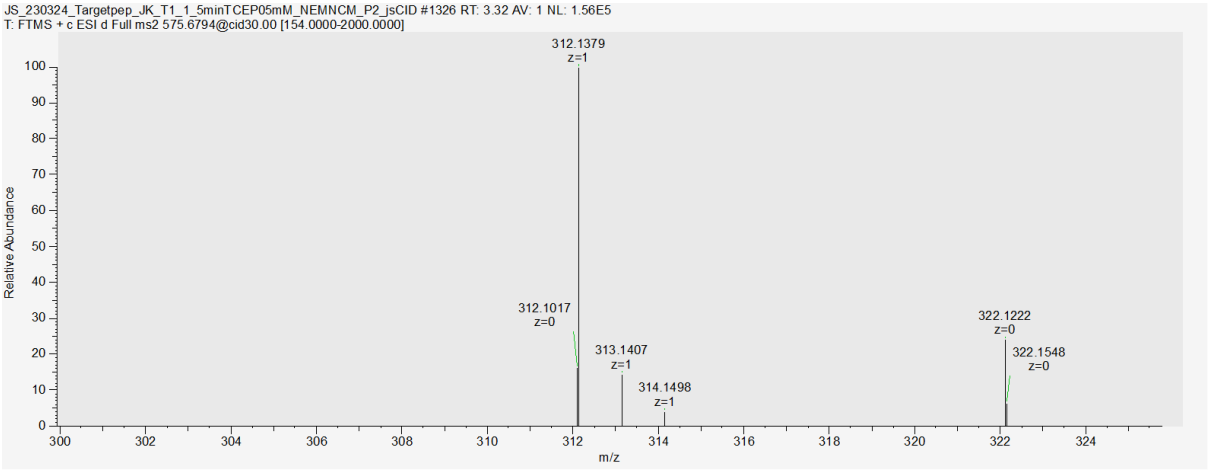

Figure 44: MS^2 spectrum of ion 575.6794, which is the molecule ion for Turg_JK_1 alkylated with two NEM and NCM groups at 5 charges. The sample is of isomer I of Turg_JK_1 after sequential reduction and alkylation. a-ion 312.1379 is present in the spectrum.

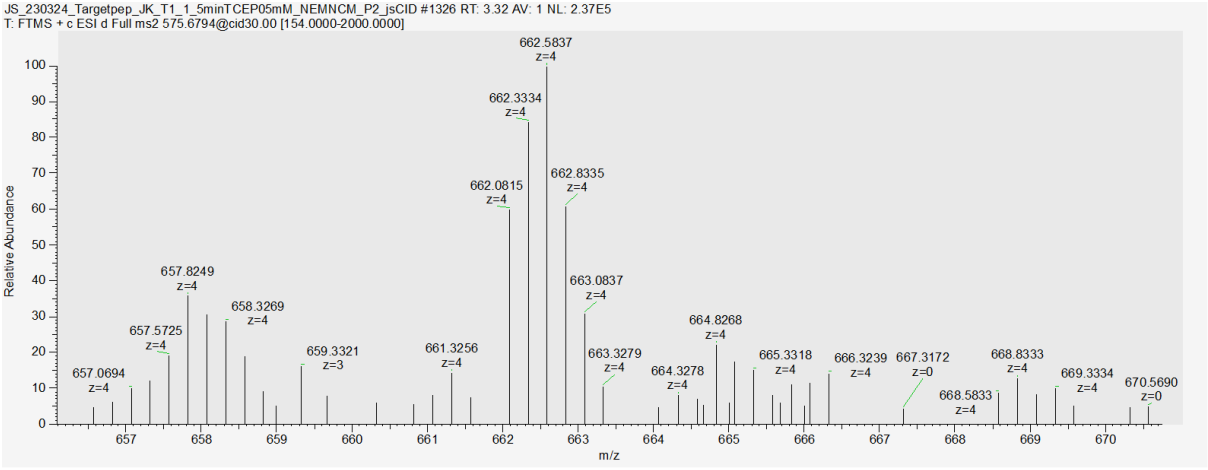

Figure 45: MS^2 spectrum of ion 575.6794, which is the molecule ion for Turg_JK_1 alkylated with two NEM and NCM groups at 5 charges. The sample is of isomer I of Turg_JK_1 after sequential reduction and alkylation. y^{+4}-ion 662.0815 is present in the spectrum.

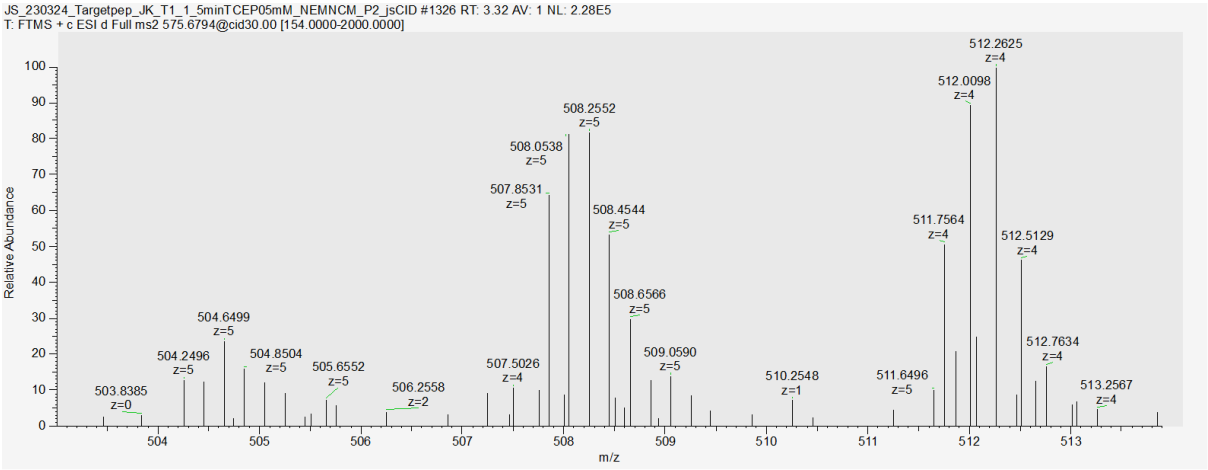

Figure 46: MS^2 spectrum of ion 575.6794, which is the molecule ion for Turg_JK_1 alkylated with two NEM and NCM groups at 5 charges. The sample is of isomer I of Turg_JK_1 after sequential reduction and alkylation. $b+H_2O^{+5}$-ion 662.0815 is present in the spectrum.

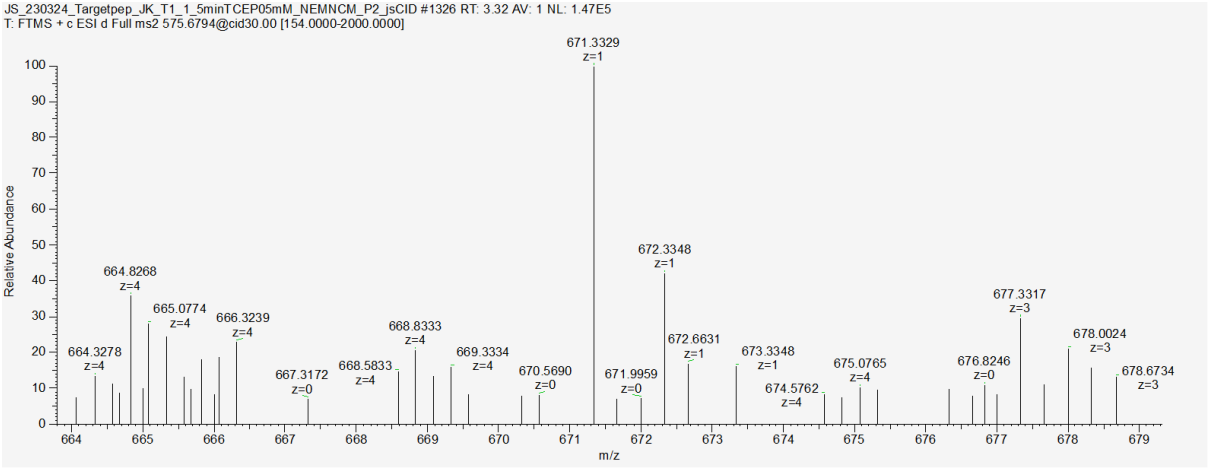

Figure 47: MS^2 spectrum of ion 575.6794, which is the molecule ion for Turg_JK_1 alkylated with two NEM and NCM groups at 5 charges. The sample is of isomer I of Turg_JK_1 after sequential reduction and alkylation. y-ion 671.3329 is present in the spectrum.

10.6 Theoretical fragments and hits of Turg_JK_1 isomer I

Table 13: Table showing the theoretical fragments of Turg_JK_1 with a 1-3/2-4 connectivity for the alkylation pattern 1-NEM/2-NCM/3-NEM/4-NCM. The ions are placed in table based on their ion type (b, y) which is seen on the left, and position in the peptide sequence which is seen in the middle. The measured ions that have a hit will have their corresponding theoretical ion highlighted in green or yellow. The hits are highlighted in green if they cannot be found in the other alkylation pattern for a 1-3/2-4 connectivity, and yellow if they are in both. The fragments highlighted in orange are common for two different fragments in the molecule and cannot be used for identification.

N-terminal																				
a-NH3	---	312.1376	498.2170	569.2541	755.3334	1037.4372	1094.4587	1250.5598	1406.6609	1503.7136	1560.7351	1617.7566	1773.8577	1929.9588	2158.0157	2286.1106	2472.1899	2754.2937	---	
a-NH3+2	---	156.5725	249.6121	285.1307	378.1703	519.2222	547.7330	625.7835	703.8341	752.3605	780.8712	809.3819	887.4325	965.4830	1079.5115	1143.5589	1236.5986	1377.6505	---	
a-NH3+3	---	---	---	---	---	---	---	417.5248	469.5585	501.9094	520.9166	539.9237	591.9574	643.9911	720.0101	762.7084	824.7348	918.7694	---	
a-NH3+4	---	---	---	---	---	---	---	---	352.4207	376.6839	390.9392	405.1946	444.2199	483.2452	540.2594	572.2831	618.8029	689.3289	---	
a-NH3+5	---	---	---	---	---	---	---	---	---	---	---	---	355.5774	386.7976	432.4090	458.0279	495.2436	551.6646	---	
a-NH3+6	---	---	---	---	---	---	---	---	---	---	---	---	---	322.4992	360.5087	381.8578	412.8711	459.8884	---	
a-NH3+7	---	---	---	---	---	---	---	---	---	---	---	---	---	---	---	327.4506	354.0334	394.3339	---	
a	---	329.1642	515.2435	586.2806	772.3599	1054.4637	1111.4852	1267.5863	1423.6874	1520.7402	1577.7617	1634.7831	1790.8842	1946.9853	2175.0422	2303.1372	2489.2165	2771.3203	---	
a+2	---	165.0857	258.1254	293.6439	386.6836	527.7355	556.2462	634.2968	712.3474	760.8737	789.3845	817.8952	895.9458	973.9963	1088.0247	1152.0722	1245.1119	1386.1638	---	
a+3	---	---	---	---	---	---	---	423.2003	475.2340	507.5849	526.5921	545.5992	597.6329	649.6666	725.6856	768.3839	830.4103	924.4449	---	
a+4	---	---	---	---	---	---	---	---	356.6773	380.9405	395.1959	409.4512	448.4765	487.5018	544.5160	576.5397	623.0596	693.5855	---	
a+5	---	---	---	---	---	---	---	---	---	---	---	---	358.9827	390.2029	435.8143	461.4333	498.6491	555.0699	---	
a+6	---	---	---	---	---	---	---	---	---	---	---	---	---	325.3370	363.3464	384.6956	415.7088	462.7261	---	
a+7	---	---	---	---	---	---	---	---	---	---	---	---	---	---	---	329.8830	356.4657	396.7663	---	
b-NH3	---	340.1326	526.2119	597.2490	783.3283	1065.4321	1122.4536	1278.5547	1434.6558	1531.7086	1588.7300	1645.7515	1801.8526	1957.9537	2186.0106	2314.1055	2500.1848	2782.2887	---	
b-NH3+2	---	170.5699	263.6096	299.1281	392.1678	533.2197	561.7304	639.7810	717.8315	766.3579	794.8686	823.3794	901.4299	979.4805	1093.5089	1157.5564	1250.5961	1391.6480	---	
b-NH3+3	---	---	---	---	---	---	---	426.8564	478.8901	511.2410	530.2482	549.2553	601.2890	653.3227	729.3417	772.0409	834.0665	928.1011	---	
b-NH3+4	---	---	---	---	---	---	---	---	359.4194	383.6826	397.9380	412.1933	451.2186	490.2439	547.2581	579.2818	625.8017	696.3276	---	
b-NH3+5	---	---	---	---	---	---	---	---	---	---	---	---	361.1763	392.3966	438.0079	463.6269	500.8428	557.2636	---	
b-NH3+6	---	---	---	---	---	---	---	---	---	---	---	---	---	327.1650	365.1745	386.5237	417.5369	464.5542	---	
b-NH3+7	---	---	---	---	---	---	---	---	---	---	---	---	---	---	---	331.4499	358.0326	398.3332	---	
b	---	357.1591	543.2384	614.2755	800.3548	1082.4587	1139.4801	1295.5812	1451.6823	1548.7351	1605.7566	1662.7780	1818.8791	1974.9803	2203.0371	2331.1321	2517.2114	2799.3152	---	
b+2	---	179.0832	272.1228	307.6414	400.6811	541.7330	570.2437	648.2943	726.3448	774.8712	803.3819	831.8926	909.9432	987.9938	1102.0222	1166.0697	1259.1093	1400.1612	---	
b+3	---	---	---	---	---	---	---	432.5319	484.5656	516.9166	535.9237	554.9308	606.9645	658.9982	735.0172	777.7159	839.7420	933.7766	---	
b+4	---	---	---	---	---	---	---	---	363.6760	387.9392	402.1946	416.4500	455.4752	494.5005	551.5147	583.5385	630.0583	700.5843	---	
b+5	---	---	---	---	---	---	---	---	---	---	---	---	364.5816	395.8019	441.4132	467.0322	504.2481	560.6689	---	
b+6	---	---	---	---	---	---	---	---	---	---	---	---	---	330.0028	368.0122	389.3614	420.3746	467.3919	---	
b+7	---	---	---	---	---	---	---	---	---	---	---	---	---	---	---	333.8822	360.4650	400.7656	---	
b+H2O	---	---	---	---	---	---	---	---	---	---	---	---	---	---	---	---	2535.2220	2817.3258	---	
b+H2O+2	---	---	---	---	---	---	---	---	---	---	---	---	---	---	---	---	1268.1146	1409.1665	---	
b+H2O+3	---	---	---	---	---	---	---	---	---	---	---	---	---	---	---	---	845.7455	939.7801	---	
b+H2O+4	---	---	---	---	---	---	---	---	---	---	---	---	---	---	---	---	634.5609	705.0869	---	
b+H2O+5	---	---	---	---	---	---	---	---	---	---	---	---	---	---	---	---	507.8502	564.2710	---	
b+H2O+6	---	---	---	---	---	---	---	---	---	---	---	---	---	---	---	---	423.3764	470.3937	---	
b+H2O+7	---	---	---	---	---	---	---	---	---	---	---	---	---	---	---	---	363.0379	403.3385	---	
		1	2	3	4	5	6	7	8	9	10	11	12	13	14	15	16	17	18	19	
-		g	K	W	A	W	e	G	R	R	P	G	G	R	R	g	K	W	e	G	- Amidated
		19	18	17	16	15	14	13	12	11	10	9	8	7	6	5	4	3	2	1	
C-terminal																					
y	---	2645.3064	2517.2114	2331.1321	2260.0950	2074.0157	1791.9118	1734.8904	1578.7893	1422.6882	1325.6354	1268.6139	1211.5925	1055.4914	899.3902	671.3334	543.2384	357.1591	75.0553	
y+2	---	1323.1568	1259.1093	1166.0697	1130.5511	1037.5115	896.4596	867.9488	789.8983	711.8477	663.3213	634.8106	606.2999	528.2493	450.1988	336.1703	---	---	---	
y+3	---	882.4403	839.7420	777.7155	754.0366	692.0101	597.9755	578.9683	526.9346	474.9009	442.5500	423.5428	404.5357	352.5020	---	---	---	---	---	
y+4	---	662.0820	630.0583	583.5385	565.7792	519.2594	448.7334	434.4781	395.4528	356.4275	332.1643	317.9089	303.6536	---	---	---	---	---	---	
y+5	---	529.8671	504.2481	467.0322	452.8248	415.6090	359.1882	347.7839	316.5637	---	---	---	---	---	---	---	---	---	---	
y+6	---	441.7238	420.3746	389.3614	377.5219	346.5087	299.4914	289.9878	---	---	---	---	---	---	---	---	---	---	---	
y+7	---	378.7643	---	---	---	---	---	---	---	---	---	---	---	---	---	---	---	---	---	
y-NH3	---	2628.2798	2500.1848	2314.1055	2243.0684	2056.9891	1774.8853	1717.8638	1561.7627	1405.6616	1308.6088	1251.5874	1194.5659	1038.4648	882.3637	654.3068	---	---	---	
y-NH3+2	---	1314.6435	1250.5961	1157.5564	1122.0378	1028.9982	887.9463	859.4356	781.3850	703.3344	654.8081	626.2973	597.7866	519.7360	441.6855	327.6571	---	---	---	
y-NH3+3	---	876.7648	834.0665	772.0400	748.3611	686.3346	592.2999	573.2928	521.2591	469.2254	436.8745	417.8673	398.8602	346.8265	---	---	---	---	---	
y-NH3+4	---	657.8254	625.8017	579.2818	561.5226	515.0027	444.4768	430.2214	391.1961	352.1709	327.9077	313.6523	299.3969	---	---	---	---	---	---	
y-NH3+5	---	526.4618	500.8428	463.6269	449.4195	412.2036	355.7829	344.3786	313.1584	---	---	---	---	---	---	---	---	---	---	
y-NH3+6	---	438.8860	417.5369	386.5237	374.6841	343.6709	296.6536	287.1500	---	---	---	---	---	---	---	---	---	---	---	
y-NH3+7	---	376.3319	---	---	---	---	---	---	---	---	---	---	---	---	---	---	---	---	---	

Table 14: Table showing the theoretical fragments of Turg_JK_1 with a 1-3/2-4 connectivity for the alkylation pattern 1-NCM/2-NEM/3-NCM/4-NEM. The ions are placed in table based on their ion type (b, y) which is seen on the left, and position in the peptide sequence which is seen in the middle. The measured ions that have a hit will have their corresponding theoretical ion highlighted in green or yellow. The hits are highlighted in green if they cannot be found in the other alkylation pattern for a 1-3/2-4 connectivity, and yellow if they are in both. The fragments highlighted in orange are common for two different fragments in the molecule and cannot be used for identification.

N-terminal																				
$_3$	---	366.1846	552.2639	623.3010	809.3803	1037.4372	1094.4587	1250.5598	1406.6609	1503.7136	1560.7351	1617.7566	1773.8577	1929.9588	2212.0626	2340.1576	2526.2369	2754.2937	---	
$_3^{+2}$	---	183.5959	276.6356	312.1541	405.1938	519.2222	547.7330	625.7835	703.8341	752.3605	780.8712	809.3819	887.4325	965.4830	1106.5349	1170.5824	1263.6221	1377.6505	---	
$_3^{+3}$	---	---	---	---	---	---	---	417.5248	469.5585	501.9094	520.9166	539.9237	591.9574	643.9911	738.0257	780.7240	842.7505	918.7694	---	
$_3^{+4}$	---	---	---	---	---	---	---	---	352.4207	376.6839	390.9392	405.1946	444.2199	483.2452	553.7711	585.7948	632.3147	689.3289	---	
$_3^{+5}$	---	---	---	---	---	---	---	---	---	---	---	---	355.5774	386.7976	443.2183	468.8373	506.0532	551.6646	---	
$_3^{+6}$	---	---	---	---	---	---	---	---	---	---	---	---	---	322.4992	369.5165	390.8657	421.8789	459.8884	---	
$_3^{+7}$	---	---	---	---	---	---	---	---	---	---	---	---	---	---	---	335.1716	361.7544	394.3339	---	
	---	383.2111	569.2905	640.3276	826.4069	1054.4637	1111.4852	1267.5863	1423.6874	1520.7402	1577.7617	1634.7831	1790.8842	1946.9853	2229.0892	2357.1841	2543.2634	2771.3203	---	
	---	192.1092	285.1489	320.6674	413.7071	527.7355	556.2462	634.2968	712.3474	760.8737	789.3845	817.8952	895.9458	973.9963	1115.0482	1179.0957	1272.1354	1386.1638	---	
	---	---	---	---	---	---	---	423.2003	475.2340	507.5849	526.5921	545.5992	597.6329	649.6666	743.7012	786.3996	848.4260	924.4449	---	
	---	---	---	---	---	---	---	---	356.6773	380.9405	395.1959	409.4512	448.4765	487.5018	558.0277	590.0515	636.5713	693.5855	---	
	---	---	---	---	---	---	---	---	---	---	---	---	358.9827	390.2029	446.6237	472.2426	509.4585	555.0699	---	
	---	---	---	---	---	---	---	---	---	---	---	---	---	325.3370	372.3543	393.7034	424.7166	462.7261	---	
	---	---	---	---	---	---	---	---	---	---	---	---	---	---	---	337.6040	364.1867	396.7663	---	
$_3$	---	394.1795	580.2588	651.2959	837.3752	1065.4321	1122.4536	1278.5547	1434.6558	1531.7086	1588.7300	1645.7515	1801.8526	1957.9537	2240.0576	2368.1525	2554.2318	2782.2887	---	
$_3^{+2}$	---	197.5934	290.6330	326.1516	419.1913	533.2197	561.7304	639.7810	717.8315	766.3579	794.8686	823.3794	901.4299	979.4805	1120.5324	1184.5799	1277.6195	1391.6480	---	
$_3^{+3}$	---	---	---	---	---	---	---	426.8564	478.8901	511.2410	530.2482	549.2553	601.2890	653.3227	747.3574	790.0557	852.0821	928.1011	---	
$_3^{+4}$	---	---	---	---	---	---	---	---	359.4194	383.6826	397.9380	412.1933	451.2186	490.2439	560.7698	592.7936	639.3134	696.3276	---	
$_3^{+5}$	---	---	---	---	---	---	---	---	---	---	---	---	361.1763	392.3965	448.8173	474.4363	511.6522	557.2636	---	
$_3^{+6}$	---	---	---	---	---	---	---	---	---	---	---	---	---	327.1650	374.1823	395.5315	426.5447	464.5542	---	
$_3^{+7}$	---	---	---	---	---	---	---	---	---	---	---	---	---	---	---	339.1709	365.7536	398.3332	---	
	---	411.2061	597.2854	668.3225	854.4018	1082.4587	1139.4801	1295.5812	1451.6823	1548.7351	1605.7566	1662.7780	1818.8791	1974.9803	2257.0841	2385.1790	2571.2583	2799.3152	---	
	---	206.1067	299.1463	334.6649	427.7045	541.7330	570.2437	648.2943	726.3448	774.8712	803.3819	831.8927	909.9432	987.9938	1129.0457	1193.0932	1286.1328	1400.1612	---	
	---	---	---	---	---	---	---	432.5319	484.5656	516.9166	535.9237	554.9309	606.9646	658.9983	753.0329	795.7312	857.7576	933.7766	---	
	---	---	---	---	---	---	---	---	363.6760	387.9392	402.1946	416.4500	455.4752	494.5005	565.0265	597.0502	643.5700	700.5843	---	
	---	---	---	---	---	---	---	---	---	---	---	---	364.5816	395.8019	452.2226	477.8416	515.0575	560.6689	---	
	---	---	---	---	---	---	---	---	---	---	---	---	---	330.0028	377.0201	398.3692	429.3825	467.3919	---	
	---	---	---	---	---	---	---	---	---	---	---	---	---	---	---	341.6032	368.1860	400.7656	---	
O	---	---	---	---	---	---	---	---	---	---	---	---	---	---	---	---	2589.2689	2817.3258	---	
O^{+2}	---	---	---	---	---	---	---	---	---	---	---	---	---	---	---	---	1295.1381	1409.1665	---	
O^{+3}	---	---	---	---	---	---	---	---	---	---	---	---	---	---	---	---	863.7612	939.7801	---	
O^{+4}	---	---	---	---	---	---	---	---	---	---	---	---	---	---	---	---	648.0727	705.0869	---	
O^{+5}	---	---	---	---	---	---	---	---	---	---	---	---	---	---	---	---	518.6596	564.2710	---	
O^{+6}	---	---	---	---	---	---	---	---	---	---	---	---	---	---	---	---	432.3842	470.3937	---	
O^{+7}	---	---	---	---	---	---	---	---	---	---	---	---	---	---	---	---	370.7589	403.3385	---	
	1	**2**	**3**	**4**	**5**	**6**	**7**	**8**	**9**	**10**	**11**	**12**	**13**	**14**	**15**	**16**	**17**	**18**	**19**	
-	**e**	**K**	**W**	**A**	**W**	**g**	**G**	**R**	**R**	**P**	**G**	**G**	**R**	**R**	**e**	**K**	**W**	**g**	**G**	**-Amidated**
	19	**18**	**17**	**16**	**15**	**14**	**13**	**12**	**11**	**10**	**9**	**8**	**7**	**6**	**5**	**4**	**3**	**2**	**1**	
C-terminal																				
	---	2591.2594	2463.1644	2277.0851	2206.0480	2019.9687	1791.9118	1734.8904	1578.7893	1422.6882	1325.6359	1268.6154	1211.5939	1055.4914	899.3902	617.2864	489.1915	303.1122	75.0553	
	---	1296.1333	1232.0859	1139.0462	1103.5276	1010.4880	896.4596	867.9488	789.8983	711.8477	663.3213	634.8106	606.2999	528.2493	450.1988	309.1469	---	---	---	
	---	864.4247	821.7263	759.6999	736.0209	673.9944	597.9755	578.9683	526.9346	474.9009	442.5500	423.5428	404.5357	352.5020	---	---	---	---	---	
	---	648.5703	616.5466	570.0267	552.2675	505.7476	448.7334	434.4781	395.4522	356.4275	332.1642	317.9089	303.6536	---	---	---	---	---	---	
	---	519.0577	493.4387	456.2223	442.0154	404.7996	359.1882	347.7839	316.5637	---	---	---	---	---	---	---	---	---	---	
	---	432.7160	411.3668	380.3536	368.5141	337.5008	299.4914	289.9878	---	---	---	---	---	---	---	---	---	---	---	
	---	371.0433	---	---	---	---	---	---	---	---	---	---	---	---	---	---	---	---	---	
$_3$	---	2574.2329	2446.1379	2260.0586	2189.0215	2002.9422	1774.8853	1717.8638	1561.7627	1405.6616	1308.6088	1251.5874	1194.5659	1038.4648	882.3637	600.2599	---	---	---	
$_3^{+2}$	---	1287.6201	1223.5726	1130.5329	1095.0144	1001.9747	887.9463	859.4356	781.3850	703.3344	654.8081	626.2974	597.7866	519.7360	441.6855	300.6336	---	---	---	
$_3^{+3}$	---	858.7491	816.0501	754.0243	730.3457	668.3189	592.2999	573.2928	521.2591	469.2254	436.8745	417.8674	398.8603	346.8265	---	---	---	---	---	
$_3^{+4}$	---	644.3137	612.2899	565.7701	548.0108	501.4910	444.4768	430.2214	391.1961	352.1709	327.9077	313.6523	299.3969	---	---	---	---	---	---	
$_3^{+5}$	---	515.6524	490.0334	452.8175	438.6101	401.3944	355.7829	344.3786	313.1584	---	---	---	---	---	---	---	---	---	---	
$_3^{+6}$	---	429.8782	408.5290	377.5158	365.6763	334.6631	296.6536	287.1500	---	---	---	---	---	---	---	---	---	---	---	
$_3^{+7}$	---	368.6109	---	---	---	---	---	---	---	---	---	---	---	---	---	---	---	---	---	

10.7 MS^2 spectra used in the disulfide elucidation of isomer III of Turg_JK_1

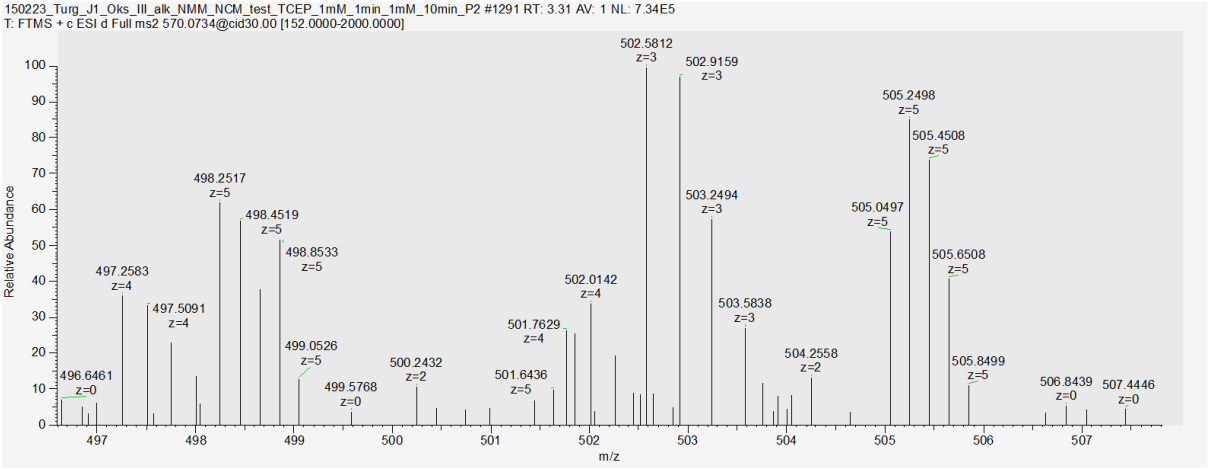

Figure 48: MS^2 spectrum of ion 570.0734, which is the molecule ion for Turg_JK_1 alkylated with two NMM and NCM groups at 5 charges. The sample is of isomer III of Turg_JK_1 after sequential reduction and alkylation. b^{+3}-ion 502.5812 is present in the spectrum.

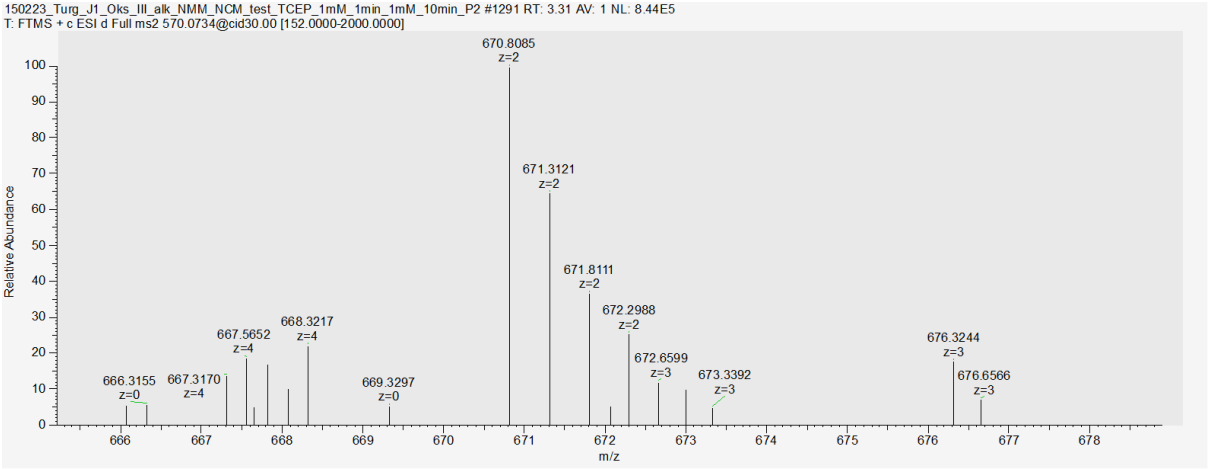

Figure 49: MS^2 spectrum of ion 570.0734, which is the molecule ion for Turg_JK_1 alkylated with two NMM and NCM groups at 5 charges. The sample is of isomer III of Turg_JK_1 after sequential reduction and alkylation. y^{+2}-ion 670.8085 is present in the spectrum.

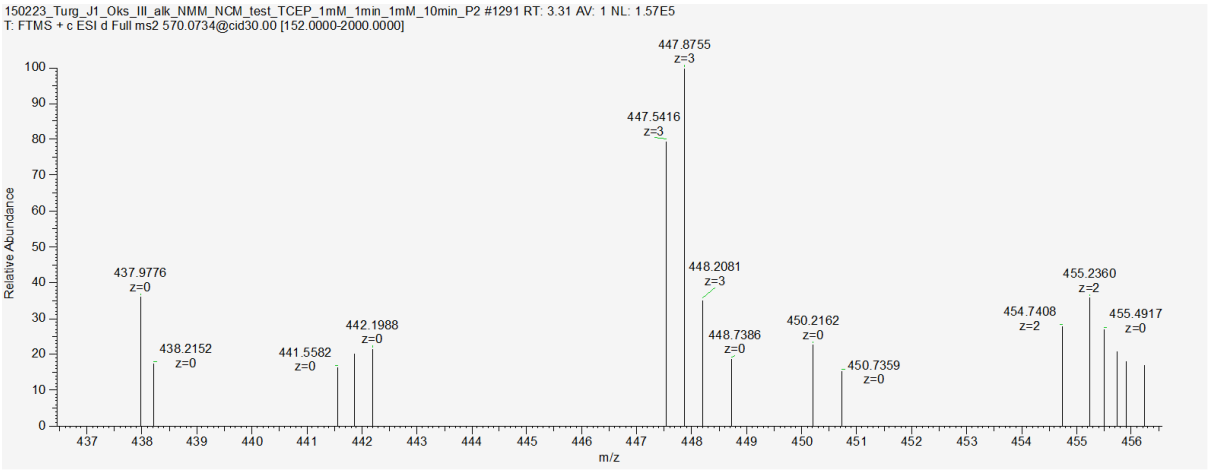

Figure 50: MS^2 spectrum of ion 570.0734, which is the molecule ion for Turg_JK_1 alkylated with two NMM and NCM groups at 5 charges. The sample is of isomer III of Turg_JK_1 after sequential reduction and alkylation. y^{+3}-ion 447.5416 is present in the spectrum.

10.8 Theoretical fragments and hits of Turg_JK_1 isomer III

Table 15: Table showing the theoretical fragments of Turg_JK_1 with a 1-2/3-4 connectivity for the alkylation pattern 1-NMM/2-NMM/3-NCM/4-NCM. The ions are placed in table based on their ion type (b, y) which is seen on the left, and position in the peptide sequence which is seen in the middle. The measured ions that have a hit will have their corresponding theoretical ion highlighted in green or yellow. The hits are highlighted in green if they cannot be found in the other alkylation pattern for a 1-2/3-4 connectivity, and yellow if they are in both.

N-terminal																				
a-NH_3	---	298.122	484.201	555.238	741.318	955.359	1012.38	1168.48	1324.58	1421.64	1478.66	1535.68	1691.78	1847.88	2129.98	2258.08	2444.16	2726.26	---	
a-NH_3^{+2}	---	149.565	242.604	278.123	371.163	478.183	506.694	584.744	662.795	711.321	739.832	768.343	846.393	924.444	1065.5	1129.54	1222.58	1363.63	---	
a-NH_3^{+3}	---	---	---	---	---	---	---	390.165	442.199	474.55	493.557	512.564	564.598	616.632	710.666	753.365	815.391	909.426	---	
a-NH_3^{+4}	---	---	---	---	---	---	---	---	331.901	356.164	370.42	384.675	423.7	462.726	533.252	565.275	611.795	682.321	---	
a-NH_3^{+5}	---	---	---	---	---	---	---	---	---	---	---	---	339.162	370.382	426.803	452.422	489.638	546.058	---	
a-NH_3^{+6}	---	---	---	---	---	---	---	---	---	---	---	---	---	308.82	355.837	377.186	408.199	455.217	---	
a-NH_3^{+7}	---	---	---	---	---	---	---	---	---	---	---	---	---	---	---	323.446	350.029	390.329	---	
a	---	315.149	501.228	572.265	758.344	972.386	1029.41	1185.51	1341.61	1438.66	1495.68	1552.7	1708.81	1864.91	2147.01	2275.11	2461.19	2743.29	---	
a^{+2}	---	158.078	251.118	286.636	379.676	486.696	515.207	593.258	671.308	719.835	748.345	776.856	854.907	932.957	1074.01	1138.06	1231.1	1372.15	---	
a^{+3}	---	---	---	---	---	---	---	395.841	447.875	480.226	499.233	518.24	570.274	622.307	716.342	759.04	821.067	915.101	---	
a^{+4}	---	---	---	---	---	---	---	---	336.158	360.421	374.676	388.932	427.957	466.982	537.508	569.532	616.052	686.578	---	
a^{+5}	---	---	---	---	---	---	---	---	---	---	---	---	342.567	373.787	430.208	455.827	493.043	549.464	---	
a^{+6}	---	---	---	---	---	---	---	---	---	---	---	---	---	311.657	358.675	380.024	411.037	458.054	---	
a^{+7}	---	---	---	---	---	---	---	---	---	---	---	---	---	---	---	325.879	352.461	392.762	---	
b-NH_3	---	326.117	512.196	583.233	769.313	983.354	1040.38	1196.48	1352.58	1449.63	1506.65	1563.67	1719.77	1875.88	2157.98	2286.07	2472.15	2754.26	---	
b-NH_3^{+2}	---	163.562	256.602	292.12	385.16	492.181	520.691	598.742	676.792	725.319	753.83	782.34	860.391	938.441	1079.49	1143.54	1236.58	1377.63	---	
b-NH_3^{+3}	---	---	---	---	---	---	---	399.497	451.531	483.882	502.889	521.896	573.93	625.963	719.998	762.696	824.723	918.757	---	
b-NH_3^{+4}	---	---	---	---	---	---	---	---	338.9	363.163	377.418	391.674	430.699	469.724	540.25	572.274	618.794	689.32	---	
b-NH_3^{+5}	---	---	---	---	---	---	---	---	---	---	---	---	344.761	375.981	432.402	458.021	495.237	551.657	---	
b-NH_3^{+6}	---	---	---	---	---	---	---	---	---	---	---	---	---	313.485	360.503	381.852	412.865	459.882	---	
b-NH_3^{+7}	---	---	---	---	---	---	---	---	---	---	---	---	---	---	---	327.445	354.028	394.329	---	
b	---	343.144	529.223	600.26	786.339	1000.38	1057.4	1213.5	1369.6	1466.66	1523.68	1580.7	1736.8	1892.9	2175.01	2303.1	2489.18	2771.28	---	
b^{+2}	---	172.075	265.115	300.634	393.673	500.694	529.205	607.255	685.306	733.832	762.343	790.854	868.904	946.955	1088.01	1152.05	1245.09	1386.15	---	
b^{+3}	---	---	---	---	---	---	---	405.173	457.206	489.557	508.564	527.571	579.605	631.639	725.674	768.372	830.398	924.433	---	
b^{+4}	---	---	---	---	---	---	---	---	343.157	367.42	381.675	395.93	434.956	473.981	544.507	576.531	623.051	693.576	---	
b^{+5}	---	---	---	---	---	---	---	---	---	---	---	---	348.166	379.386	435.807	461.426	498.642	555.063	---	
b^{+6}	---	---	---	---	---	---	---	---	---	---	---	---	---	316.323	363.34	384.69	415.703	462.72	---	
b^{+7}	---	---	---	---	---	---	---	---	---	---	---	---	---	---	---	329.878	356.461	396.761	---	
b+H_2O	---	---	---	---	---	---	---	---	---	---	---	---	---	---	---	---	2507.19	2789.29	---	
b+H_2O^{+2}	---	---	---	---	---	---	---	---	---	---	---	---	---	---	---	---	1254.1	1395.15	---	
b+H_2O^{+3}	---	---	---	---	---	---	---	---	---	---	---	---	---	---	---	---	836.402	930.436	---	
b+H_2O^{+4}	---	---	---	---	---	---	---	---	---	---	---	---	---	---	---	---	627.553	698.079	---	
b+H_2O^{+5}	---	---	---	---	---	---	---	---	---	---	---	---	---	---	---	---	502.244	558.665	---	
b+H_2O^{+6}	---	---	---	---	---	---	---	---	---	---	---	---	---	---	---	---	418.705	465.722	---	
b+H_2O^{+7}	---	---	---	---	---	---	---	---	---	---	---	---	---	---	---	---	359.034	399.334	---	
	1	**2**	**3**	**4**	**5**	**6**	**7**	**8**	**9**	**10**	**11**	**12**	**13**	**14**	**15**	**16**	**17**	**18**	**19**	
-	**d**	**K**	**W**	**A**	**W**	**d**	**G**	**R**	**R**	**P**	**G**	**G**	**R**	**R**	**e**	**K**	**W**	**e**	**G**	**-Amidated**
	19	**18**	**17**	**16**	**15**	**14**	**13**	**12**	**11**	**10**	**9**	**8**	**7**	**6**	**5**	**4**	**3**	**2**	**1**	
C-terminal																				
y	---	2631.29	2503.2	2317.12	2246.08	2060	1845.96	1788.94	1632.84	1476.74	1379.68	1322.66	1265.64	1109.54	953.437	671.333	543.238	357.159	75.0553	
y^{+2}	---	1316.15	1252.1	1159.06	1123.54	1030.5	923.483	894.972	816.922	738.871	690.345	661.834	633.323	555.273	477.222	336.17	---	---	---	
y^{+3}	---	877.768	835.07	773.044	749.365	687.338	615.991	596.984	544.95	492.917	460.566	441.559	422.551	370.518	---	---	---	---	---	
y^{+4}	---	658.5781	626.5544	580.0346	562.275	515.756	462.245	447.99	408.965	369.939	345.676	331.421	317.165	---	---	---	---	---	---	
y^{+5}	---	527.064	501.445	464.229	450.022	412.806	369.998	358.593	327.373	---	---	---	---	---	---	---	---	---	---	
y^{+6}	---	439.388	418.039	387.026	375.186	344.173	308.499	298.996	---	---	---	---	---	---	---	---	---	---	---	
y^{+7}	---	376.762	---	---	---	---	---	---	---	---	---	---	---	---	---	---	---	---	---	
y-NH_3	---	2614.26	2486.17	2300.09	2229.05	2042.97	1828.93	1771.91	1615.81	1459.71	1362.66	1305.63	1248.61	1092.51	936.411	654.307	---	---	---	
y-NH_3^{+2}	---	1307.64	1243.59	1150.55	1115.03	1021.99	914.97	886.459	808.409	730.358	681.832	653.321	624.81	546.76	468.709	327.657	---	---	---	
y-NH_3^{+3}	---	872.093	829.395	767.368	743.689	681.663	610.316	591.308	539.275	487.241	454.89	435.883	416.876	364.842	---	---	---	---	---	
y-NH_3^{+4}	---	654.322	622.298	575.778	558.019	511.499	457.989	443.733	404.708	365.683	341.419	327.164	312.909	---	---	---	---	---	---	
y-NH_3^{+5}	---	523.659	498.04	460.824	446.616	409.401	366.592	355.188	323.968	---	---	---	---	---	---	---	---	---	---	
y-NH_3^{+6}	---	436.55	415.201	384.188	372.348	341.335	305.661	296.158	---	---	---	---	---	---	---	---	---	---	---	
y-NH_3^{+7}	---	374.33	---	---	---	---	---	---	---	---	---	---	---	---	---	---	---	---	---	

Table 16: Table showing the theoretical fragments of Turg_JK_1 with a 1-3/2-4 connectivity for the alkylation pattern 1-NCM/2-NCM/3-NMM/4-NMM. The ions are placed in table based on their ion type (b, y) which is seen on the left, and position in the peptide sequence which is seen in the middle. The measured ions that have a hit will have their corresponding theoretical ion highlighted in green or yellow. The hits are highlighted in green if they cannot be found in the other alkylation pattern for a 1-3/2-4 connectivity, and yellow if they are in both.

N-terminal																				
$a-NH_3$	---	366.1846	552.2639	623.3010	809.3803	1091.4841	1148.5056	1304.6067	1460.7078	1557.7606	1614.7821	1671.8035	1827.9046	1984.0057	2198.0470	2326.1419	2512.2212	2726.2624	---	
$a-NH_3^{+2}$	---	183.5959	276.6356	312.1541	405.1938	546.2457	574.7564	652.8070	730.8576	779.3839	807.8947	836.4054	914.4560	992.5065	1099.5271	1163.5746	1256.6143	1363.6349	---	
$a-NH_3^{+3}$	---	---	---	---	---	---	---	435.5404	487.5741	519.9250	538.9322	557.9394	609.9731	662.0068	733.3538	776.0522	838.0786	909.4257	---	
$a-NH_3^{+4}$	---	---	---	---	---	---	---	---	365.9324	390.1956	404.4510	418.7063	457.7316	496.7569	550.2672	582.2909	628.8108	682.3211	---	
$a-NH_3^{+5}$	---	---	---	---	---	---	---	---	---	---	---	---	366.3867	397.6070	440.4152	466.0342	503.2501	546.0583	---	
$a-NH_3^{+6}$	---	---	---	---	---	---	---	---	---	---	---	---	---	331.5070	367.1806	388.5297	419.5429	455.2165	---	
$a-NH_3^{+7}$	---	---	---	---	---	---	---	---	---	---	---	---	---	---	---	333.1694	359.7521	390.3294	---	
a	---	383.2111	569.2905	640.3276	826.4069	1108.5107	1165.5322	1321.6333	1477.7344	1574.7871	1631.8086	1688.8301	1844.9312	2001.0323	2215.0735	2343.1685	2529.2478	2743.2890	---	
a^{+2}	---	192.1092	285.1489	320.6674	413.7071	554.7590	583.2697	661.3203	739.3708	787.8972	816.4079	844.9187	922.9692	1001.0198	1108.0404	1172.0879	1265.1275	1372.1481	---	
a^{+3}	---	---	---	---	---	---	---	441.2159	493.2496	525.6006	544.6077	563.6149	615.6486	667.6823	739.0294	781.7277	843.7541	915.1012	---	
a^{+4}	---	---	---	---	---	---	---	---	370.1891	394.4522	408.7076	422.9630	461.9883	501.0135	554.5238	586.5476	633.0674	686.5777	---	
a^{+5}	---	---	---	---	---	---	---	---	---	---	---	---	369.7921	401.0123	443.8205	469.4395	506.6554	549.4636	---	
a^{+6}	---	---	---	---	---	---	---	---	---	---	---	---	---	334.3448	370.0183	391.3675	422.3807	458.0542	---	
a^{+7}	---	---	---	---	---	---	---	---	---	---	---	---	---	---	---	335.6017	362.1845	392.7618	---	
$b-NH_3$	---	394.1795	580.2588	651.2959	837.3752	1119.4791	1176.5005	1332.6016	1488.7027	1585.7555	1642.7770	1699.7984	1855.8995	2012.0007	2226.0419	2354.1368	2540.2161	2754.2574	---	
$b-NH_3^{+2}$	---	197.5934	290.6330	326.1516	419.1913	560.2432	588.7539	666.8045	744.8550	793.3814	821.8921	850.4029	928.4534	1006.5040	1113.5246	1177.5721	1270.6117	1377.6323	---	
$b-NH_3^{+3}$	---	---	---	---	---	---	---	444.8721	496.9058	529.2567	548.2638	567.2710	619.3047	671.3384	742.6855	785.3838	847.4102	918.7573	---	
$b-NH_3^{+4}$	---	---	---	---	---	---	---	---	372.9311	397.1943	411.4497	425.7051	464.7303	503.7556	557.2659	589.2897	635.8095	689.3198	---	
$b-NH_3^{+5}$	---	---	---	---	---	---	---	---	---	---	---	---	371.9857	403.2060	446.0142	471.6332	508.8491	551.6573	---	
$b-NH_3^{+6}$	---	---	---	---	---	---	---	---	---	---	---	---	---	336.1728	371.8464	393.1955	424.2088	459.8823	---	
$b-NH_3^{+7}$	---	---	---	---	---	---	---	---	---	---	---	---	---	---	---	337.1686	363.7514	394.3287	---	
b	---	411.2061	597.2854	668.3225	854.4018	1136.5056	1193.5271	1349.6282	1505.7293	1602.7821	1659.8035	1716.8250	1872.9261	2029.0272	2243.0684	2371.1634	2557.2427	2771.2839	---	
b^{+2}	---	206.1067	299.1463	334.6649	427.7045	568.7564	597.2672	675.3177	753.3683	801.8947	830.4054	858.9161	936.9667	1015.0172	1122.0378	1186.0853	1279.1250	1386.1456	---	
b^{+3}	---	---	---	---	---	---	---	450.5476	502.5813	534.9322	553.9394	572.9465	624.9802	677.0139	748.3610	791.0593	853.0857	924.4328	---	
b^{+4}	---	---	---	---	---	---	---	---	377.1878	401.4510	415.7063	429.9617	468.9870	508.0123	561.5226	593.5463	640.0661	693.5764	---	
b^{+5}	---	---	---	---	---	---	---	---	---	---	---	---	375.3910	406.6113	449.4195	475.0385	512.2544	555.0626	---	
b^{+6}	---	---	---	---	---	---	---	---	---	---	---	---	---	339.0106	374.6841	396.0333	427.0465	462.7200	---	
b^{+7}	---	---	---	---	---	---	---	---	---	---	---	---	---	---	---	339.6010	366.1838	396.7611	---	
$b+H_2O$	---	---	---	---	---	---	---	---	---	---	---	---	---	---	---	---	2575.2533	2789.2945	---	
$b+H_2O^{+2}$	---	---	---	---	---	---	---	---	---	---	---	---	---	---	---	---	1288.1303	1395.1509	---	
$b+H_2O^{+3}$	---	---	---	---	---	---	---	---	---	---	---	---	---	---	---	---	859.0893	930.4363	---	
$b+H_2O^{+4}$	---	---	---	---	---	---	---	---	---	---	---	---	---	---	---	---	644.5688	698.0791	---	
$b+H_2O^{+5}$	---	---	---	---	---	---	---	---	---	---	---	---	---	---	---	---	515.8565	558.6647	---	
$b+H_2O^{+6}$	---	---	---	---	---	---	---	---	---	---	---	---	---	---	---	---	430.0483	465.7218	---	
$b+H_2O^{+7}$	---	---	---	---	---	---	---	---	---	---	---	---	---	---	---	---	368.7567	399.3340	---	
	1	**2.0000**	**3.0000**	**4.0000**	**5.0000**	**6.0000**	**7.0000**	**8.0000**	**9.0000**	**10.0000**	**11.0000**	**12.0000**	**13.0000**	**14.0000**	**15.0000**	**16.0000**	**17.0000**	**18.0000**	**19.0000**	
-	**e**	**K**	**W**	**A**	**W**	**e**	**G**	**R**	**R**	**P**	**G**	**G**	**R**	**R**	**d**	**K**	**W**	**d**	**G**	**-Amidated**
	19	**18.0000**	**17.0000**	**16.0000**	**15.0000**	**14.0000**	**13.0000**	**12.0000**	**11.0000**	**10.0000**	**9.0000**	**8.0000**	**7.0000**	**6.0000**	**5.0000**	**4.0000**	**3.0000**	**2.0000**	**1.0000**	
C-terminal																				
y	---	2563.2281	2435.1331	2249.0538	2178.0167	1991.9374	1709.8336	1652.8121	1496.7110	1340.6099	1243.5571	1186.5357	1129.5142	973.4131	817.3120	603.2708	475.1758	289.0965	75.0553	
y^{+2}	---	1282.1177	1218.0702	1125.0306	1089.5120	996.4723	855.4204	826.9097	748.8591	670.8086	622.2822	593.7715	565.2607	487.2102	409.1596	302.1390	---	---	---	
y^{+3}	---	855.0809	812.3826	750.3561	726.6771	664.6507	570.6160	551.6089	499.5752	447.5415	415.1906	396.1834	377.1763	325.1426	---	---	---	---	---	
y^{+4}	---	641.5625	609.5387	563.0189	545.2596	498.7398	428.2139	413.9585	374.9332	335.9079	311.6447	297.3894	283.1340	---	---	---	---	---	---	
y^{+5}	---	513.4514	487.8324	450.6166	436.4092	399.1933	342.7725	331.3682	300.1480	---	---	---	---	---	---	---	---	---	---	
y^{+6}	---	428.0441	406.6949	375.6817	363.8422	332.8290	285.8117	276.3081	---	---	---	---	---	---	---	---	---	---	---	
y^{+7}	---	367.0388	---	---	---	---	---	---	---	---	---	---	---	---	---	---	---	---	---	
$y-NH_3$	---	2546.2016	2418.1066	2232.0273	2160.9902	1974.9109	1692.8070	1635.7856	1479.6845	1323.5834	1226.5306	1169.5091	1112.4877	956.3866	800.2854	586.2442	---	---	---	
$y-NH_3^{+2}$	---	1273.6044	1209.5569	1116.5173	1080.9987	987.9591	846.9072	818.3964	740.3459	662.2953	613.7689	585.2582	556.7475	478.6969	400.6464	293.6258	---	---	---	
$y-NH_3^{+3}$	---	849.4054	806.7070	744.6806	721.0016	658.9751	564.9405	545.9334	493.8997	441.8660	409.5150	390.5079	371.5007	319.4670	---	---	---	---	---	
$y-NH_3^{+4}$	---	637.3058	605.2821	558.7623	541.0030	494.4832	423.9572	409.7019	370.6766	331.6513	307.3881	293.1327	278.8774	---	---	---	---	---	---	
$y-NH_3^{+5}$	---	510.0461	484.4271	447.2113	433.0039	395.7880	339.3672	327.9629	296.7427	---	---	---	---	---	---	---	---	---	---	
$y-NH_3^{+6}$	---	425.2063	403.8572	372.8439	361.0044	329.9912	282.9739	273.4703	---	---	---	---	---	---	---	---	---	---	---	
$y-NH_3^{+7}$	---	364.6065	---	---	---	---	---	---	---	---	---	---	---	---	---	---	---	---	---	

10.9 Bioactivity testing for Turg_JS_001

Table 17: MIC of Turg_JS_001 against several bacteria. "OXY" stands for Oxytetracycline and is used as a control. Ink time means incubation time.

SAMPLE	E.C ATCC 25922	C.G ATCC 13032	S.A ATCC 9144	P.A ATCC 27853	B.S ATCC 23857	S.E ATCC RP62A	N=	COMMENTS
Turg_JS_001								
Isomer I	>250	7,8	-	125*	125	>250	3	
Isomer II	125	1,95	-	205	31,2	62,5	3	
Isomer III	>250	1,95	-	62,5*	7,8	31,2	3	
OXY	1,25	0,31	0,08	10	20	0,62	3	
Ink time	24h	24h	24h	24h	24h	24h		

*) 50% hemming. Ingen 100%

S.a vokste ugjevnt